

DOTTORATO DI RICERCA IN  
INGEGNERIA INFORMATICA E DELL' AUTOMAZIONE  
XXV CICLO - ING/INF04



UNIVERSITA' DEGLI STUDI DI FIRENZE  
Dipartimento di Sistemi e Informatica

# Performance-oriented Adaptive Switching Control

A Dissertation submitted in partial satisfaction  
of the requirements for the degree of  
Doctor of Philosophy

Daniele Mari

Ph.D Coordinator: Prof. Luigi Chisci

Tutors: Prof. Edoardo Mosca  
Prof. Giorgio Battistelli

December 2012

## Acknowledgements

First, I would like express my sincere gratitude to Prof. Edoardo Mosca for introducing me to the Control Theory. His passion, rigour and competence have aroused my interest to the Adaptive Control, which has been the main topic of my research activity. I am also indebted to him for creating the opportunity for me to spend part of my Ph.D. course studying at the University of Wyoming (UW), where I lived an unforgettable experience. Also, I would like express my deep gratitude to Prof. Giorgio Battistelli. He supported me during all my Ph.D. with constant encouragements and advices. I am grateful to him for his friendship and for the invaluable experience I gained through the discussions with him during these years. I am forever grateful to Pietro Tesi for his sincere friendship and for his precious help in all my research activity. The constant discussions with him in and out of the university, his considerations and countless advices have inspired my work and allowed me to grow up as a researcher.

I'm also indebted to Prof. Margareta Stefanovic for the time she dedicated me during the period I was at UW, as well as for her generosity and kindness. I greatly profited from my interaction with her to deepen my understanding on the switching control.

During my activity, I had the opportunity to interact with many researchers. In this respect, I am especially grateful to Armando Riccardi for giving me the opportunity to collaborate with the Astrophysical Observatory of Florence. I thank him for his generosity, patience and friendship, his precious advices helped me to broaden my studies and under his supervision I experienced a fabulous experimental research. Also, I would like thank Guido Agapito and Simone Baldi for all discussions which have enriched my doctoral studies. Irrespective of the distance, they constantly offered me all their support and friendship. I am thankful to Andrei Neamtu, Daniela Selvi, Claudio Fantacci and Giovanni Mugnai for the time they shared with me in the lab while discussing on control, estimate and other small talks. It was great time for me. A special thank goes to Goutham Kamath for making me feel at home when I was at UW. I am also sincerely thankful to Gurudatha Pai, Bharath Nayak, Sharath A S, Kaushik S V, Sahana Shenoy, Pallavi Choudhuri and Stephon Mendez. They made my experience at Laramie simply wonderful.

I am forever and deeply grateful to my closest friends Francesco Lenzi, Giacomo Tizzanini, Francesco Banci, Gloria Bargelli, Lorenzo Vinerbi and Marzia Donati for their constant support, encouragement and love. A special thank goes to Martina and Clarissa Piras for coloring all these years with their smiles. All they have inspired my life more than they can know.

Finally, I am forever grateful to my parents, Claudia and Valeriano, for their constant support and love. Also, I would like thank my uncle Sauro and my aunt Rosaria and all the rest of my family for their encouragement.

Above all, thanks to my love Irene Balzani for making each day of my life a beautiful day. This thesis is dedicated to her.

*to Irene*

## Abstract

# Performance-oriented Adaptive Switching Control

Daniele Mari

This thesis addresses the problem of controlling uncertain multivariable systems by means of adaptive switching control (ASC) schemes. Indeed, in many real applications, a large number of actuator and/or sensors may be employed so as to achieve the desired control task, thus requiring to treat the process as a typical multi-input/multi-output system. In particular, the attention is directed to model-based switching schemes and the goal is to develop solutions which aim at improving transient/regime performance. The main feature of the examined architecture is that stability does not depend on model distribution and performance improvements can be achieved without increasing the number of models.

Part I aims at extending a model-based control approach, so far restricted to single-input/single-output systems, to a general multivariable setting. The proposed scheme relies on a “high-level” unit, called the supervisor, which at any time can switch on in feedback with the process one controller from a finite family of candidate controllers. The supervisor performs routing/scheduling tasks by monitoring suitable data-based test functionals. In addition, a possible modification to the original scheme is introduced, whereby switching among fixed candidate controllers can be suitably combined with an adaptive mechanism, this idea being of interest for on-line implementation of highly performing ASC schemes.

Part II addresses the problem of the control transfer in model-based ASC schemes. Indeed, the switching is a source of nonlinearity and can cause variations of closed loop dynamics yielding significant performance degradations. To cope with this event, the proposed technique aims at promptly recovering an adequate closed-loop behavior and it exploits the model distribution/uncertainty structure so as to suitably reset of the state of the switched-on controller, in accordance with the regime behavior predicted by the a-priori information. From an implementation viewpoint, the technique is flexible enough so as to allow the designer to trade off performance vs. memory and/or computational complexity, even when the process is described by a continuous distribution of models.

Since simulations of adaptive control systems are often useful for performance evaluation, Part III focuses on a numerical multivariable example.

# Contents

<b>Abstract</b>	<b>iv</b>
<b>1 Introduction</b>	<b>1</b>
1.1 Switching Strategy . . . . .	4
1.1.1 Adaptive Tuning in Switching Control . . . . .	7
1.2 Transfer of the Control Action . . . . .	9
<b>2 Problem Framework: Square Systems</b>	<b>12</b>
<b>I Controller Selection Strategy</b>	<b>15</b>
<b>3 Model-based Switching Control for Uncertain Square Systems</b>	<b>16</b>
3.1 Supervisory Control System and Switching Logic . . . . .	19
3.2 Test Functionals-based selection . . . . .	20
3.2.1 Reference-loop Identification in case of Square Systems . . . . .	22
3.3 Stability Inference and Performance Requirements . . . . .	25
3.4 Main results . . . . .	28
3.4.1 Tracking Properties . . . . .	30
3.5 ASC scheme Implementation Aspects . . . . .	32
3.6 Concluding Remarks . . . . .	34
<b>A Reference-loop Identification in case of Non-Square Systems</b>	<b>35</b>

<b>B Performance-oriented Controller Tuning: Some Remarks</b>	<b>41</b>
B.1 Model distribution-based Performance: An example . . . . .	42
B.2 Fine Controller Tuning Algorithm . . . . .	45
B.2.1 Implementation Issues . . . . .	47
B.3 ASC Scheme with Fine Controller Tuning . . . . .	48
B.3.1 Tuning-based Performance: An Example (Continued) . . . . .	51
B.4 Concluding Remarks and Open Problems . . . . .	52
<b>C Proofs</b>	<b>54</b>
<b>II Control Transfer</b>	<b>60</b>
<b>4 Performance-Oriented Transfer for Model-based Switching Schemes</b>	<b>61</b>
4.1 Overall Problem . . . . .	63
4.2 State-shared multicontroller implementation . . . . .	64
4.3 Optimal conditioning . . . . .	68
4.3.1 Time-Weighted cost . . . . .	76
4.4 Robust Conditioning . . . . .	76
4.5 An Example . . . . .	80
4.5.1 State reset map vs. dynamic compensation . . . . .	83
4.6 Concluding Remarks . . . . .	87
<b>III Simulative Example</b>	<b>91</b>
<b>5 A Four Carts Example</b>	<b>92</b>
5.1 First Scenario: Monodimensional Uncertainty . . . . .	94
5.2 Second Scenario: Bidimensional Uncertainty . . . . .	100
5.3 Concluding Remarks . . . . .	105
<b>Conclusions</b>	<b>108</b>
<b>Bibliography</b>	<b>110</b>

# Chapter 1

## Introduction

“In everyday language, *to adapt* means to change a behavior to conform to new circumstances. Intuitively, an adaptive controller is thus a controller that can modify its behavior in response to changes in the dynamics of the process and the character of the disturbances” [SS11].

In this thesis we deal with the problem of controlling multivariable linear processes in presence of large-scale modelling uncertainty, *i.e.* processes described by models whose structure and parameters are not all a priori known to the designer. Large uncertainty is typically the case where no single controller can guarantee a desired behaviour when connected with the process so, Robust Control design techniques, as the one described in [ZDG95, GL95, DFT90], turn out to be ineffective. Also, in many control engineering applications, the process may exhibit significant / fast variations of its dynamics and accordingly, it could be required a control law such to compensate such variations by responding as quickly as process dynamics changes. This is the case, for example, of the problem of fight-control systems [SL92, NRR93, BG97]. In such applications, Gain-Scheduling techniques have succeeded the classical Adaptive Control approach. In both ones, the control architecture, as shown in Figure 1.1, consists of two loops: an inner loop, the ordinary control system, composed of the process and the controller, and an outer loop which comprises the tuning mechanism / gain-scheduler. Tuning mechanism adapts in a continuous manner the parameters of the feedback compensator, based on the data directly measured from the closed loop system [Mos95, IS96]. However, this solution turns out to be poorly applicable in situations where process dynamics is subjected to fast variations. Gain-scheduler

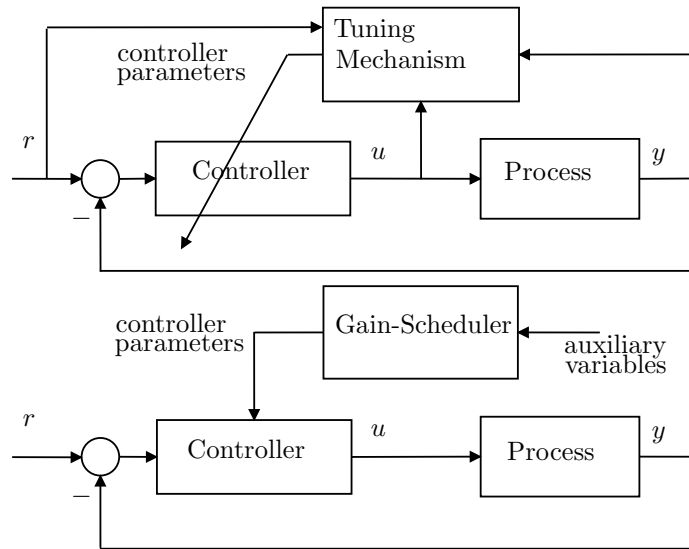


**Figure 1.1:** Top: Adaptive Control scheme. Bottom: Gain-Scheduling Control scheme.

accommodates, on the contrary, changes in the control action by means of a look-up table associating the controller parameters to the value of auxiliary variables which carry information about the dynamic regime of the process [SA90, RS00]. Typically, these variables provide no feedback from the actual performance of the closed loop system with the consequence that unstable trends can occur in the inner loop without the gain-scheduling unit be able to detect them.

*Adaptive Switching Control* (ASC) schemes can be viewed as an adaptive variant of Gain-Scheduling. The main idea behind this method to approach the problem of handling process with large uncertainty / abrupt variations consists in employing adaptive logic-based switching among a family of pre-computed controllers. To do that, ASC schemes make use of an outer loop which comprises an high level supervision unit, called *supervisor*, such to select the current controller based on recorded process data. Controllers are a-priori designed to guarantee for each dynamic regime of the process a satisfactory behavior. Advantages with respect to pre-existing control approaches are evident. First, stability / higher performance can be always achieved by increasing the number of controllers; second, the switching rule, its nature being adaptive, can quickly detect the dynamic mode which currently characterizes the process behavior so that the most suitable controller can be



## *Chapter 1. Introduction*

instantly switched-on in feedback with the process. Thereby, once obtained a family of fixed controllers, the control problem consists in appropriately orchestrating the switching. Switching among controllers is actually a crucial aspect, as it may generate bad transients with adverse effects on closed loop performance and, in some case, it can lead to instability. For this reason, in the last two decades many research efforts have been devoted to the development of appropriate switching logics – monograph [Lib03] and survey papers [KSe01, HLe01, AD08] provide an overview of this topic.

This thesis stems from the consideration that a switching logic, even if well designed, could not be sufficient to keep high performance at each situation where the control system could be in. Of course, control action transfer at the times of switching is a source of nonlinearity and can cause dramatic transients for the process. Also, using a finite number of fixed controllers does not allow in general to achieve an exact adaptation of the control law to the process dynamics. To end, the switching logic should be independent of the “geometry” of the process. Indeed, in many real processes, such as industrial plants, aircrafts and communication networks, a large number of actuator and/or sensors may be employed in order to achieve the desired control task, thus requiring to treat the process as a typical multi-input / multi-output system.

This thesis is so divided in order to provide some suggestion for each one of the above mentioned questions. The framework of the control problem is specified in Chapter 2. Part I concerns the adaptive switching logic applied to a generic multivariable system. In particular, Chapter 3 refers to square systems, while the extension to the non-square systems is carried out in Appendix A. Appendix B provides some remarks on the design of a dedicated tuning mechanism to be combined with the switching logic of Chapter 3, in case the aim be to increase the closed loop performance without destroying the properties given by the switching logic. Part II deals with the problem to transfer the control action, controllers being actually dynamic system, which time evolution depends on their implementation into the ASC scheme. Chapter 4 discusses a multicontroller architecture which appears adequate to be implemented in ASC schemes and also a parameter is detected such to be adaptively changed so as to have a performance-oriented transfer. Eventually, Chapter 5 in Part III considers a linear multivariable system and provides some numerical results.

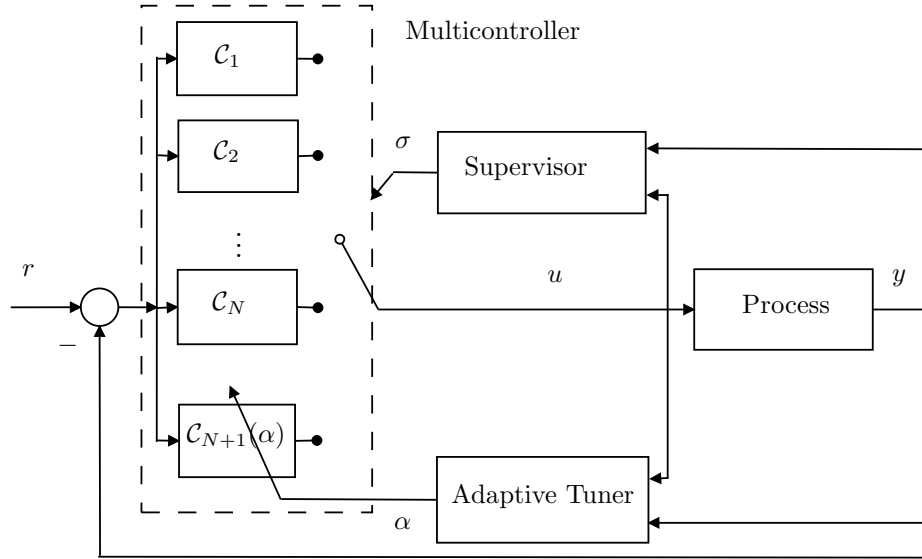


**Figure 1.2:** Adaptive Switching Control scheme with Tuning Mechanism.

Figure 1.2 sums up the three blocks characterizing the supervisory control scheme, namely supervisor, multicontroller and, possibly, adaptive tuner. Because of the modular nature of the scheme, property of each block can be separately analysed. The remainder of this chapter introduces the topics handled in this thesis and it briefly resumes the solutions proposed to design each block, thus highlighting the new contributions.

## 1.1 Switching Strategy

Control of processes with large dynamic uncertainties requires the use of multiple linear time-invariant controllers  $\mathcal{C}_1, \mathcal{C}_2, \dots, \mathcal{C}_N$  whenever no single controller can guarantee adequate performance for each process configuration. In this respect, a high-level unit, called *Supervisor*, is devoted to select the controller to be put in feedback with the process at each time. To carry out the selection, the supervisor has access to the input / output records of the process and, by monitoring a family of data-based test functionals  $\Pi(t) := \{\Pi_1(t), \Pi_2(t), \dots, \Pi_N(t)\}, t \in \{0, 1, \dots\}$ , decides whether the currently switched-on controller is adequate and, in the negative, replaces it by another candidate controller. Each functional  $\Pi_i(t)$  quantifies the suitability of the controller  $\mathcal{C}_i$  to be placed in feed-

back with the process, given the data up to time  $t$ . The supervisor updates the index  $\sigma(t) \in \{1, 2, \dots, N\}$  based on a switching logic

$$\sigma(t+1) = l(\sigma(t), \Pi(t)).$$

Hysteresis-based switching logics (HSL) as the one considered in Chapter 3 have the advantage, along with avoiding chattering (namely, infinitely fast switching [HLM03b, HLM03a]), to enjoy properties given by the HSL Lemma 3.1.1 [MMG92], which provides conditions under which the switching stops in a finite time and, the test functional associated to the final controller is bounded. To cope with this lemma, it is convenient to design test functionals in order to satisfy basic assumptions of the HSL lemma, *i.e.*, irrespective of switching sequence  $\sigma^t$ , to guarantee that i) each test functional admits limit as  $t \rightarrow \infty$  and, ii) at least one test functional keeps bounded as  $t \rightarrow \infty$ . Nonetheless, the main goal of a switching control scheme has to be the one to select the right controller without exciting unstable dynamics of the process. In this respect, we consider the input-output stability in a  $l_2$  sense, so defined for the specific system represented in Figure 1.2: the (switched) inner loop of Figure 1.2 is input-output  $l_2$  stable if there exist two non-negative reals  $c_1$  and  $c_2$  such that

$$\|z^t\| \leq c_1 + c_2 \|r^t\|, \quad \forall t \in \{0, 1, \dots\},$$

where  $z := [u' \ y']'$  and  $\|x^t\| := \sqrt{\sum_{k=0}^t |x(k)|^2}$ . Hence, an appropriate test function should be such to satisfy the assumptions i) and ii) of the HSL lemma and also, the boundedness of the  $\Pi_f(t)$  as  $t \rightarrow \infty$ , where the subscription  $f$  indicates the final switching index, should reflect the input-output  $l_2$  stability above defined [ST97, SWPS07, SS11].

The switching strategy presented in Part I has been proposed in [BBM<sup>+</sup>11a, BBM<sup>+</sup>12] and, it is an extension to the multivariable setting of the ASC scheme proposed for the first time in [BBMT10]. The latter consists in a model-based switching scheme, based on the assumption that a process model is associated to each controller. So, a model distribution  $\mathcal{M}_1, \mathcal{M}_2, \dots, \mathcal{M}_N$ , is a-priori available, describing the process uncertainty. Models and controllers allows the designer to determine a family of reference loops  $(\mathcal{M}_i/\mathcal{C}_i)$ ,  $i = 1, 2, \dots, N$ , each one representing the feedback interconnection between the model  $\mathcal{M}_i$  with the controller  $\mathcal{C}_i$ . Let  $\mathcal{P}$  indicate the real process, then  $(\mathcal{P}/\mathcal{C}_i)$  denotes the  $i$ 'th potential loop. In [BBMT10],  $\Pi_i(t)$  evaluates the discrepancy between  $(\mathcal{P}/\mathcal{C}_i)$  and  $(\mathcal{M}_i/\mathcal{C}_i)$  in response to a fictitious signal  $v_i$ , known as *virtual reference*. Leaving the details to Chapter

## Chapter 1. Introduction

3, it can be obtained by solving, if it is possible, the following equation

$$v_i(t) = y(t) + \mathcal{C}_i^{-1} u(t),$$

*i.e.* in words, the virtual reference is the sequence which would reproduce the process input-output sequences, respectively,  $u^t$  and  $y^t$ , should the process be fed-back by the candidate controller  $\mathcal{C}_i$ , irrespective of the way  $u^t$  and  $y^t$  are generated. With obvious meaning of symbols, virtual reference  $v_i$  is hence such that  $z = (\mathcal{P}/\mathcal{C}_i) v_i$ , while one has  $[u'_i \ y'_i]' =: z_i = (\mathcal{M}_i/\mathcal{C}_i) v_i$ . According to that, test functional is obtained as the following percentage discrepancy

$$\begin{aligned} \Pi_i(t) &:= \max_{k \leq t} \Lambda_i(k), \\ \Lambda_i^{1/2}(t) &:= \frac{\|\tilde{z}_{i/i}^t\|}{\|(z - \tilde{z}_{i/i})^t\|}, \quad \tilde{z}_i(t) := z(t) - z_i(t). \end{aligned}$$

which turns out to be computable for each candidate controller  $\mathcal{C}_i$ , irrespective of the fact that  $\mathcal{C}_i$  could be on-line or off-line, thus avoiding pre-routing routines. Essentially, the overall switching strategy carry out a *Reference Loop Identification* task: closer the behavior of  $(\mathcal{P}/\mathcal{C}_i)$  to the one of  $(\mathcal{M}_i/\mathcal{C}_i)$  in response to  $v_i$ , higher the probability that  $\mathcal{C}_i$  be selected.

Notice that the use of the max operator allows to satisfy assumption i) of the HSL lemma, while assumption ii) turns out to be satisfied provided that the minimal / reasonable requirement that at least one controller exists such to be stabilizing for each process configuration (see Section 3.2.1). Sections 3.3 and 3.4 tackle the main contributions of the chapter and show how such test functionals could be able to infer stability of the candidate controllers. Further, Theorem 3.4.1 resumes the conditions under which the switched system of Figure 1.2 keeps input-output  $l_2$  stable and also, Theorem 3.4.2 provides a simple variation to the original form of the test functional apt to guarantee offset-free with respect to a generic class of reference produced by linear time-invariant exo-systems. The main contribution of the chapter consists in proving that such results hold irrespective of the “geometry” of the process. In particular, the original interpretation of discrepancy between potential and reference loop need not hold in case number of outputs be greater than number of inputs, since the virtual reference need not exist. In this respect, Appendix A discusses a possible modification of the virtual reference definition which makes it possible to recover the interpretation in terms of discrepancy for any process geometry. Nevertheless,

from Section 3.5, one can conclude that the adopted test functional  $\Pi_i(t)$  is always on-line computable by prefiltering the prediction error based on the nominal model  $\mathcal{M}_i$ , see Lemma 3.5.1.

ASC schemes, while retaining the fundamental ideas of adaptive control [Mos95, IS96], enjoy potential advantages over traditional continuous adaptation [Mor95, NB97, HLM03b]: i) fast adaptation due to the discontinuous fashion of the controller selection ii) modularity of the control architecture. Because of the latter one, the dynamic of the supervisor does not affect the inner loop behavior between two switching instants and, integration into the inner loop of pre-designed control structures is possible, without having the need to continuously parametrize the controller structure. Further, the use of pre-designed control structures allows to circumvent shortcomings in the controller synthesis, such as danger of stabilizability loss of the identified model, which is typically encountered in formulating adaptive control as a recursive tuning control problem. However, the adoption of a finite number of controllers may prevent from achieving optimal performance because of possible detuning arising from the discrete nature of the controller family in contrast with the possibly continuous nature of the process uncertainty. Even more importantly, satisfactory trade-offs between the conflicting objectives of number of candidate controllers (hence memory/computational load) and desired performance need not even exist in some cases, especially if the process uncertainty set is large. Intuitively, higher performance is achievable by suitably increasing the number of reference loops, such a result being formalized in Proposition 3.4.1.

### 1.1.1 Adaptive Tuning in Switching Control

The main contribution of Appendix B consists in proposing a way to combine an ASC scheme with a controller tuning algorithm in order to enjoy positive features of both the techniques: Speed (from switching) and accuracy (from adaptive tuning) of the control system response. In particular, the tuning algorithm is thought to be applied to the ASC logic described in Chapter 3 [BBM<sup>+</sup>11b]. The essential of the idea is the following. Let switching mechanism select the controller  $\mathcal{C}_f$  at the time  $t_*$ , then  $(\mathcal{M}_f/\mathcal{C}_f)$  can be thought as the desired behavior to be achieved. If  $\mathcal{C}(\alpha)$  denotes a linear time-invariant controller in a given class parametrized by the vector  $\alpha$ , belonging to some set  $\Theta_\alpha \subset \mathbb{R}^{n_\alpha}$ , then the goal can be to tune  $\alpha$  so that  $(\mathcal{P}/\mathcal{C}(\alpha))$  approaches as much as possible  $(\mathcal{M}_f/\mathcal{C}_f)$ . Such objective

Chapter 1. Introduction

can be carried out by means of the virtual reference concept. Indeed, the innovative idea is the one to parametrize the virtual reference with respect to  $\alpha$  as follows

$$v_\alpha(t) = y(t) + \mathcal{C}^{-1}(\alpha) u(t),$$

and hence, assuming available a batch of data  $z_*^t$ , the controller tuning can be therefore obtained through the minimization, with respect to  $\alpha$ , of the following criterion

$$\Lambda^{1/2}(\alpha, t_*) := \frac{\| (z - z_\alpha)^{t_*} \|}{\| z_\alpha^{t_*} \|}, \quad \alpha \in \Theta_\alpha,$$

where  $z_\alpha := [u'_\alpha \ y'_\alpha]'$ ,  $u_\alpha$  and  $y_\alpha$  representing the desired behavior on basis on  $(\mathcal{M}_f/\mathcal{C}_f)$  and the current value of  $\alpha$ . Notice that the functional to minimize is obtained by parametrizing the test functional used in the switching rule of the previous section, the idea being the one to carry out a sort of *Reference Loop Adaptation* task: to adapt  $\mathcal{C}(\alpha)$  in a continuously way in order that  $(\mathcal{P}/\mathcal{C}(\alpha))$  behaves as closely as possible to  $(\mathcal{M}_f/\mathcal{C}_f)$  in response to  $v_\alpha$ . Section B.2 explains in detail the tuning algorithm and it discusses the inheriting implementation issues. The originality of the proposed implementation is that, while tuning algorithm is running, the process continues to be managed by the supervisor. So tuning and switching has to be thought as two disjoint blocks, i.e. operating in a separate way. Once the new controller, named  $\mathcal{C}_{N+1}$ , get available, the corresponding nominal model  $\mathcal{M}_{N+1}$  is obtained as described in Section B.3 and, in particular, Theorem B.3.1 provides the conditions whereby the properties of switching scheme continue to hold in case the new reference loop  $(\mathcal{M}_{N+1}/\mathcal{C}_{N+1})$  be inserted in the switching algorithm. So,  $\mathcal{C}_{N+1}$  is added to the pre-existing controller family and the related  $\Pi_{N+1}$  to the family  $\Pi(t)$ . In the practice, to fairly compare  $\Pi_{N+1}$  with all the other  $\Pi_i$ 's, the switching scheme is simply modified by resetting all candidate test functionals at time  $t_+ > t_*$ , i.e. for any  $i = 1, \dots, N + 1$

$$\begin{aligned} \Pi_i(t) &:= \max_{t_+ \leq k \leq t} \Lambda_i(k) \\ \Lambda_i^{1/2}(t) &:= \frac{\| \tilde{z}_i|_{t_+}^t \|}{\| (z - \tilde{z}_i)|_{t_+}^t \|}, \quad t \in \mathbb{Z}_{t_+}, \end{aligned}$$

where  $\mathbb{Z}_{t_+} := \{t_+, t_+ + 1, \dots\}$  and,  $x|_{t_1}^{t_2} := \{x(t_1), \dots, x(t_2)\}$ ,  $t_1 < t_2$ . Section B.4 concludes the discussion by enumerating the current open problems.

The idea of combining switching and tuning schemes for adaptive control is not new in the literature, see for example [NB97, NX00]. However, different from [NB97, NX00], the

control design procedure is here formulated as a parameter optimization problem in which the optimization is carried directly out the controller parameters, with no intermediate process model identification effort, as in a typical data-driven approach [HGGL98]. Different from [HGGL98], the proposed procedure needs of a minimum interaction with the process, the data set being collected only one time by any controller stabilizing the process. The latter is in general a positive characteristics and, most of all for an adaptive procedure to be combined with a switching scheme. The tuning procedure alone has been applied also to Adaptive Optics problems, as the tuning of Adaptive Secondary Mirrors for Ground-based Large Telescopes – the interest reader can refer to [ABB<sup>+</sup>11, ABM<sup>+</sup>12] for more details on control problems related to Adaptive Optics.

## 1.2 Transfer of the Control Action

Switching control schemes deal with changing operating dynamic mode of the inner loop, caused by a substitution of the control law due to the instantaneous switching between two different controllers. When a switching occurs, the difference between the outputs of the active controller at the time of switching and the off-line controller to be switched on can cause dramatic transients in the dynamics of the inner loop, such phenomenon being called “bump”. The noticeable manifestation of the bump phenomenon is a jump in the process input, and most importantly a significant deterioration of the actual closed-loop performance with respect to the ideal or expected performance following a controller switching. Numerous approaches, known as bumpless transfer techniques, have been proposed in the last years to reduce the bumps after switching [AW96, GA96, TW00, ZT02, ZT05, CS06]. However, the concept of bumpless transfer has never been precisely formalized [ZT02] and it is sometimes misunderstood, as noted in [PVH96]. A common statement which conveys the idea of bumpless transfer is that of switching smoothly as possible from one controller to another where the notion of smoothness is understood in the most cases related to the continuity property (in the mathematical sense) of the process inputs at the switching instants, that is, input signals which does not experience a jump or discontinuity in time when switching between controllers [AW96]. Such a definition makes sense only for continuous-time systems while in a discrete time setting the acceptance of bumpless transfer can be the one to minimize the jump at the process input in some way as defined in [GA96, TW00]. In any case, guaranteeing continuity in time or a small jump at the switching instants does

not preclude the inner loop from exhibiting very poor transients with the new on line controller. However, in some case the primary goal of controller switching can be to promptly recover an adequate input / output process behavior, not to assure smooth control transitions. Indeed, ASC schemes usually manage processes concerned with the case where the their dynamics can vary and produce abrupt and significant performance degradations of the feedback loop, indeed suddenly unstable closed-loops. So, switching between controllers aims at realizing fast transitions which maintain the performance of closed-loop systems. In such cases hence jumps or abrupt changes in the inputs of the process are actually inherent to such control strategies. However, the underlying control objective constraints should not be violated by the transients induced by such instantaneous events. Therefore, it is appropriate to consider control switching as bumpless when the follow-up transients are reduced or possibly eliminated from the closed-loop system behavior albeit the occurrence of jumps in process inputs and the performance still remains good after switching. This notion of bumpless transfer has been termed conditioned transfer in [P VH96]. It is worth noticing that this notion applies indifferently to continuous time or discrete time systems and conveys the idea that switching should take place without perturbing the closed-loop system to depart from its desired performance.

According to the above motivations, Part II deals with a conditioned transfer approach which has been thought to be suitably used in model-based ASC schemes, along with both set-point regulation and tracking problems [BMMT]. The block dedicated to the control transfer is the *Multicontroller*. In Figure 1.2, the multicontroller is represented as the parallel connection of  $N$  controllers, where  $N - 1$  controllers are off-line and only is active, all being alimented by the error signals  $(r - y)$ , as a typical “multisystem” implementation [AW97]. Although such an architecture be the most intuitive, it has evident drawbacks: i) the states of off-line controllers are unpredictably preconditioned before switching ii) so that, unstable controller can have outputs diverging before being active; iii) implementation load increases with the number of controllers and, iv) bumpless transfer solutions, suited for such an architecture, need to use additional circuitry [TW00, ZT05, AW97]. Let  $\{F_i, G_i, H_i, K_i\}$  be a state-space realization of the  $i$ -th controller  $\mathcal{C}_i$ ,  $i = 1, 2, \dots, N$ . In Chapter 4, an alternative multicontroller realization is adopted as the following

$$\left. \begin{aligned} q(t+1) &= F_{\sigma(t)} q(t) + G_{\sigma(t)} (r(t) - y(t)) \\ u(t) &= H_{\sigma(t)} q(t) + K_{\sigma(t)} (r(t) - y(t)) \end{aligned} \right\}$$



which has the peculiarity to have an unique vector  $q(t)$ , the switching reducing to change the gain matrices according to the switching sequence  $\sigma(t)$ , dictated by the supervisor. This “hybrid linear” architecture allows for sidestepping the limits of multisystem one and, it is commonly used for supervisory control of sampled-data systems [BBMT10, BMST10, CHP04, ZMF00]. Indeed, though not reflecting optimal-oriented features, it is such to: i) allow the use of unstable controllers and ii) require a low computational load, the computational cost being invariant to the number of candidate controllers.

The main contribution of Chapter 4 consists in proposing a method such to minimize the transient effects due to switching and to recover as soon as possible the desired behavior, without increasing the computational cost needed to implement a hybrid linear system. The idea of the method stems from the fact that transient after switching is due to the states of the inner loop at the time of switching. In this respect, the exosystem generating the reference signals and the processor have states which can not be manipulated however, the one of the multicontroller can be arbitrarily set at each time. So, one can condition the state  $q$  of the multicontroller at the time of switching in order to recover as soon as possible some pre-specified desired behavior. In Section 4.3, the desired behavior is specified to be the steady state dynamics of the closed loop  $(\mathcal{P}/\mathcal{C}_{\sigma(t_s)})$ , where  $\mathcal{C}_{\sigma(t_s)}$  is the controller which is switched on at the switching time  $t_s$ . Accordingly, the multicontroller state is reinitialized so as to minimize the discrepancy between actual and steady-state closed-loop behaviors, the sense of the minimization being specified in Section 4.3. The reinitialization consists in a linear map as in classical initial value compensation / controller state resetting schemes [Joh00, HIKH09, YSTH96, HM98, PHGne] and depends *affinely* by a pre-computed set of constant gains on the same closed-loop data as the ones in input to the supervisor. In particular, Section 4.3 describes how to obtain such a set of gains by solving *off-line* performance-oriented control problems suitably defined in case the process be supposed to be coincident with one of the available nominal models. Section 4.4 proposes an innovative procedure to suitably “robustify” the solution of Section 4.3 so as to still provide explicit, though suboptimal, solutions in case the process uncertainty be a continuum (and so, not completely representable by a finite model distribution) and only a finite number feedback-gain matrices is allowed such to allow the designer to trade off performance vs. memory savings and/or computational complexity.

## Chapter 2

# Problem Framework: Square Systems

This chapter aims at framing the control problem and providing the basic assumptions which are considered in the body of the thesis.

We tackle the problem of guaranteeing stability / performance of uncertain multi-variable processes, where the uncertainty is “somewhat” structured. The process is denoted by a map  $\mathcal{P} : \mathbb{R}^p \mapsto \mathbb{R}^p$  with a structure depending on a finite number of parameters, each one taking value in some set. According to that, let  $\theta$  indicate the vector of parameters and  $\Theta$  the parameters uncertainty set, namely  $\theta \in \Theta \subseteq \mathbb{R}^{n_\theta}$ , with  $n_\theta$  number of parameters. Then, it is possible to define the set  $\mathcal{P}$  containing all possible configurations / modes of the process as follows

$$\mathcal{P} := \{\mathcal{P}(\theta), \theta \in \Theta\}, \quad (2.1)$$

where each element  $\mathcal{P}(\theta)$  represents a particular configuration of the process.

Hereafter, we deal with discrete-time, strictly causal, square (with dimension  $p \geq 1$ ), linear and time invariant (LTI) dynamic systems and will assume that matrix fraction descriptions (MFDs, for short) of the process such as the following

$$\mathcal{P}(\theta) : A^{-1}(\theta, d) B(\theta, d) = N(\theta, d) D^{-1}(\theta, d), \quad (2.2)$$

are available, where  $d$  stands for the unit backward shift operator and

$$\begin{aligned} A(\theta, d) &= I_p + \mathcal{A}_1(\theta)d + \cdots + \mathcal{A}_{n_a}(\theta)d^{n_a}, \\ B(\theta, d) &= \mathcal{B}_1(\theta)d + \cdots + \mathcal{B}_{n_b}(\theta)d^{n_b}, \end{aligned}$$

are polynomial matrices of dimensions  $p \times p$  with strictly Schur greatest common left divisor (g.c.l.d.). Similar definitions apply also to the right MFD  $N(\theta, d) D^{-1}(\theta, d)$ . Note that no constraint needs to be specified about the way the vector  $\theta$  affects the coefficients of polynomials  $A(\theta, d)$  and  $B(\theta, d)$  (and accordingly,  $N(\theta, d)$  and  $D(\theta, d)$ ).

**Remark 2.0.1** The reason for considering a discrete-time setting is that our interest is mainly directed to sampled-data processes to be managed by digital control systems. The polynomial formulation is, moreover, motivated by the ultimate goal to provide a control architecture which exploits the only information regarding to the input-output process records, the state of the process being unknown / not accessible in the most of the practical cases.

Based on the uncertainty set  $\Theta$ , a family of  $N$  controllers

$$\mathcal{C} = \{\mathcal{C}_i, i \in \overleftarrow{N}\} \quad (2.3)$$

is supposed to be a-priori designed. Namely, each process configuration in the set  $\mathcal{P}$  should be satisfactorily controlled by at least one of the controllers  $\mathcal{C}_i$ , so as that  $\mathcal{C}$  turns out to provide some sort of *covering property* [ABD<sup>+</sup>01]. More specifically, the attention is focused on one-degree-of-freedom LTI controllers, each one characterized by MFDs as follows

$$\mathcal{C}_i : R_i^{-1}(d) S_i(d) = Y_i(d) X_i^{-1}(d), \quad (2.4)$$

where

$$\begin{aligned} R_i(d) &= I_m + \mathcal{R}_{i1}d + \cdots + \mathcal{R}_{i n_r} d^{n_r}, \\ S_i(d) &= \mathcal{S}_{i0} + \mathcal{S}_{i1}d + \cdots + \mathcal{S}_{i n_s} d^{n_s}, \end{aligned}$$

are polynomial matrices of dimensions  $p \times p$  with strictly Schur g.c.l.d.. As beforehand, a similar definition applies to the right MFDs  $Y_i(d) X_i^{-1}(d)$ .

Before proceeding, the loop which can be obtained by the feedback connection between the process  $\mathcal{P}(\theta)$  and the pre-designed controller  $\mathcal{C}_i$  will be indicated as  $(\mathcal{P}(\theta)/\mathcal{C}_i)$  and referred to as the  $i$ -th *potential loop* with respect to the configuration  $\mathcal{P}(\theta)$ . According to that, the basic requirement of the control problem can be stated as follows.

Chapter 2. Problem Framework: Square Systems

- a1.** For every process configuration  $\mathcal{P}(\theta) \in \mathcal{P}$ , there is at least one controller  $\mathcal{C}_i \in \mathcal{C}$  such to guarantee internal stability of the feedback loop  $(\mathcal{P}(\theta)/\mathcal{C}_i)$ .

Assumption **a1** is sufficient to have well-posedness of the control problem, the process being always stabilizable by at least one controller and also, it allows to determine the minimum number of controllers to be used relatively to the process uncertainty. Hereafter, we will name assumption **a1** as *feasibility condition*.

The second assumption, which will turn out to be essential to carry on this dissertation, is the following.

- a2.** Each controller  $\mathcal{C}_i, i \in \overleftarrow{N}$ , is designed with respect to a process model  $\mathcal{M}_i$ .

Assumption **a2** is reasonable from a practical viewpoint, the controller  $\mathcal{C}_i$  being pre-designed, in most of the cases, based on a model representing a particular dynamic mode of the process. Thus, let us assume available a family

$$\mathcal{M} := \{\mathcal{M}_i, i \in \overleftarrow{N}\} \quad (2.5)$$

of  $N$  discrete-time strictly causal LTI dynamic systems with MFDs

$$\mathcal{M}_i : \quad A_i^{-1}(d) B_i(d) = N_i(d) D_i^{-1}(d), \quad (2.6)$$

where

$$\begin{aligned} A_i(d) &= I_p + \mathcal{A}_{i1}d + \cdots + \mathcal{A}_{in_a}d^{n_a}, \\ B_i(d) &= \mathcal{B}_{i1}d + \cdots + \mathcal{B}_{in_b}d^{n_b}, \end{aligned}$$

are polynomial matrices of dimensions  $p \times p$  with strictly Schur g.c.l.d.. Similar definitions apply to the right MFDs  $N_i(d) D_i^{-1}(d)$ . The family  $\mathcal{M}$  is hence taken as a representative set of all possible process configurations and form, along with  $\mathcal{C}$ , a finite family

$$\mathcal{F} := \{(\mathcal{M}_i/\mathcal{C}_i), i \in \overleftarrow{N}\} \quad (2.7)$$

of internally stable feedback loops, each one designed to fulfil desired prescriptions.

In (2.7) and hereafter,  $(\mathcal{M}_i/\mathcal{C}_i)$  denotes the  $i$ -th *reference-loop* or *nominal-loop*, which consists of the nominal model  $\mathcal{M}_i$  with the corresponding feedback controller  $\mathcal{C}_i$ .

**PART I**  
**Controller Selection Strategy**

## Chapter 3

# Model-based Switching Control for Uncertain Square Systems

In many control systems, such as industrial plants, aircrafts, and communication networks, a large number of actuators and/or sensors are employed in order to achieve desired control tasks. In these control applications, the inputs and outputs cannot be usually grouped into pairs, and treated as if they were separate single-input single-output (SISO) sub-systems, because the interactions between a generic input and any given output can be non-negligible. Consequently, one has to tackle the control design as a genuine multiple-input multi-output (MIMO) problem. The situation is even more complicated whenever the multivariable system to be controlled is poorly known. One of the approaches for controlling uncertain plants is the introduction of feedback adaptation. The extension of adaptive control algorithms developed for SISO systems to a MIMO setting is non trivial. Some MIMO adaptive control algorithms based on the model reference approach and the pole placement approach can be found in [SB89, Tao03]. In recent years, adaptive switching control (ASC) has emerged as an alternative to conventional continuous adaptation, providing an attractive framework for combining tools from adaptive and robust control [MMG92, HLM03b, FAP06, SWPS07, BBMT10]. ASC usually embeds a finite family of precomputed candidate controllers  $\{\mathcal{C}_1, \mathcal{C}_2, \dots, \mathcal{C}_N\}$  and a *supervisor*  $\mathcal{S}$  which selects at any time the controller to be switched-on in feedback with the process: the selection being based on the input/output process records [Mor95]. Although the ASC literature

is quite vast, most of the works deal with the SISO case with notable exceptions being [WG94, CN94, SP97, CD99].

Present chapter addresses the problem of controlling an uncertain square system by means of ASC schemes [BBM<sup>+</sup>12, BBM<sup>+</sup>11a], see Figure 3.1 for a typical scheme. In particular, we focus on a scheme which combines Multi-Model architectures with the Unfalsified control, proposed in [BBMT10, BBMT11] for SISO systems. Such scheme exploits a supervisory unit which performs in real-time both the *scheduling task* (when to switch) and the *routing task* (which controller to select), by monitoring test functionals, pairwise associated with the given candidate controllers, as indicators of controller suitability. Each test functional provides a measure of percentage discrepancy between the *potential loop*, made up by the uncertain process in feedback with the candidate controller, and a *reference loop* related to the same candidate controller. In this way, the selection of the controller bases on identifying which dynamics, among those associated to the reference loops, is the best one to be reproduced by the process. Section 3.2 explains, more in detail, this selection idea with particular attention to the square systems. In general, the adopted test functional can be obtained by exploiting the concept of a *virtual reference*. However, while in the SISO / square systems, this tool does not pose particular questions, the situation becomes more intricate for the non-square systems since, in this case, such virtual references need not exist. Appendix A is devoted to the analysis of the latter case and provides a constructive proof that, irrespective of the existence of such virtual references, the proposed approach still maintains its intuitive interpretation of discrepancy. The most appealing feature of this ASC scheme consists in the ability to make inference of the stability properties of the resulting switched system, as depicted in Figure 3.1. Once a stable behavior for the switched system is guaranteed, selection rule follows performance requirements based on the family of reference loops. According to that, Sections 3.3 and 3.4 carry out an analysis of the main characteristics and results regarding to the use of such test functionals along with the hysteresis-based switching rule, as defined in Section 3.1. Eventually, Section 3.5 accounts for implementation aspects.

Let  $\mathbb{S}$  denote the linear space of all the real-valued sequences on  $\mathbb{Z}_+ := \{0, 1, \dots\}$ . Given a vector-valued real sequence  $x \in \mathbb{S}$  of dimension  $n$ ,  $x^t$  denotes its time truncation up to time  $t$ , *i.e.*,  $x^t := \{x(0), x(1), \dots, x(t)\}$ , with  $x(k) \in \mathbb{R}^n$ . Hereafter, we consider the

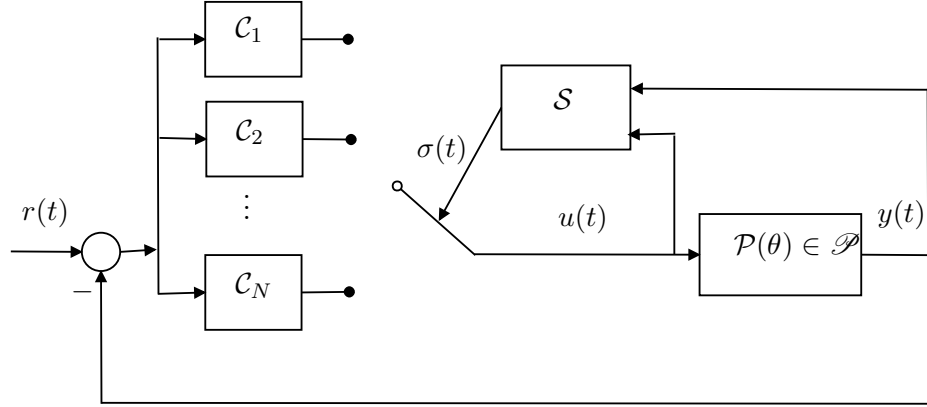


**Figure 3.1:** Typical ASC arrangement.

space  $l_2(\mathbb{Z}_+)$  of all vector-valued real sequences with bounded  $l_2$ -norm defined as

$$\|x^t\|^2 := \sum_{k=0}^t |x(k)|^2, \quad (3.1)$$

where  $|\cdot|$  denote the Euclidean norm. Namely, the space  $l_2(\mathbb{Z}_+)$  denotes the linear space of the sequences belonging to  $\mathbb{S}$  with bounded energy. Then, the following notion of input-output  $l_2$ -stability is adopted in the reminder of the chapter.

**Definition 3.0.1** A causal system  $\mathcal{H}$  with input  $w = \{w_i, i \in \underline{m}\}$ ,  $\underline{m} := \{1, 2, \dots, m\}$  and output  $v = \{v_j, j \in \underline{p}\}$ ,  $\underline{p} := \{1, 2, \dots, p\}$  is said to be input-output  $l_2$ -stable if, for every input  $w \in \mathbb{S}$ , there exist finite positive reals  $c_i$ ,  $i = 1, 2$ , such that

$$\|v^t\| \leq c_1 + c_2 \|w^t\|, \quad \forall t \in \mathbb{Z}_+, \quad (3.2)$$

where  $v$  denotes the system output response to the input  $w$ .

The constant  $c_1$  allows for consideration of systems with non-zero initial state. It should be emphasized that stability of the system  $\mathcal{H}$  requires that (3.2) holds true, possibly with different constants  $c_1$ ,  $c_2$ , for any possible input. Before proceeding, some comments are in order. For clarity of exposition, in the sequel, the analysis will be carried out assuming zero process initial conditions, that means

$$y(k) = u(k) = 0, \quad k = -1, -2, \dots, \quad (3.3)$$



and absence of noises/disturbances. Nonetheless, the results to be presented can be readily extended to the general case along the same lines as those of [BBMT10, BMST10]. In accordance with the mentioned restrictions, next definition is introduced in order to avoid possible ambiguities.

**Notation.** Given an LTI dynamic system with transfer matrix  $F(d)$ , and left MFD,  $F(d) = G^{-1}(d)H(d)$ , with input  $u$  and output  $y$ , by the notation  $y(t) = F(d)u(t)$  we mean that the sequence  $y(t)$ ,  $t \in \mathbb{Z}_+$ , is computed via the following difference equation ( $\det G_0 \neq 0$ )

$$\sum_{k=0}^{n_G} G_k y(t-k) = \sum_{k=0}^{n_H} H_k u(t-k), \quad y(k) = u(k) = 0, \quad k = -1, -2, \dots, \quad (3.4)$$

where  $G(d) = \sum_{k=0}^{n_G} G_k d^k$  and  $H(d) = \sum_{k=0}^{n_H} H_k d^k$ , with  $d$  the unit backward shift operator.

### 3.1 Supervisory Control System and Switching Logic

By referring to Figure 3.1, let the *switched* system be represented as follows

$$\left. \begin{aligned} y(t) &= \mathcal{P}(\theta, u)(t) \\ u(t) &= \mathcal{C}_{\sigma(t)}(r - y)(t) \end{aligned} \right\} \quad (3.5)$$

where  $t \in \mathbb{Z}_+$ ,  $\mathcal{P} : \Theta \times \mathbb{R}^p \mapsto \mathbb{R}^p$ ,  $p \geq 1$ , denotes the map describing the input-output behavior of the process as follows

$$A(\theta, d) y(t) = B(\theta, d) u(t) \quad (3.6)$$

with input  $u(t) \in \mathbb{R}^p$  and output  $y(t) \in \mathbb{R}^p$ , while  $r(t) \in \mathbb{R}^p$  represents the reference to be tracked by the process output. Finally, the map  $\sigma : \mathbb{Z}_+ \mapsto \overleftarrow{N}$ ,  $\overleftarrow{N} := \{1, 2, \dots, N\}$ , refers to the controller switching sequence: The subscript  $\sigma(t)$  identifying, among all  $N$  available candidate controllers, the one connected in feedback to the process at time  $t$ , thus defining the configuration of the switching controller  $\mathcal{C}_{(\cdot)}$ . Hereafter, the linear time-varying feedback system (3.5) will be denoted by  $(\mathcal{P}(\theta)/\mathcal{C}_{\sigma(\cdot)})$ .

The unit generating the sequence  $\sigma^t$  is the so-called supervisor  $\mathcal{S}$ . It handles the input-output records to the process up the current time  $t$  and selects which controller to connect in feedback to the process at the time  $t$ . Accordingly, the switching controller  $\mathcal{C}_{\sigma(t)}$  turns out to coincide with one element  $\mathcal{C}_i$  from the finite family  $\mathcal{C}$  of pre-designed controllers.

In order to decide which candidate controller has to be placed in feedback with process, the supervisor embodies a family

$$\Pi := \{\Pi_i, i \in \overleftarrow{N}\} \quad (3.7)$$

of test functionals such that, in broad terms,  $\Pi_i(t)$  quantifies the suitability of the  $i$ -th candidate controller  $\mathcal{C}_i$  to be placed in feedback with the process  $\mathcal{P}(\theta)$ , given the data up to time  $t$ . In particular, we will make use of the well-known *hysteresis switching logic* (HSL) which computes at each step the least index  $i_*(t)$  in  $\overleftarrow{N}$  such that  $\Pi_{i_*(t)}(t) \leq \Pi_i(t), \forall i \in \overleftarrow{N}$ . Then, the switching sequence  $\sigma$  is given by <sup>1</sup>

$$\left. \begin{aligned} \sigma(t+1) &= l(\sigma(t), \Pi(t)), & \sigma(0) &= i_0 \in \overleftarrow{N} \\ l(i, \Pi(t)) &= \begin{cases} i, & \text{if } \Pi_i(t) < \Pi_{i_*(t)}(t) + h \\ i_*(t), & \text{otherwise} \end{cases} \end{aligned} \right\} \quad (3.8)$$

where the constant  $h > 0$  determines the hysteresis value.

Next lemma establishes the limiting behavior of the switched system  $(\mathcal{P}(\theta)/\mathcal{C}_{\sigma(\cdot)})$  subject to (3.8), provided that the family of cost indices  $\Pi$  be suitably chosen. Let  $\Sigma$  denote the class of all possible switching sequences  $\sigma^t$  giving rise to (3.5). Consider the following assumptions.

**hsl<sub>1</sub>**. For each  $\sigma^t \in \Sigma$  and  $i \in \overleftarrow{N}$ ,  $\Pi_i(t)$  admits a limit (even infinite) as  $t \rightarrow \infty$ ;

**hsl<sub>2</sub>**. For each  $\sigma^t \in \Sigma$ , there exist integers  $\mu \in \overleftarrow{N}$  such that  $\Pi_\mu(\cdot)$  is bounded

**Lemma 3.1.1 HSL Lemma** [MMG92]. Let  $\sigma^t$  the switching sequence resulting from (3.5) with (3.8). Then, for any initial condition and reference  $r$ , if **hsl<sub>1</sub>** and **hsl<sub>2</sub>** hold, there is a finite time  $t_f \in \mathbb{Z}_+$ , after which no more switching occurs. Moreover,  $\Pi_{\sigma(t_f)}(\cdot)$  is bounded.

## 3.2 Test Functionals-based selection

In the *Unfalsified Control*, proposed for the first time in [ST97], the idea consists in cleverly design the test functionals family so as to detect any instability trends exhibited

---

<sup>1</sup>Alternative to (3.8), a multiplicative HSL, where  $l(i, \Pi(t)) = i$  if  $(1+h)\Pi_i(t) < \Pi_{i_*(t)}(t)$  - the so called *scale-independent* HSL [ABD<sup>+</sup>01] - can be considered.

by the switched system (3.5). In particular, the key property to be required to the family  $\Pi$  is known with the name of *cost detectability property* [SWPS07].

**Definition 3.2.1** Given the family  $\Pi$ , as defined in (3.7), and the controller set  $\mathcal{C}$  in (2.3), the pair  $(\Pi/\mathcal{C})$  is said to be  *$l_2$ -cost detectable* if for every sequence  $\mathcal{C}_\sigma^t \in \mathcal{C}$  with finitely many switching times and final switched-on controller  $\mathcal{C}_f \in \mathcal{C}$ , the following statements are equivalent: 1)  $\Pi_f(t)$  keeps bounded as  $t \rightarrow \infty$ ; 2) Input-output  $l_2$  stability of the system  $(\mathcal{P}(\theta)/\mathcal{C}_{\sigma(t)})$  mapping  $r$  into  $z = (u, y)$  is *unfalsified* by the sequence  $(r, z)^t$ .

The concept of unfalsified stability of a system stems from the model-free / data-driven paradigm which aims at adjusting the parameters of the switching controller  $\mathcal{C}_{\sigma(\cdot)}$  from time to time without a-priori information about dynamics characteristics of the process and, by only using a single infinite-length experiment. Notice also that, safe operations with  $\Pi$  need no hypothesis neither on the structure of the uncertainty set  $\Theta$  nor on the (linear / non-linear) nature of the process. In broad terms, stability of the system  $(\mathcal{P}(\theta)/\mathcal{C}_{\sigma(\cdot)})$  is *unfalsified* by the (recorded) sequence  $(r, z)^t$  if there exist finite nonnegative reals  $a_1$  and  $a_2$  such to guarantee the stability requirement so as specified in Definition 3.0.1, *i.e.*

$$\|z^t\| \leq a_1 + a_2 \|r^t\|, \quad \forall t \in \mathbb{Z}_+. \quad (3.9)$$

Otherwise, the stability of the system is said to be falsified by  $(r, z)^t$ .

Notice that cost-detectability property enables test functionals to be used in the HSL. The test functionals proposed in [SWPS07, SS08] allow to select in a finite time a final controller yielding, in an  $l_2$ -sense, a finite affine gain from the reference  $r$  to the process data  $z$ , under the minimal requirement consisting in the feasibility of the control problem (see Assumption **a1** in Chapter 2). However, these functionals can yield a critical behavior for the switched system as they need not provide protection against the temporary insertion in the loop of destabilizing controllers. Indeed, significant initial transients and temporary trends to divergence are typically experienced before the final controller be switched-on.

The basic idea of the Multi-Model Unfalsified ASC scheme, proposed for the first time in [BBMT10], stems from the possibility to combine the Unfalsified philosophy with *Multiple-Models* architectures, studied in [ABD<sup>+</sup>01, HLM03a, Mor97], in order to overcome the limits of classical unfalsified schemes by exploiting the advantages of the use of multiple models, based on Assumption **a2**.

In the Multi-Model ASC schemes a dynamical nominal model is associated with every candidate controller and the supervisor compare norms of sequences of estimation errors based on the various nominal models. According to that, the controller associated to the nominal model yielding the prediction error norm of minimum magnitude is believed to be the most suitable one. Such functionals do not exhibit the cost detectability property and stability properties of the switched system is typically only guaranteed if the process is tightly approximated by at least one nominal model, as analysed in [HLM03a]. On the contrary, learning transients can be typically made small at the cost of very dense nominal model distribution.

Eventually, the smart intuition which has given rise to the ASC scheme in [BBMT10] was the possibility to use multiple models into the unfalsified approach and so, to enjoy the positive features of both approaches. Indeed, it has been experienced, see [BBMT10, BBMT11, BBM<sup>+</sup>12], that the time duration of learning transients decreases and, also stability is ensured if, for any element in the process uncertainty set  $\Theta$ , there is at least one stabilizing candidate controller, irrespective of the models distribution density. Contrarily to Multi-Model schemes, stability robustness against un-modelled dynamics in the large is hence automatically guaranteed.

Next section reviews the basic idea of the Multi-Models Unfalsified ASC architecture with particular attention to the case of multivariable square systems. The case of non-square systems is discussed in Appendix A.

### 3.2.1 Reference-loop Identification in case of Square Systems

Given a family  $\mathcal{F}$  of candidate reference loops, see (2.7), for each process configuration a desired behavior is known, which would be opportune to reproduce by the switching rule, once stability is guaranteed. For this reason, test functionals are designed so as to carry out a *reference-loop identification* task. In broad terms, the aim consists in selecting a candidate controller  $\mathcal{C}_\sigma$  in such a way that  $(\mathcal{P}(\theta)/\mathcal{C}_\sigma)$  behaves as close as possible to one of the candidate reference loops in  $\mathcal{F}$ . Accordingly, the overall idea of the Multi-Model Unfalsified approach can be formulated based on satisfying the two following goals.

- 1) *Basic goal.* The loop  $(\mathcal{P}(\theta)/\mathcal{C}_\sigma)$  exhibit a stable behavior in response to the sequence of the reference  $r^t$ .

- 2) *Ideal goal.* At time  $t$ , the controller index  $\sigma(t)$  in (3.8) be updated, based on the test functionals

$$\Pi_i(t) = \max_{k \leq t} \frac{\|[(\mathcal{P}(\theta)/\mathcal{C}_i)r - (\mathcal{M}_i/\mathcal{C}_i)r]^k\|}{\|[(\mathcal{M}_i/\mathcal{C}_i)r]^k\|}, \quad (3.10)$$

where  $(\mathcal{P}(\theta)/\mathcal{C}_i)r$  and  $(\mathcal{M}_i/\mathcal{C}_i)r$  denote the behavioral data produced by the loops  $(\mathcal{P}(\theta)/\mathcal{C}_i)$  and  $(\mathcal{M}_i/\mathcal{C}_i)$ , respectively, in response to the reference  $r$ .

**Remark 3.2.1** The use of the max operator allows to satisfy Assumption **hsl**<sub>1</sub> of HSL Lemma, and, in general, it means that the search for the controller minimizing the discrepancy between actual and nominal behavior is carried out with respect to the *whole* observation interval up to the current time  $t$ .

**Remark 3.2.2** One of the advantages of using percentage criteria is essentially that, in case of large uncertain process dynamic range, it is possible to have a different cost associated to each index  $i \in \overleftarrow{N}$ . Test functionals in normalized form like (3.10) thus help to avoid possible biases associated with the controller selection. More details about this topic can be found in [VS95, MA01].

The test functional (3.10) allows to compare the performance levels achievable by the use of each candidate controller,  $(\mathcal{P}(\theta)/\mathcal{C}_i)$  exhibiting an input-output stable behavior / being not falsified by couple  $(r, z)$  (using the terminology of [SWPS07]) if and only if  $\Pi_i(t)$  stays bounded for  $t \rightarrow \infty$ . Indeed the sequence  $[(\mathcal{M}_i/\mathcal{C}_i)r]^k$  in (3.10) keeps bounded by construction; on the contrary,  $[(\mathcal{P}(\theta)/\mathcal{C}_i)r]^k$  grows unbounded in case the potential loop  $(\mathcal{P}(\theta)/\mathcal{C}_i)$  show an unstable behavior in response to the reference  $r$ . Hence, Assumption **hsl**<sub>2</sub> turns out to be satisfied under the preliminary hypothesis of feasibility of the control problem. Unfortunately, on line computation of (3.10) is impossible without using logics like pre-routing, which in general have to be ruled out because typically cause large and long-lasting learning transients. In fact, on line computation of (3.10) would require to compute the response of  $(\mathcal{P}(\theta)/\mathcal{C}_i)$  to  $r$  for each of the  $N$  candidate controllers, which is not possible unless all controllers are sequentially tested or,  $N$  exact copies of the process  $\mathcal{P}(\theta)$  are available, each one connected with a candidate controller.

The unfalsified approach provides, under certain conditions, a tool for side-stepping the above mentioned problem. At each time and for each candidate controller, one computes

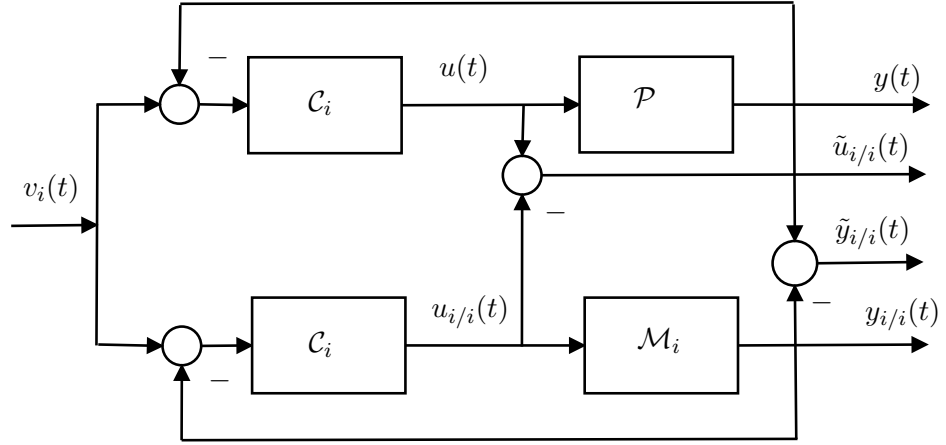


**Figure 3.2:** Detail of a Multi-Model Unfalsified ASC scheme: notice that, with  $\tilde{z}_{i/i} = \begin{bmatrix} \tilde{u}'_{i/i} & \tilde{y}'_{i/i} \end{bmatrix}' := z - z_{i/i}$ .

(if possible) the solution  $v_i(t) \in \mathbb{R}^p$  of the following difference equation

$$S_i(d)v_i(t) = R_i(d)u(t) + S_i(d)y(t). \quad (3.11)$$

In words,  $v_i^t$  equals the  $i$ -th *virtual reference* sequence which would reproduce the recorded input-output sequences, respectively,  $u^t$  and  $y^t$ , should the process  $\mathcal{P}(\theta)$  be fed-back by the candidate controller  $\mathcal{C}_i$ , irrespective of the way  $u^t$  and  $y^t$  are generated. Let

$$z(t) := \begin{bmatrix} u(t) \\ y(t) \end{bmatrix}, \quad (3.12)$$

this means that, being  $(\mathcal{P}(\theta)/\mathcal{C}_{\sigma(\cdot)})$  the linear (time-varying) transformation (3.5) mapping the  $r$  into  $z$ , we have

$$z = (\mathcal{P}(\theta)/\mathcal{C}_{\sigma(\cdot)}) r = (\mathcal{P}(\theta)/\mathcal{C}_i) v_i.$$

In the sequel, the virtual reference concept will be rearranged as follows. For each reference-loop  $(\mathcal{M}_i/\mathcal{C}_i)$ , we define the closed-loop response of  $(\mathcal{M}_i/\mathcal{C}_i)$  to  $v_i$  as

$$\left. \begin{aligned} y_{i/i}(t) &= \mathcal{M}_i(u_{i/i})(t) \\ u_{i/i}(t) &= \mathcal{C}_i(v_i - y_{i/i})(t) \end{aligned} \right\} \quad (3.13)$$

Accordingly, by letting  $z_{i/i} = (\mathcal{M}_i/\mathcal{C}_i)v_i := \begin{bmatrix} u'_{i/i} & y'_{i/i} \end{bmatrix}'$ , the test functionals (3.10) turns out to be modified as follows

$$\Pi_i(t) = \max_{k \leq t} \frac{\|[(\mathcal{P}(\theta)/\mathcal{C}_i)v_i - (\mathcal{M}_i/\mathcal{C}_i)v_i]^k\|}{\|[(\mathcal{M}_i/\mathcal{C}_i)v_i]^k\|}. \quad (3.14)$$

In (3.14), numerical questions arise relating to the computation of sequences  $v_i^t$ 's. The virtual references are always well-defined in case of square systems (see [BBMT10] for the analysis in the particular case of SISO systems) and questions arise only on their numerical computation: the solution of (3.11) is actually “numerically stable” only if the determinant of the polynomial matrix  $S_i(d)$  is strictly Schur. Appendix A shows how handling virtual references in case  $S_i(d)$  is not strictly Schur and also in the more general case of non-square systems, where the virtual reference need not even exist, with the consequence that the original interpretation in terms of discrepancy between potential and nominal loops falls down.

### 3.3 Stability Inference and Performance Requirements

Before comparing the performance levels of the candidate loops  $(\mathcal{P}(\theta)/\mathcal{C}_i)$ 's, it is necessary to be able to make inference on their stability properties. The main feature of the Multi-Model Unfalsified ASC scheme is actually that one to associate the boundedness of the test functional  $\Pi_i(\cdot)$  to the internal stability of the loop  $(\mathcal{P}(\theta)/\mathcal{C}_i)$ . In order to show the validity of the latter sentence, it is convenient to rewrite (3.14) as follow

$$\Pi_i(t) := \max_{k \leq t} \Lambda_i(k), \quad (3.15)$$

$$\Lambda_i^{1/2}(t) := \frac{\|\tilde{z}_{i/i}^t\|}{\|(z - \tilde{z}_{i/i})^t\|}, \quad (3.16)$$

where  $\tilde{z}_{i/i} := z - z_{i/i}$ , as shown in Figure 3.2.

Coprime factor model error representations [GL95], hereafter briefly recalled for the reader's benefit, are a convenient framework to work with. Let the uncertain process  $\mathcal{P}(\theta)$  in (3.5) be represented, as in Figure 3.3, in the coprime factor perturbed form based

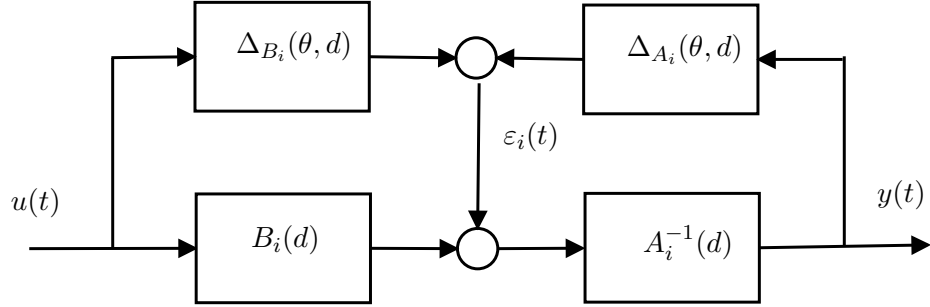


**Figure 3.3:** Coprime model error representation.

on the nominal model  $\mathcal{M}_i$

$$\mathcal{P}(\theta) : \begin{cases} A_i(d) y(t) = B_i(d) u(t) + \varepsilon_i(t) \\ \varepsilon_i(t) = \Delta_{A_i}(\theta, d) y(t) + \Delta_{B_i}(\theta, d) u(t) \end{cases} \quad (3.17)$$

where

$$\Delta_{A_i}(\theta, d) := A_i(d) - A(\theta, d), \quad \Delta_{B_i}(\theta, d) := B(\theta, d) - B_i(d), \quad (3.18)$$

and  $\varepsilon_i(t) \in \mathbb{R}^p$  represents the equation error. Accordingly, let us define

$$\Delta_{\theta/i}(d) := [\Delta_{B_i}(\theta, d) \quad \Delta_{A_i}(\theta, d)], \quad (3.19)$$

and consider the polynomial matrices

$$\Xi_{i/i}(d) := A_i(d)X_i(d) + B_i(d)Y_i(d), \quad (3.20)$$

$$\Xi_{\theta/i}(d) := A(\theta, d)X_i(d) + B(\theta, d)Y_i(d), \quad (3.21)$$

whose determinants equal the characteristic polynomials of the  $i$ -th reference loop and, respectively, the  $i$ -th potential loop. In particular, the first one is strictly Schur by construction for all  $i$ 's  $\in \overleftarrow{N}$ ,  $(\mathcal{M}_i/\mathcal{C}_i)$  being internal stable – see Assumption **a2**; while, the second one turns out to be strictly Schur at least for one index  $i$  in the set  $\overleftarrow{N}$ , as assured through the feasibility condition – see Assumption **a1**.

Next lemma allows us to establish the main features of (3.15)-(3.16) in terms of stability inference / cost detectability property.



**Lemma 3.3.1** Consider the rational matrices

$$Q_{i/i}(d) := \begin{bmatrix} Y_i(d) \\ X_i(d) \end{bmatrix} \Xi_{i/i}^{-1}(d), \quad (3.22)$$

$$Q_{\theta/i}(d) := \begin{bmatrix} Y_i(d) \\ X_i(d) \end{bmatrix} \Xi_{\theta/i}^{-1}(d). \quad (3.23)$$

Then,

$$Q_{\theta/i}(d) - Q_{i/i}(d) = Q_{\theta/i}(d) \Delta_{\theta/i}(d) Q_{i/i}(d). \quad (3.24)$$

*Proof.* See Appendix C. □

From Lemma 3.3.1, one can conclude that

$$\begin{aligned} \tilde{z}_i(t) &= Q_{i/i}(d) \Delta_{\theta/i}(d) z(t) \\ &= Q_{\theta/i}(d) \Delta_{\theta/i}(d) [I - Q_{i/i}(d) \Delta_{\theta/i}(d)] z(t) \\ &= Q_{\theta/i}(d) \Delta_{\theta/i}(d) (z(t) - \tilde{z}_i(t)). \end{aligned} \quad (3.25)$$

and so, under the assumption of zero initial conditions, the following condition

$$\|\tilde{z}_i^t\| \leq \|Q_{\theta/i} \Delta_{\theta/i}\|_{\infty} \|(z - \tilde{z}_i)^t\|, \quad (3.26)$$

holds, where  $\|\cdot\|_{\infty}$  indicates the  $H_{\infty}$ -norm of a linear system. Accordingly, the boundedness of (3.16) depends on the one of  $\|Q_{\theta/i} \Delta_{\theta/i}\|_{\infty}$ , namely on the internal stability of the loop  $(\mathcal{P}(\theta)/\mathcal{C}_i)$ . In fact, for the switched-on controller, say  $\mathcal{C}_i$ , the corresponding test functional in (3.16) can grow unbounded if and only if  $\mathcal{C}_i$  does not stabilize the proces, this property being connected with the cost detectability condition of Definition 3.2.1. In Section 3.4, it will be shown more accurately how, based on (3.26), it is possible to ensure input-output  $l_2$ -stability of the switched system (3.5).

Different from stability robustness, high performance depends on the distribution  $\mathcal{M}$  of models. Some comments are in the following. Given any configuration of the process  $\mathcal{P}(\theta)$ , let us define  $S(\mathcal{P}(\theta)) \subseteq \overleftarrow{N}$  as the set of all indices  $s \in \overleftarrow{N}$  such that the potential loop  $(\mathcal{P}(\theta)/\mathcal{C}_s)$  is internally stable. Obviously, from Assumption **a1**, it follows that  $S(\mathcal{P}(\theta)) \neq \emptyset$  holds for any  $\theta \in \Theta$  and, for that  $\theta$  the finite values

$$\beta_i(\theta) := \|Q_{\theta/i} \Delta_{\theta/i}\|_{\infty} \leq \|Q_{\theta/i}\|_{\infty} \|\Delta_{\theta/i}\|_{\infty}, \quad \forall i \in S(\mathcal{P}(\theta)) \quad (3.27)$$

turn out to quantify the distance between the  $i$ -th potential loop from the related reference loop. Accordingly, smaller

$$\beta(\theta) := \min_{i \in S(\mathcal{P}(\theta))} \beta_i(\theta), \quad (3.28)$$

higher the performance achievable in correspondence of the process configuration  $\mathcal{P}(\theta)$ . Notice that, for each  $i$  belonging to  $S(\mathcal{P}(\theta))$ , “closer” the nominal model  $\mathcal{M}_i$  to  $\mathcal{P}(\theta)$ , smaller the value  $\beta_i(\theta)$ , the latter being depending on the magnitude of coprime perturbations  $\|\Delta_{\theta/i}\|_\infty$ . The closeness of the process configuration to a nominal model can be thought as a guaranty of performance in case, under Assumption **a2**, the reference loops reflect desired behaviors<sup>2</sup>.

### 3.4 Main results

This section provides the main result characterizing the Multi-Model Unfalsified ASC scheme, which consists in assuring stable behavior of the switched system  $(\mathcal{P}(\theta)/\mathcal{C}_{(\cdot)})$  when the supervisory unit  $\mathcal{S}$  exploits the test functional defined as in (3.15)-(3.16). In this respect, (3.25) would be sufficient *per se* to prove the input-output  $l_2$ -stability of the switched system. In addition, conditions on the uncertainty set  $\Theta$  are derived, such to allow a performance-oriented design of the models distribution.

Starting from the last mentioned task, we asserts that whenever the process uncertainty set  $\Theta$  is compact and, also, it is a priori known, then the distribution  $\mathcal{M}$  can be designed dense enough in  $\mathcal{P}$  so as to ensure that, for any  $\theta \in \Theta$ , there exist indices  $i \in \overleftarrow{N}$ , yielding stable loops  $(\mathcal{P}(\theta)/\mathcal{C}_i)$  and such that

$$\beta(\theta) < \beta,$$

where the positive real  $\beta$  is a performance parameter. More specifically, the following result can be stated, whose proof follows along the same lines of the SISO case and can found in [BBMT11].

---

<sup>2</sup>It is well to notice that the two terms of the rightmost member of (3.27) are disjoint with respect to stability / performance requirements. Indeed, the index  $i$  in  $Q_{\theta/i}(d)$  refers only to the controller  $\mathcal{C}_i$  and so, the norm  $\|Q_{\theta/i}\|_\infty$  accounts for the stability of  $(\mathcal{P}(\theta)/\mathcal{C}_i)$ . On the contrary, the index  $i$  in  $\Delta_{\theta/i}(d)$  considers only the model  $\mathcal{M}_i$ ,  $\|\Delta_{\theta/i}\|_\infty$  thus defining a measure of the process/model distance, irrespective of stability property of  $(\mathcal{P}(\theta)/\mathcal{C}_i)$ .

**Proposition 3.4.1** Let  $\Theta$  be a compact set, and the map  $\theta \mapsto \mathcal{P}(\theta)$  continuous on  $\Theta$ . Then, for any positive real  $\beta$ , there always exists a finite model family such that:

$$\max_{\theta \in \Theta} \beta(\theta) := \bar{\beta} < \beta, \quad (3.29)$$

where  $\beta(\theta)$  is defined as in (3.28).

A model distribution for which property (3.29) holds will be denoted by  $\mathcal{M}(\bar{\beta})$ . Now, the main result of this section can be stated.

**Theorem 3.4.1** Consider the switched system (3.5) under zero initial conditions. Let the sequence  $\sigma^t$  be selected in accordance with the HSL (3.8), with test functionals as in (3.15)-(3.16). Then, under the feasibility condition **a1**, for any reference  $r \in \mathbb{S}$ , the switched system is input-output  $l_2$ -stable. Further, under a model distribution  $\mathcal{M}(\bar{\beta})$  the total number of switches  $N_\sigma$  is bounded as follows

$$N_\sigma \leq N \left\lceil \frac{\bar{\beta}^2}{h} \right\rceil, \quad (3.30)$$

where  $\lceil \alpha \rceil$  denotes the smallest integer greater than or equal to  $\alpha \in \mathbb{R}_+$ .

*Proof.* See Appendix C. □

**Remark 3.4.1** It can be shown that Theorem 3.4.1 also extends to the cases of nonzero process initial conditions and/or nonzero disturbances. As for the first issue, see [BBMT10]. In relation to the latter issue, a detailed discussion on how to ensure cost-detectability in noisy environments can be found in [BMST10].

According to the next lemma, one can assert that safe behavior of the switched system (3.5) can be ensured by means of (3.15)-(3.16) even if uncertainty set  $\Theta$  is not a compact and / or the process does not reflect a linear behavior.

**Lemma 3.4.1** Consider the switched system  $(\mathcal{P}(\theta)/\mathcal{C}_i)$ . Then, the family of test functionals  $\Pi(t) := \{\Pi_i(t), i \in \overleftarrow{N}\}$ , with  $\Pi_i(t)$  as in (3.15)-(3.16), along with the controller family  $\mathcal{C}$ , as in (2.3), yields a cost detectable pair  $(\Pi, \mathcal{C})$ , provided that the polynomial matrices  $S_i(d)$ 's,  $i \in \overleftarrow{N}$ , see (2.4), have no roots on the unit circle, i.e.  $\det S_i(d) \neq 0$  if  $d = e^{j\omega}$ ,  $\omega \in [-\pi, \pi]$ .

*Proof.* See Appendix C. □

To sum up, Proposition 3.4.1 and Theorem 3.4.1 show that the Multi-Model Unfalsified ASC scheme accounts for both the issues of performance and stability robustness, respectively. In fact, while stable behavior of  $(\mathcal{P}(\theta)/\mathcal{C}_{\sigma(\cdot)})$  is guaranteed under the only feasibility condition, performance can be achieved by designing the nominal model distribution  $\mathcal{M}$  dense enough in  $\mathcal{P}$ . More specifically, the smaller  $\beta$ , the smaller (for any possible process configuration)  $\beta(\theta)$  and hence, the closer the behavior of the final closed-loop  $(\mathcal{P}(\theta)/\mathcal{C}_f)$  to the behavior of the corresponding reference loop  $(\mathcal{M}_f/\mathcal{C}_f)$ . However, although stability robustness can be obtained by means of a small number of pre-computed controllers, in many cases guaranteeing high performance (which means keeping  $\bar{\beta}$  small) needs of a number of controllers too high to be managed by a moderate memory / computational load. Appendix B deals with this problem and provides some remarks about the possibility to combine an algorithm of fine controller tuning with the proposed ASC scheme.

### 3.4.1 Tracking Properties

Hereafter, we discuss how previous results can be extended so as to ensure asymptotic tracking. Assume that the reference  $r(t) \in \mathbb{R}^p$  be such that

$$\Phi(d)r(t) = 0, \tag{3.31}$$

where  $\Phi(d) := \phi(d) I_p$ , with  $\phi(d)$  is a polynomial with simple roots on the unit circle and  $\phi(0) = 1$ . This amounts to assuming that  $r(t)$  is a bounded sequence.

Consider a left MFD of the process configuration  $\mathcal{P}(\theta)$ , as specified by (2.2). Necessary and sufficient condition for the existence of a linear time-invariant controller ensuring asymptotic tracking is the following [DG75].

- a3.** The polynomial matrices  $B(\theta, d)$  and  $\Phi(d)$  are left coprime, for each  $\theta \in \Theta$ .

Multiplying (3.31) by  $A(\theta, d)$  and (3.6) by  $\Phi(d)$ , and subtracting the resulting equations, we obtain

$$A(\theta, d) \Phi(d) e(t) = B(\theta, d) \eta(t). \tag{3.32}$$

where  $e(t) = r(t) - y(t)$  is the tracking error and  $\eta(t) := \Phi(d)u(t)$ . In such a case, any stabilizing controller  $\mathcal{C}_i$  of the form

$$\Phi(d)u(t) = Y_i(d)X_i^{-1}(d)e(t), \quad (3.33)$$

ensures asymptotic tracking. Such a controller has transfer matrix  $\Phi^{-1}(d)Y_i(d)X_i^{-1}(d)$  and, in agreement with the so-called *Internal Model Principle*, incorporates the model of the reference to be tracked [DG75, FW76, Mos95, WF79].

Using (3.32) and (3.33), the switched system (3.5) can be therefore rewritten as

$$\left. \begin{aligned} e(t) &= \mathcal{P}_n(\theta, \eta)(t) \\ \eta(t) &= \mathcal{C}_{\sigma(t)}(e)(t) \end{aligned} \right\} \quad (3.34)$$

where  $\mathcal{P}_n(\theta)$  denotes the “new” process with input  $\eta$ , output  $e$  and transfer matrix as in (3.32). Essentially, this means that the tracking problem for system (3.5) is transformed into an equivalent zero-regulation problem for (3.34).

By exploiting such an equivalence, a simple approach for ensuring, along with stability, the offset-free tracking property, consists in designing the family  $\mathcal{F}$  of nominal loops  $(\mathcal{M}_i/\mathcal{C}_i)$ ’s so as to satisfy the following conditions.

- a4.** For each candidate model  $\mathcal{M}_i$ , the polynomial matrices  $B_i(d)$  and  $\Phi(d)$  are left co-prime.
- a5.** Each candidate controller  $\mathcal{C}_i$  stabilizes the corresponding model  $\mathcal{M}_i$ , and ensures offset-free tracking in the sense of (3.33).

Under such design conditions, we can modify the test functional (3.16) by replacing  $z$  with  $\zeta := [\eta' e']'$ , and, similarly,  $z_{i/i}$  with  $\zeta_{i/i} := [\eta'_{i/i} (v_i - y_{i/i})']'$ , where  $\eta_{i/i}$  is given by  $\eta_{i/i}(t) = \Phi(d)u_{i/i}(t)$ , while  $v_i$  is obtained by solving  $S_i(d)v_i(t) = R_i(d)e(t) + S_i(d)\eta(t)$ . This leads to

$$\Lambda_i^{1/2}(t) := \frac{\|\tilde{\zeta}_{i/i}^t\|}{\|(\zeta - \tilde{\zeta}_{i/i})^t\|}, \quad (3.35)$$

where  $\tilde{\zeta}_{i/i} := \zeta - \zeta_{i/i}$ . The so-modified test functional now provides a measure of discrepancy between potential and nominal loops with respect to system (3.34), by which we get at once the following.

**Theorem 3.4.2** Consider the switched system (3.5) under zero initial conditions. Let the sequence  $\sigma^t$  be selected in accordance with the HSL (3.8), with test functionals as in (3.15)-(3.35). Let  $r(t)$  satisfy (B.6) and assume that condition **a3** holds. Further assume that  $\mathcal{F}$  has been designed so as to satisfy conditions **a4** and **a5**. Then, under the feasibility condition **a1**, the switched system (3.5) is input-output  $l_2$ -stable and offset-free, i.e.  $e(t) \rightarrow 0$  as  $t \rightarrow \infty$ .

*Proof.* See Appendix C. □

**Remark 3.4.2** Notice that, given any reference  $r(t) \in \mathbb{R}^p$  such that

$$\tilde{\Phi}(d) r(t) = 0, \quad (3.36)$$

where  $\tilde{\Phi}(d)$  is a polynomial matrix with  $\tilde{\Phi}(0) = I_p$ , the use of a polynomial matrix  $\Phi(d)$  as in (3.31) guarantees asymptotic tracking provided that  $\phi(d) = \det \tilde{\Phi}(d)$ . Although conservative, the use of  $\Phi(d)$  in place of  $\tilde{\Phi}(d)$  turns out to be a convenient choice from a controller design viewpoint. To see that, suppose to use  $\tilde{\Phi}(d)$ . Then, one set the condition  $-A(\theta, d) \tilde{\Phi}^{-1}(d) = \bar{\Phi}^{-1}(\theta, d) \bar{A}(\theta, d)$ , with  $\bar{\Phi}(\theta, d)$  and  $\bar{A}(\theta, d)$  left coprime and such that  $\det \bar{\Phi}(\theta, d) = \det \tilde{\Phi}(d)$  and  $\det \bar{A}(\theta, d) = \det A(\theta, d)$ , for each  $\theta \in \Theta$ . Hence, Assumption **a3** becomes the following [DG75, WF79]: The polynomial matrices  $B(\theta, d)$  and  $\bar{\Phi}(\theta, d)$  are externally skew prime for each  $\theta \in \Theta$ , i.e. there exist two polynomial matrices  $\hat{\Phi}(\theta, d)$  and  $\hat{B}(\theta, d)$  of suitable dimensions such that  $\bar{\Phi}(\theta, d) B(\theta, d) = \hat{B}(\theta, d) \hat{\Phi}(\theta, d)$ , with  $\det \hat{\Phi}(\theta, d) = \det \bar{\Phi}(\theta, d)$  and,  $B(\theta, d)$  and  $\hat{\Phi}(\theta, d)$  right coprime for each  $\theta \in \Theta$  (see Corollary 1 in [WF79]). So, multiplying (3.36) by  $\bar{A}(\theta, d)$  and (3.6) by  $\bar{\Phi}(\theta, d)$ , with simple algebra one obtain

$$\bar{A}(\theta, d) \tilde{\Phi}(d) e(t) = \hat{B}(\theta, d) \eta(\theta, t),$$

where  $\eta(\theta, t) := \hat{\Phi}(\theta, d) u(t)$ . Hence, the controller guaranteeing asymptotic tracking depends, in general, on  $\theta$ , its transfer matrix being  $\hat{\Phi}^{-1}(\theta, d) Y_i(d) X_i^{-1}(d)$ , and turns out to be impractical unless  $\hat{\Phi}(\theta, d) = \hat{\Phi}(d)$  for each  $\theta \in \Theta$ .

### 3.5 ASC scheme Implementation Aspects

In this section, we discuss the main implementation aspects related to the computation of (3.16) and (3.35). For simplicity of exposition, consider at time the former. As

it is possible to see, the proposed ASC methodology hinges upon the computation of the sequence  $\tilde{z}_{i/i}$ . In this respect, Appendix C allows us to assert that  $\tilde{z}_{i/i}$  can be obtained via the difference  $z - z_{i/i}$ , where  $z_{i/i}$ 's can be always computed by running reference-loops suitably modified (see Figure A.2) driven by a modified virtual reference, without posing any question related to numerical aspects. Nonetheless, it is convenient to provide an alternative tool for computing  $\tilde{z}_{i/i}$ , consisting in suitably filtering the input-output process records.

**Lemma 3.5.1** Consider the vector valued sequence  $\tilde{z}_{i/i}$  in (3.16). Then, under zero process initial conditions one has that

$$\tilde{z}_{i/i}(t) = \begin{bmatrix} -Y_i(d) \\ X_i(d) \end{bmatrix} \Xi_{i/i}^{-1}(d) \epsilon_i(t) \quad (3.37)$$

exactly holds, where  $\epsilon_i(t) := A_i(d)y(t) - B_i(d)u(t)$  represents the prediction error based on  $\mathcal{M}_i$ .

*Proof.* See Appendix C. □

**Remark 3.5.1** Notice that  $\varepsilon_i(t) = \epsilon_i(t)$ ,  $\forall t \geq 0$ , holds in case of zero initial conditions, see (3.3), since in such a case (3.6) holds  $\forall t \geq 0$ . Non zero initial condition are treated more in detail in [BBMT10].

**Remark 3.5.2** The prefiltering of the prediction error (3.37) was already suggested for SISO systems, see [BBMT10], as an alternative procedure for computing (3.14) in the presence of non-minimum phase controllers, *viz.* in case the computation of the  $v_i$ 's were not numerically stable, so as the one of (3.14). Note also that, Lemma 3.5.1 reinforces the interpretation of (3.16) in terms of identification for control. For similar uses of filtering the prediction error in the framework of identification for control, the reader is referred to [MN95, Gev93].

**Remark 3.5.3** Along the same lines of the proof of Lemma 3.5.1 in Appendix C, it is straightforward to see that  $\zeta_{i/i}$  can be obtained as  $z_{i/i}$  by (3.37) and  $\epsilon_i$  given by  $\epsilon_i(t) = A_i(d)e(t) - B_i(d)\eta(t)$ .

A second main aspect related to the implementation of the ASC scheme of Figure 3.1 concerns how arranging the multicontroller  $\mathcal{C}_{(\cdot)}$ . The way of transferring the control action from a controller to an other one is actually a critical aspect and influences, in the negative, the behavior of the overall switching scheme. Into the control loop, each switching inevitably yields non-linear effects, which entities are usually unpredictable. Supervisor can not prevent such phenomenons, they being due to the time-varying nature of the switched system (3.5). However, it is possible to implement the multicontroller through clever architectures, so as to prevent / reduce such undesirable effects. Part II of this thesis is devoted to the analysis of the control transfer problem.

### 3.6 Concluding Remarks

This chapter has discussed the problem of controlling uncertain square systems by means of an ASC scheme which selects the right controller among a family of pre-designed controllers. Selection is carried out by comparing test functionals suitably chosen to evaluate the suitability of each controller to be connected in feedback with the process. Specifically, the analysis concerns the Multi-Model Unfalsified ASC approach, introduced in [BBMT10] for handling SISO systems. The approach has been extended to generic multivariable systems (the case of non-square systems is considered in Appendix A) and, it is possible to see that, by suitably redefining the test functionals, the same stability and performance features characterizing the SISO systems carry over to the generic multivariable case with no additional assumptions on the process to be controlled. In particular, it is shown that, under the only reasonable requirements to have a stabilizing controller for each process configuration, a stable behavior of the switched system in response to a generic bounded reference signal is guaranteed. In addition, a simple variant of the basic scheme has been proposed which ensures, along with stability, the offset-free tracking with respect to signals originated through LTI exosystems.



## Appendix A

# Reference-loop Identification in case of Non-Square Systems

The main problem when one have to handle non-square systems is that the ideal goal of the reference-loop identification task (see Section 3.2.1) can become meaningless. Indeed, the virtual reference, obtained by solving (3.11), need not even exist and, accordingly, the original interpretation in terms of discrepancy between potential and nominal loops falls down.

As known, in square systems (so as for SISO cases) questions originate only on numerical aspects. However, it is sufficient that the determinant of polynomial matrix  $S_i(d)$  be strictly Schur to get  $v_i$  well-defined. In order to analyse what happen to the virtual reference based on the “geometry” of the system, some results of linear algebra are briefly recalled [ZDG95].

**Lemma A.0.1** Consider the linear equation

$$Gx = L, \tag{A.1}$$

where  $G \in \mathbb{R}^{m \times p}$ , and  $L \in \mathbb{R}^m$  are given matrices. Then, the following statements are equivalent:

- i) there exists a solution  $x \in \mathbb{R}^p$ ;
- ii) the columns of  $L \in \text{Im } G$ .

## Appendix A. Reference-loop Identification in case of Non-Square Systems

Furthermore, the solution, if it exists, is unique if and only if  $G$  has full column rank.

**Lemma A.0.2** Consider the linear equation (A.1), where  $m \leq p$  and  $G$  has full row rank, *i.e.*,  $\text{rank } G = m$ . Then, the solution, if any, can be expressed as

$$x = G^\dagger L + (I_p - G^\dagger G)\gamma, \quad (\text{A.2})$$

where  $\gamma \in \mathbb{R}^p$  while  $G^\dagger := G'(GG')^{-1}$  denotes right pseudo-inverse of  $G$ .

More in detail, the first term  $G^\dagger L$  of (A.2) represents one particular solution of (A.1); in particular, it is the solution of minimum Euclidean norm among all solutions. The second term  $(I_p - G^\dagger G)\gamma$  of (A.2) embodies all solutions of linear equation  $Gx = 0_m$ , *viz.*  $(I_p - G^\dagger G)\gamma \in \text{Ker}(G)$ . When  $m = p$  and  $\text{rank}(G) = m$ , then  $G^\dagger = G^{-1}$  and the (A.1) has only one solution given by  $x = G^{-1}L$ .

Before proceeding, let us assume that the process  $\mathcal{P}(\theta)$  have  $m$  inputs, *i.e.*  $u(t) \in \mathbb{R}^m$ , and  $p$  outputs, *i.e.*  $y(t) \in \mathbb{R}^p$ . Accordingly, polynomial matrices  $S_i(d)$  and  $R_i(d)$  have dimensions  $m \times p$  and  $m \times m$ , respectively. Then, let us rewrite (3.11) as follows

$$\mathcal{S}_{i0}v_i(t) = R_i(d)u(t) + S_i(d)y(t) + [\mathcal{S}_{i0} - S_i(d)]v_i(t) := \xi_i(t). \quad (\text{A.3})$$

Based on Lemmas A.0.1 and A.0.2 and (A.3), the following conclusions can be drawn regarding the existence of the virtual reference with respect to the geometry of the process.

- 1) Case  $m = p$ . If  $\mathcal{S}_{i0}$  has full column rank, the virtual reference

$$v_i(t) = \mathcal{S}_{i0}^{-1}\xi_i(t) \quad (\text{A.4})$$

always exists unique.

- 2) Case  $m < p$ . If  $\mathcal{S}_{i0}$  has full row rank,  $(\mathcal{S}_{i0}\mathcal{S}'_{i0})$  is invertible and all the possible  $v_i$ 's are given by

$$v_i(t) = \mathcal{S}'_{i0}\xi_i(t) + (I_p - \mathcal{S}'_{i0}\mathcal{S}_{i0})\nu(t), \quad (\text{A.5})$$

where  $\nu(t) \in \mathbb{R}^p$  is an arbitrary signal.

- 3) Case  $m > p$ . The virtual reference  $v_i$  need not exist unless  $\xi_i(t) \in \text{Im } \mathcal{S}_{i0}$ .

Appendix A. Reference-loop Identification in case of Non-Square Systems

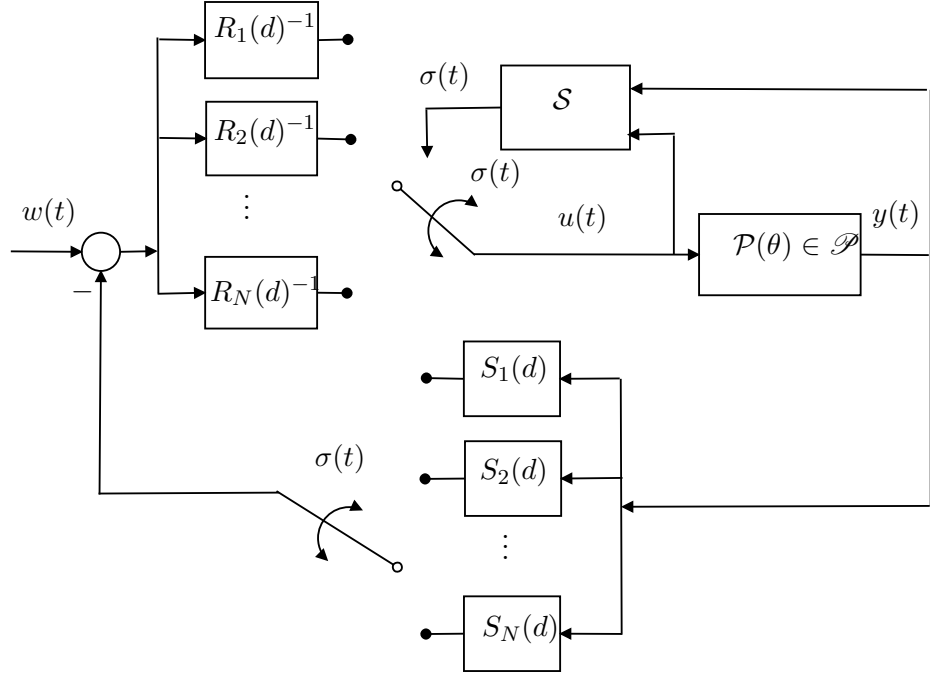


**Figure A.1:** Equivalent representation of the ASC scheme of Figure 3.1 based on the observer-form implementation of the switching controller  $\mathcal{C}_{\sigma(\cdot)}$ .

Note that in the cases 1 and 2, equation (3.11) is numerically stable, provided that the polynomial matrix  $S_i(d)$  be such that  $\det(S_i(d))$  and  $\det(S_i(d)' S_i(d))$  are strictly Schur polynomials, respectively. However, it is the case 3 which motivates the adoption of a virtual reference different from the one used in (3.11). To this end, let

$$w(t) := S_{\sigma(t)}(d)r(t) \quad (\text{A.6})$$

be a modified real reference. In accordance to (A.6), an representation of the switched system (3.5), equivalent to that one of Figure 3.1, is depicted in Figure A.1, where the polynomial matrices  $R_i(d)$  and  $S_i(d)$  are now in the forward path and, respectively, in the backward path of control loop, known as “observer-form implementation”<sup>1</sup>. Thereby, we

<sup>1</sup>In the unfalsified control, observer-form implementation of the controllers has been proposed for the first time in [DAL07] in order to remove the restrictive assumption on the controllers family, which requires all the candidate controllers be minimum-phase and biproper. Let us assume the controller  $\mathcal{C}_i$  be switched-on,

Appendix A. Reference-loop Identification in case of Non-Square Systems

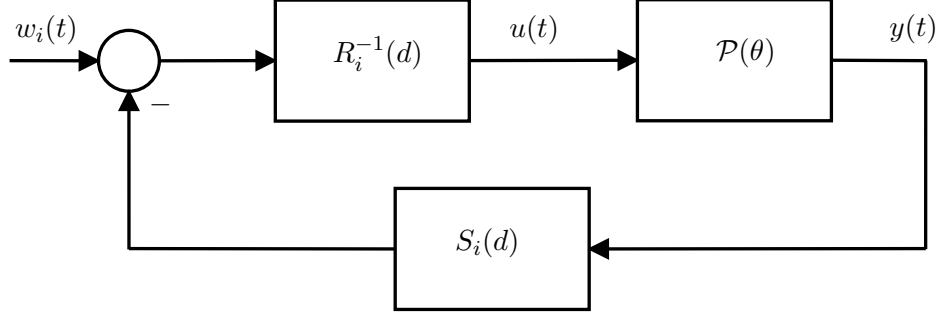


**Figure A.2:** New  $i$ -th potential control loop, referred to as  $(\widehat{\mathcal{P}(\theta)}/\widehat{\mathcal{C}_i})$ .

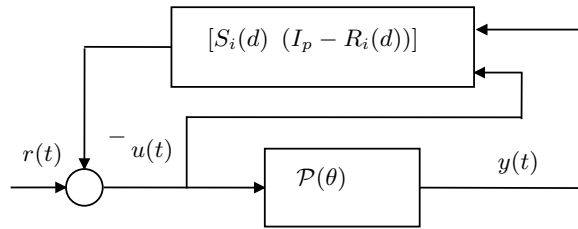
can consider, in place of  $v_i$ , the signal

$$w_i(t) = R_i(d)u(t) + S_i(d)y(t), \quad (\text{A.7})$$

so that the  $i$ -th potential control loop of Figure 3.2 becomes the one depicted in Figure A.2. In the light of (A.7) and Figure A.2, we can therefore replace the test functionals in (3.14) by

$$\Pi_i(t) = \max_{k \leq t} \frac{\left\| \left[ (\widehat{\mathcal{P}(\theta)}/\widehat{\mathcal{C}_i})w_i - (\widehat{\mathcal{M}_i}/\widehat{\mathcal{C}_i})w_i \right]^k \right\|}{\left\| \left[ (\widehat{\mathcal{M}_i}/\widehat{\mathcal{C}_i})w_i \right]^k \right\|}, \quad (\text{A.8})$$

then observer form implementation of the controller, proposed in [DAL07], is equivalent to the feedback interconnection as shown in the following figure



which clearly justifies why this configuration is referred to as the observer-form. Note that, by substituting the signal  $w(t)$ , as in (A.6), in the place of  $r(t)$ , observer-form implementation turns out to be equivalent to the typical one-degree-of-freedom implementation. Similar controller implementation is also utilized in [DLVL09] for validating controllers by using closed-loop data. The reader is referred to [ZDG95] for further discussion on the observer-based controllers and the link to the controller implementation in above figure.

Appendix A. Reference-loop Identification in case of Non-Square Systems

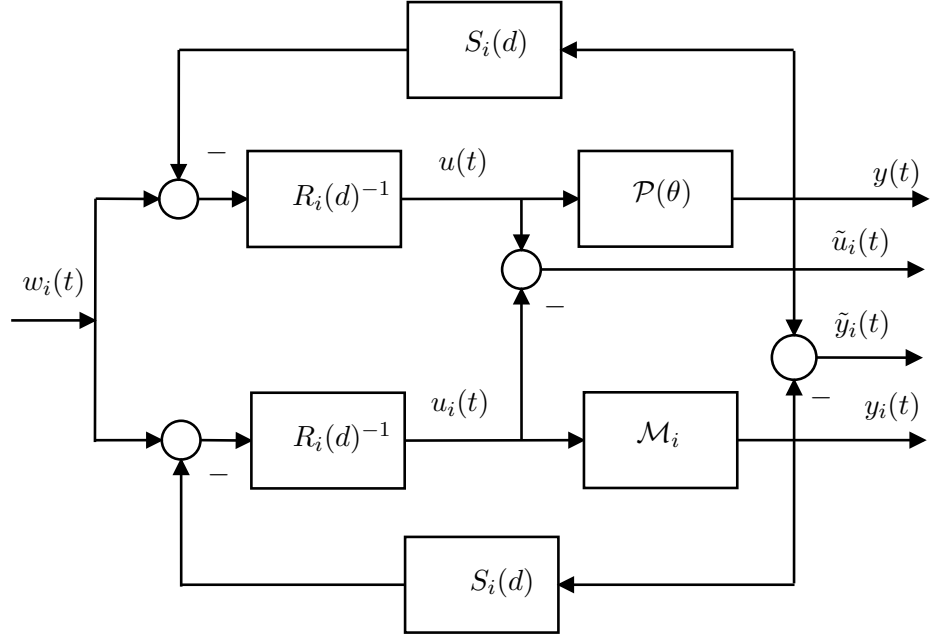


**Figure A.3:** Details of a Multi-Model Unfalsified ASC scheme with candidate controllers implemented via the observer-form.

where, with obvious meaning of the symbols,  $(\widehat{\mathcal{P}(\theta)/\mathcal{C}_i})$  and  $(\widehat{\mathcal{M}_i/\mathcal{C}_i})$  denote the  $i$ -th potential loop and the  $i$ -th reference loop, respectively, where the controller  $\mathcal{C}_i$  implemented in the observer form. Consistently with the observer-form arrangement, functional (A.8) can be equivalently rewritten as follows

$$\Pi_i(t) := \max_{k \leq t} \Lambda_i(k), \quad (\text{A.9})$$

$$\Lambda_i^{1/2}(t) := \frac{\| \tilde{z}_i^t \|}{\| (z - \tilde{z}_i)^t \|}, \quad (\text{A.10})$$

with  $\tilde{z}_i := z - z_i$ , where

$$z = (\widehat{\mathcal{P}(\theta)/\mathcal{C}_i}) w_i$$

stems from (A.7) and  $z_i = (\widehat{\mathcal{M}_i/\mathcal{C}_i}) w_i := [u_i' \ y_i']'$ ,  $i \in \overleftarrow{N}$ , as shown in Figure A.3.

## Appendix A. Reference-loop Identification in case of Non-Square Systems

Notice that, in contrast with (3.16), the test functional (A.10) is always well-defined, since (A.7) is always numerically stable <sup>2</sup>. This leads us to make the following comments.

- (i) From a conceptual point of view, approach based on (A.8) still maintains an interpretation in terms of discrepancy between potential and nominal loops, both driven by a virtual reference signal. In particular, as much the sequences  $w_i^t$ 's approximate the sequence  $w^t$ , as the solution obtained by (A.9)-(A.10) approaches the ideal goal, *i.e.*  $z^t \approx [(\mathcal{P}(\theta)/\mathcal{C}_i) r]^t$  and  $z_i^t \approx [(\mathcal{M}_i/\mathcal{C}_i) r]^t$ .
- (ii) From a practical point of view, even when  $v_i$  keeps bounded, the approach based on (A.9)-(A.10) does not pose questions related to numerical aspects/implementation. It can be seen as the direct counterpart of the pre-existing approach based on (3.14) for SISO systems [MCMS07].

Eventually, the merit of (A.8) is to recover, for non-square systems, an interpretation of the test functional in terms of discrepancy between potential and nominal loop (which is, in broad terms, a form of identification for control) even in case the classical virtual references  $v_i$ 's in (3.11) do not exist. Obviously, there is no need to implement the switching controller  $\mathcal{C}_{(\cdot)}$  as in Figure A.1. Indeed, the test functionals (A.10) are only used in order to update the controller switching index into the switching logic (3.8) and, as for the square case, can be computed by filtering the prediction error as described in Lemma 3.5.1.

---

<sup>2</sup>For SISO systems, test functionals based on  $w_i$  were indeed considered in order to obtain numerically stable solutions in the presence of non-minimum phase controllers, without the need to reconfigure the control action [MCMS07].

## Appendix B

# Performance-oriented Controller Tuning: Some Remarks

In recent years, ASC schemes have emerged as an alternative to conventional continuous adaptation in order to control processes in presence of large model uncertainties. Compared to conventional forms of adaptation, switching control offers the definite advantage that controller selection is carried out by means of logic-based switching rather than continuous tuning, thus allowing fast (discontinuous) adaptation of the control system. In this respect, [Mor95] provides a general overview of the topic.

Adaptive switching control has been approached by several diversified techniques, within both model-free control [FB86, ST97, SWPS07] and, model-based control [NX00, Mor95, ZMF00, PK01, HLM03a, BBMT10]. Although these contributions originate from fundamentally different approaches, the common idea is to have a *finite* family of pre-designed candidate controllers, so that, for each possible process model in the process uncertainty set, at least one of the controllers performs satisfactorily. However, the adoption of a finite number of candidate controllers may prevent from achieving optimal performance because of possible detuning arising from the discrete nature of the controller family in contrast with the possibly continuous nature of the process uncertainty. Even more importantly, satisfactory trade-offs between the conflicting objectives of number of candidate controllers (hence memory/computational load) and desired performance need not even exist in some cases, especially if the process uncertainty set is large.

## Appendix B. Performance-oriented Controller Tuning: Some Remarks

In this appendix, the aim consists in proposing an architecture which combines an ASC scheme with a controller tuning algorithm in order to enjoy of positive features of both the techniques: Speed (from switching) and accuracy (from tuning) of the control system response. In particular, the tuning algorithm is thought to be applied to the ASC scheme described in Chapter 3 [BBM<sup>+</sup>11b]. The idea is the following. Given a family of  $N$  pre-designed candidate controllers, one of these is first selected via switching; then, by means of an appropriate tuning mechanism, which is discussed in Section B.2, the parameters of a new controller are adjusted so as to design the  $(N + 1)$ -th candidate controller, potentially yielding higher performance. The peculiarity is that, while tuning algorithm is running, the process continues to be managed by the supervisor. Tuning and switching has to be thought as two disjoint blocks, *i.e.* operating in a separate way. Once tuning procedure stops and the new controller is ready to be used, then it is added to the pre-existing controller family. More details on the combination between switching scheme and tuning algorithm are provided in Section B.3, even if some problem is still open. Section B.4 takes care of the current open problems. It has to be pointed out that the idea of combining switching and tuning schemes for adaptive control is by no means new in the literature, see for example [NB97, NX00]. However, despite the similarities, the approach developed hereafter differs from that in [NB97, NX00], since the control design procedure is formulated as a parameter optimization problem in which the optimization is carried directly on the controller parameters, with no intermediate process model identification effort. Further, different from existing data-driven controller tuning techniques, as for example that one in [HGGL98], the algorithm proposed hereafter need of a minimum interaction with the process, the latter being a positive characteristics for an adaptive procedure to be combined with a switching scheme.

### B.1 Model distribution-based Performance: An example

The switching scheme built via the adoption of (3.15)-(3.16) allows one to consider adaptive control systems in which both the issues of robustness and performance can be taken into account. In fact, while stability is guaranteed under the only feasibility condition **a1**, performance requirements can be achieved by designing the nominal model distribution  $\mathcal{M}$  dense enough in  $\mathcal{P}$ . In broad terms, fixed a desired value for  $\beta$ , it is necessary to design a model distribution  $\mathcal{M}(\bar{\beta})$  with  $\bar{\beta} \leq \beta$ , where  $\bar{\beta}$  is defined as in (3.29). As previously said,



Appendix B. Performance-oriented Controller Tuning: Some Remarks

	$K_{P_{\theta_i}}$	$K_{I_{\theta_i}}$	Stability Interval
$\mathcal{C}_1$	0.98	0.98	$\theta \in [0.3, 0.946)$
$\mathcal{C}_2$	0.36	0.68	$\theta \in [0.3, 2.174)$
$\mathcal{C}_3$	0.08	0.3	$\theta \in [0.3, 3.5]$

**Table B.1:** Controllers coefficients.

the smaller  $\beta$ , the closer (for any possible process in  $\mathcal{P}$ ) the behavior of the final closed-loop ( $\mathcal{P}(\theta)/\mathcal{C}_f$ ) to the behavior of the reference-loop ( $\mathcal{M}_f/\mathcal{C}_f$ ).

However, further aspects arise concerning (3.29). In many cases, it may in fact be difficult to achieve a desired  $\bar{\beta}$ , while retaining a moderate memory/computational load. To see this, consider for simplicity a SISO problem ( $p = 1$ ) which consists in controlling an oscillatory uncertain system  $\mathcal{P}(\theta)$  [APH98], with continuous-time transfer function

$$P(\theta, s) = \frac{b(\theta)}{A(s)} = \frac{9\theta}{(s+1)(s^2+s+9)}, \quad (\text{B.1})$$

where  $\theta \in [0.3, 3.5]$ . For each  $\theta$ , the corresponding controller  $\mathcal{C}_\theta$  has been selected as the one among all proportional-integral (PI) controllers  $\tilde{\mathcal{C}}_\theta$  with continuous-time transfer function

$$\tilde{\mathcal{C}}_\theta(s) = \frac{\tilde{S}_\theta(s)}{\tilde{R}_\theta(s)} = \frac{\tilde{K}_{P_\theta} s + \tilde{K}_{I_\theta}}{s}, \quad (\text{B.2})$$

satisfying the weighted  $\mathcal{H}_\infty$  mixed-sensitivity criterion [Kwa91]

$$C_\theta(s) = \inf_{(\tilde{K}_{P_\theta}, \tilde{K}_{I_\theta})} \sup_{\omega > 0} \frac{|A(j\omega)|^2}{|\tilde{\chi}_\theta(j\omega)|^2} \left( |j\omega|^2 + \left| V(j\omega)(\tilde{K}_{I_\theta} + j\omega \tilde{K}_{P_\theta}) \right|^2 \right),$$

where  $V(s) := 1/(1 + s/\omega_v)$ ,  $\omega_v := 1.88$  rad/s, while  $\tilde{\chi}_\theta(s) := A(s)s + b(\theta)(\tilde{K}_{P_\theta}s + \tilde{K}_{I_\theta})$ . Three different continuous-time controllers  $\mathcal{C}_{\theta_i}$  have been designed relatively to the nominal process models  $\mathcal{M}_{\theta_i}$  corresponding to the following three values:

- $\theta_1 = 0.3$ ;
- $\theta_2 = 1$ ;
- $\theta_3 = 3.5$ .

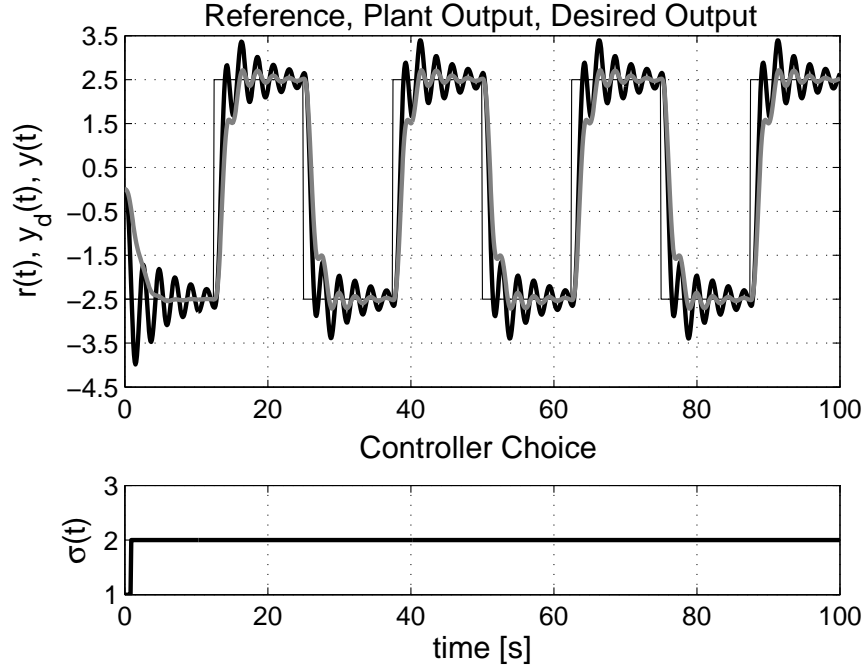


**Figure B.1:** Switching mechanism with pre-designed controllers. Legend: Reference (thin black), process output (bold black), desired output (bold grey).

The discrete-time nominal models  $\mathcal{M}_i$  and related controllers  $\mathcal{C}_i$  are the ones resulting from the use of an input zero-order holder with sampling time  $T_s$  equal to 0.1 s, and the subscript  $i$  corresponds to  $\theta_i$ ,  $i \in \overleftarrow{3}$ . In particular, the controllers have transfer functions

$$C_i(d) = \frac{S_i(d)}{R_i(d)} = \frac{(K_{P_i} + K_{I_i}) - K_{P_i} d}{1 - d}, \quad (\text{B.3})$$

with  $K_{P_i} = K_{P_{\theta_i}}$  and  $K_{I_i} = K_{I_{\theta_i}} T_s$ . The coefficients  $K_{P_i}$  and  $K_{I_i}$  are reported in Table B.1, along with the corresponding stability intervals.

The reference  $r(t)$  to be tracked is a square-wave with zero-mean, amplitude 2.5 and period 50 s. The controller index is selected by the rule (3.8) with (3.15)-(3.16), and hysteresis constant  $h$  set equal to 0.1<sup>1</sup>.

Assume that  $\theta = 1.5$ , and let  $\sigma(0) = 1$ . Fig. B.1 shows that  $\mathcal{C}_2$  is switched-on as the final controller right after start-up. However,  $(\mathcal{P}(1.5)/\mathcal{C}_2)$  does not behave as desired,

<sup>1</sup>All simulations reported hereafter consider a case with zero process initial conditions and zero noises and disturbances.

Appendix B. Performance-oriented Controller Tuning: Some Remarks

$N$	3	6	9	12	15	18	> 80
$\bar{\beta}$	2.402	1.316	0.897	0.675	0.529	0.472	< 0.1

**Table B.2:** Dependence of  $\bar{\beta}$  from  $N$ .

its closed-loop response being drastically different compared to the desired one given by the reference-loop ( $\mathcal{M}_2/\mathcal{C}_2$ ).

To achieve definite performance improvements, one is forced to increase the number  $N$  of candidate reference-loops. To this end, we have constructed  $\mathcal{M}(\bar{\beta})$  model distributions for various values of  $\bar{\beta}$  covering the whole uncertainty interval  $[0.3, 3.5]$ , where for each  $N$ , the models have been logarithmically distributed over the such an interval. Table B.2 indicates that  $N > 80$  is needed so as to achieve a value of  $\bar{\beta}$  less than the hysteresis constant  $h$  and makes the selection rule sensible to the performance requirements.

An alternative procedure for enhancing the performance is hereafter proposed and it is presented for the particular case of SISO systems.

## B.2 Fine Controller Tuning Algorithm

Let  $\mathcal{C}_f$  denote the final controller selected according to (3.8) with (3.15)-(3.16). According to data,  $\mathcal{C}_f$  is therefore recognized as the controller such that the closed-loop behaves as closely as possible to one of the  $N$  candidate reference-loops. Consequently, among all candidate reference-loops, ( $\mathcal{M}_f/\mathcal{C}_f$ ) yields the reference-loop behavior more likely to be achievable by designing a new controller.

To this end, let  $\mathcal{C}(\alpha)$  denote a controller in a given class parametrized by the vector  $\alpha$  which belongs to some set  $\Theta_\alpha \subseteq \mathbb{R}^{n_\alpha}$ , which transfer function is given by

$$C(\alpha, d) = \frac{S(\alpha, d)}{R(\alpha, d)} \quad (\text{B.4})$$

where  $S(\alpha, d) := s_0(\alpha) + s_1(\alpha)d + \dots + s_{n_r}(\alpha)d^{n_r}$  and  $R(\alpha, d) := 1 + r_1(\alpha)d + \dots + r_{n_r}(\alpha)d^{n_r}$  are here polynomials. Then, the corresponding virtual reference  $v_\alpha \in \mathbb{R}^p$  can be computed by solving the difference equation

$$S(\alpha, d) v_\alpha(t) = R(\alpha, d) u(t) + S(\alpha, d) y(t), \quad (\text{B.5})$$

Appendix B. Performance-oriented Controller Tuning: Some Remarks

which, as for (3.11), is such that  $z = (\mathcal{P}(\theta)/\mathcal{C}_{\sigma(\cdot)}) r = (\mathcal{P}(\theta)/\mathcal{C}(\alpha)) v_\alpha$ . A suitable variable to describe the desired closed-loop behavior can be the complementary sensitivity of the reference-loop ( $\mathcal{M}_f/\mathcal{C}_f$ )

$$W_f(d) := \frac{M_f(d) C_f(d)}{1 + M_f(d) C_f(d)} = \frac{B_f(d) S_f(d)}{\chi_f(d)}. \quad (\text{B.6})$$

where  $M_f(d) := B_f(d)/A_f(d)$  and  $C_f(d) := S_f(d)/R_f(d)$  denote the transfer functions of nominal model  $\mathcal{M}_f$  and controller  $\mathcal{C}_f$ , respectively, while  $\chi_f(d) := A_f(d) R_f(d) + B_f(d) S_f(d)$  is the closed loop characteristic polynomial of ( $\mathcal{M}_f/\mathcal{C}_f$ ). According to (B.6), one can generate the signals

$$\left. \begin{aligned} y_\alpha(t) &= W_f(d) v_\alpha(t) \\ u_\alpha(t) &= C(\alpha, d) (v_\alpha(t) - y_\alpha(t)) \end{aligned} \right\} \quad (\text{B.7})$$

which represent the desired behavior in response to the reference  $v_\alpha$ . In particular,  $y_\alpha$  indicates the desired process output while  $u_\alpha$  is the signal which should be the input to the process, if the latter was connected with the controller  $\mathcal{C}(\alpha)$  and its output coincided with the desired one  $y_\alpha$ .

Assuming available a batch of data  $z^t$ , the controller tuning can be therefore obtained through the minimization, with respect to  $\alpha$ , of the following criterion

$$\Lambda^{1/2}(\alpha, t) := \frac{\| (z - z_\alpha)^t \|}{\| z_\alpha^t \|}, \quad \alpha \in \Theta_\alpha, \quad (\text{B.8})$$

where  $z_\alpha := [u_\alpha \ y_\alpha]^t$ . In view of (B.6), the optimization criterion (B.8) simply amounts to finding the vector  $\alpha$  such that  $(\mathcal{P}(\theta)/\mathcal{C}(\alpha))$  in response to  $v_\alpha$  behaves, as closely as possible, to the desired behavior given by (B.7).

**Remark B.2.1** Notice that, the functional (B.8) has the same structure of the one used in the switching rule, see (3.16). By the tuning algorithm, indeed, the idea consists in carrying out a sort of *reference loop adaptation* task, where the controller is selected from an infinite set of controllers parametrized by the vector  $\alpha$ .

The solution can be obtained based on an iterative gradient-descent approach

$$\alpha_{j+1} = \alpha_j - \eta_j H_j^{-1} \frac{\partial \Lambda}{\partial \alpha}(\alpha_j, t) \quad (\text{B.9})$$

initialized from  $\alpha_0 := \hat{\alpha}_f$ , where  $\hat{\alpha}_f$  denotes the parameter vector associated to  $\mathcal{C}_f$ . As usual,  $H_j$  is some appropriate positive definite matrix, *e.g.* the Hessian of  $\Lambda(\alpha_j, t)$ , while  $\eta_j$

## Appendix B. Performance-oriented Controller Tuning: Some Remarks

is a positive scalar which determines the step size. As can be easily checked, the gradient  $\partial\Lambda/\partial\alpha$  is given by

$$\frac{\partial}{\partial\alpha}\Lambda(\alpha, t) = -\frac{2}{\|z_\alpha^t\|^2} \sum_{k=0}^t \left\{ [z_\alpha(k) + (\Lambda(\alpha, t) - 1) z_\alpha(k)]' \frac{\partial}{\partial\alpha} z_\alpha(\alpha, k) \right\} \quad (\text{B.10})$$

where

$$\frac{\partial}{\partial\alpha} z_\alpha(\alpha, k) := \begin{bmatrix} \partial u_\alpha(k)/\partial\alpha \\ \partial y_\alpha(k)/\partial\alpha \end{bmatrix} \quad (\text{B.11})$$

Based on (B.5)-(B.6), the gradient  $\partial\Lambda(\alpha, t)/\partial\alpha$  can be therefore computed from collected data as follows

$$\frac{\partial}{\partial\alpha} z_\alpha(\alpha, k) = \begin{bmatrix} (1 - W_f(d))C'(\alpha, d) y(k) \\ -W_f(d)C^{-2}(\alpha, d)C'(\alpha, d) u(k) \end{bmatrix} \quad (\text{B.12})$$

with  $C'(\alpha, d) := \partial C(\alpha, d)/\partial\alpha$ .

**Remark B.2.2** Notice that, the above minimization procedure has similarities with the Iterative Feedback Tuning (IFT) approach of [HGGL98], since optimization is carried out directly on the controller parameters, with no intermediate process model identification effort. The main difference is that, here, thanks to the virtual reference variable  $v_\alpha$ , it is not required that  $\mathcal{C}(\alpha)$  be connected in feedback with the process in order to update the controller parameters. We note, also, that such a procedure can be extracted from the switching context and used for the data-based design of a controller for an unknown / uncertain process.

### B.2.1 Implementation Issues

As for  $v_i$ 's in (3.11), numerical constraints exist also in the computation of the virtual reference for SISO systems. Indeed, numerical computation of the  $v_\alpha$  in (B.5) requires that  $S(\alpha, d)$  be strictly Schur. While the results considered here hinge upon such an assumption, a way for sidestepping this problem could be to show that the same conclusions hold true for possible non-stable invertible controllers, provided that modified virtual references be appropriately defined, see Appendix A and [DAL07]. However, a possible way to active the tuning mechanism in presence of nonminimum-phase candidate controllers consists in letting  $S(\alpha, d) := \tilde{S}(\alpha, d) S_f^u(d)$ , where  $S_f^u(d)$  is fixed and contains all roots of  $S_f(d)$  into and on the unit circle (on the contrary,  $S_f^s(d)$  contains all the others and hence

## Appendix B. Performance-oriented Controller Tuning: Some Remarks

$S_f(d) := S_f^u(d) S_f^s(d)$ . Then a virtual signal  $\tilde{v}_\alpha(t) := S_f^u(d) v_\alpha(t)$ , can be computed by solving

$$\tilde{S}(\alpha, d) \tilde{v}_\alpha(t) = R(\alpha, d) u(t) + S(\alpha, d) y(t).$$

In this respect,  $\tilde{S}(\alpha, d)$  has to keep strictly Schur.

Similarly, numerical computation of (B.7) and (B.12) may not be feasible if  $\mathcal{C}(\alpha)$  and/or its gradient with respect to  $\alpha$ , namely  $\partial\mathcal{C}(\alpha, d)/\partial\alpha$ , are unstable, *i.e.*  $R(\alpha, d)$  is not strictly Schur. Appropriate procedures for coping with this situation can be found in ([HGGL98]). However, as elaborated next in more detail, though the developments of this appendix can be generalized so as to cover the case where  $\mathcal{C}(\alpha)$  and/or the gradient of  $\mathcal{C}(\alpha)$  are unstable, stability of the map from  $v_\alpha$  to  $u_\alpha$  in (B.7) is required to extend Theorem 3.4.1 to the case where switching and tuning are combined. A possible way for allowing the use of unstable candidate controllers is to let  $R(\alpha, d) := \tilde{R}(\alpha, d) R_f^u(d)$ , where  $R_f^u(d)$  is a fixed polynomial containing all roots of  $R_f(d)$  into and on the unit circle, consistently  $R_f^s(d)$  contains all other roots of  $R_f(d)$ , namely  $R_f(d) = R_f^s(d) R_f^u(d)$ . Accordingly,  $u_\alpha$  in (B.7) can be computed as

$$u_\alpha(t) = \frac{A_f(d) R_f^s(d) \tilde{S}(\alpha, d)}{\chi_f(d) \tilde{R}(\alpha, d)} \tilde{v}_\alpha(t),$$

which yields a stable map, provided that  $\tilde{R}(\alpha, d)$  keeps strictly Schur. Consistently,  $y_\alpha$  in (B.7) becomes

$$y_\alpha(t) = \frac{B_f(d) S_f^s(d)}{\chi_f(d)} \tilde{v}_\alpha(t).$$

Enforcing  $\tilde{S}(\alpha, d)$  and  $\tilde{R}(\alpha, d)$  to be strictly Schur can be approached in many ways, *e.g.* by resorting to constrained optimization routines, or by the use of penalty functions [Ber96, Sny05].

### B.3 ASC Scheme with Fine Controller Tuning

The controller design scheme, though iterative, does not require  $\mathcal{C}(\alpha)$  to be connected in feedback with the process in order to update the vector  $\alpha$ , since the idea is based on virtual experiments. Such a feature makes it possible to improve the performance of the switching scheme of Chapter 3, while retaining guaranteed stability properties.

Appendix B. Performance-oriented Controller Tuning: Some Remarks

Given  $t_* \in \mathbb{Z}_+$ ,  $t_* > 0$ , such that  $\sigma(t) = f \in \overleftarrow{N}$  for  $t \geq t_*$ , let  $\mathcal{C}(\alpha_*)$  with transfer function

$$C(\alpha_*, d) = \frac{S(\alpha_*, d)}{R(\alpha_*, d)} \quad (\text{B.13})$$

be the controller resulting from the minimization of  $\Lambda(\alpha, t_*)$  by means of (B.9), where

$$\left. \begin{aligned} \alpha_0 &:= \hat{\alpha}_f, \quad f \in \overleftarrow{N} \\ W_f(d) &= \frac{M_f(d)C_f(d)}{1+M_f(d)C_f(d)} = \frac{B_f(d)S_f(d)}{X_f(d)} \\ \alpha_* &:= \alpha_\varrho \end{aligned} \right\} \quad (\text{B.14})$$

$\hat{\alpha}_f$  being associated to  $\mathcal{C}_f$ , while  $\varrho$  represents the number of iterations. In accordance with (B.6), the transfer function  $M_{\alpha_*}(d)$  of the nominal model  $\mathcal{M}_{\alpha_*}$  corresponding to  $\mathcal{C}(\alpha_*)$  can be therefore obtained from the open-loop transfer function of  $(\mathcal{M}_f/\mathcal{C}_f)$ , *i.e.* by solving

$$M_{\alpha_*}(d)C(\alpha_*, d) = M_f(d)C_f(d). \quad (\text{B.15})$$

Integration of the tuning scheme into the switching one is hence simply achieved by adding the  $(N+1)$ -th reference-loop  $(\mathcal{M}_{N+1}/\mathcal{C}_{N+1}) := (\mathcal{M}_{\alpha_*}/\mathcal{C}(\alpha_*))$  to the initial family of candidate reference-lops  $\mathcal{F}$ , which therefore becomes

$$\mathcal{F}_e := \{(\mathcal{M}_i/\mathcal{C}_i), i \in \overleftarrow{N+1}\}. \quad (\text{B.16})$$

Clearly, the feasibility condition **a1** is not destroyed by the introduction of an additional candidate controller in the family  $\mathcal{C}$ . Accordingly, by restricting to the case  $p = 1$ , one concludes that the ASC scheme of Chapter 3 combined with the above described tuning algorithm continues to guarantee input-output  $l_2$  stability of the switched system (3.5) in accordance to Theorem 3.4.1, provided that the new reference loop  $(\mathcal{M}_{N+1}/\mathcal{C}_{N+1})$  be internally stable. This is captured by the next lemma.

**Lemma B.3.1** Given an arbitrary  $t_* \in \mathbb{Z}_+$ ,  $t_* > 0$ , let  $\mathcal{C}_{N+1}$  be the controller resulting from the minimization of  $\Lambda(\alpha, t_*)$  by means of (B.9)-(B.14). Furthermore, let  $\mathcal{M}_{N+1}$  denote the corresponding nominal model computed via (B.15). Then, provided that  $\mathcal{C}_{N+1}$  be stable, causal, stably and causally invertible (CSCI), the reference-loop  $(\mathcal{M}_{N+1}/\mathcal{C}_{N+1})$  is internally stable.

*Proof.* The proof simply follows from the fact that internal stability of  $(\mathcal{M}_{N+1}/\mathcal{C}_{N+1})$  is equivalent to the stability of its generalized sensitivity matrix  $T_{N+1}(d)$

Appendix B. Performance-oriented Controller Tuning: Some Remarks

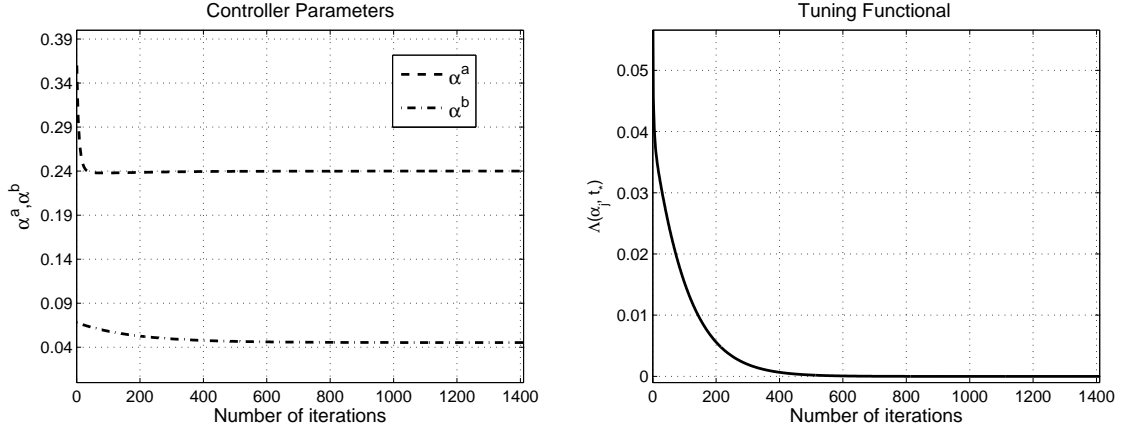


**Figure B.2:** Left: Controller parameter vector  $\alpha_k$ ; Right: Test functional  $\Lambda(\alpha_k, t_*)$ ,  $k = 1, 2, \dots, \varrho = 1400$ .

$$\begin{aligned}
 T_{N+1}(d) &:= (1 + M_{N+1}(d)C_{N+1}(d))^{-1} \begin{bmatrix} -M_{N+1}(d)C_{N+1}(d) & C_{N+1}(d) \\ M_{N+1}(d) & -1 \end{bmatrix} \\
 &= \begin{bmatrix} -W_f(d) & C_{N+1}(d)(1 - W_f(d)) \\ W_f(d)/C_{N+1}(d) & -(1 - W_f(d)) \end{bmatrix} \quad (\text{B.17})
 \end{aligned}$$

which is stable.  $\square$

**Remark B.3.1** Notice that the same conclusions of Lemma B.3.1 hold true if  $C_{N+1}(d) = C_f^u(d)C_{N+1}^s(d)$ , where  $C_f^u(d)$  contains all the unstable zeros and poles of  $\mathcal{C}_f$ , and with  $C_{N+1}^s(d)$  stable and minimum-phase.

Given  $(\mathcal{M}_{N+1}/\mathcal{C}_{N+1})$ , the control scheme is simply modified by adding at some instant  $t_+ \in \mathbb{Z}_+$ ,  $t_+ > t_*$ , the test functional corresponding to  $(\mathcal{M}_{N+1}/\mathcal{C}_{N+1})$  into the switching logic. Notice that, in practice, to fairly compare  $\Pi_{N+1}$  with all the other  $\Pi_i$ 's, all candidate test functionals are reset at time  $t_+$ , *i.e.*

$$\Pi_i(t) := \max_{t_+ \leq k \leq t} \Lambda_i(k) \quad (\text{B.18})$$

$$\Lambda_i^{1/2}(t) := \frac{\|\tilde{z}_{i/i}|_{t_+}^t\|}{\|(z - \tilde{z}_{i/i})|_{t_+}^t\|}, \quad t \in \mathbb{Z}_{t_+}, \quad i \in \overleftarrow{N+1} \quad (\text{B.19})$$



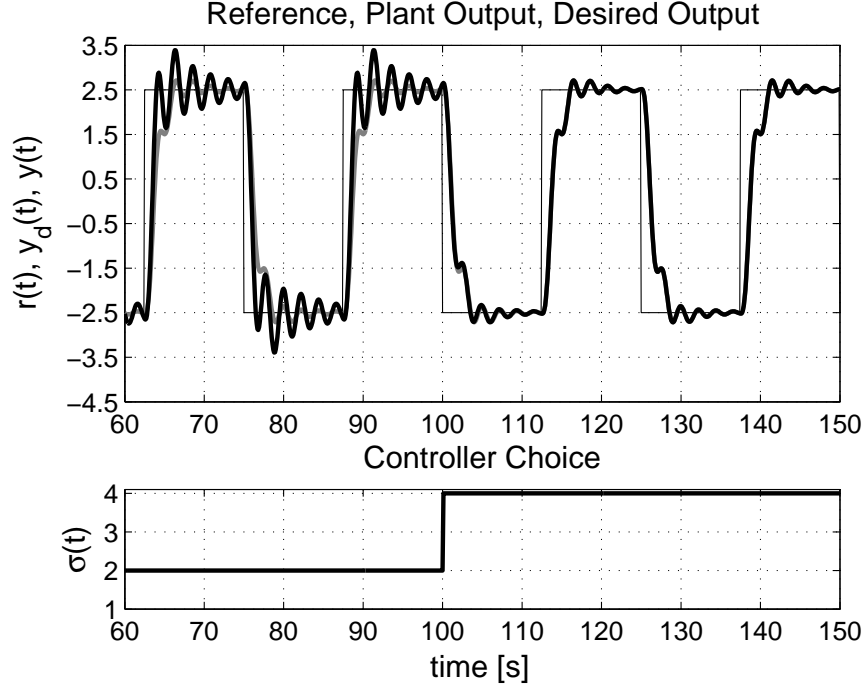


**Figure B.3:** Switching mechanism with real-time controller design. Legend: Reference (thin black), process output (bold black), desired output (bold grey).

where  $\mathbb{Z}_{t_+} := \{t_+, t_+ + 1, \dots\}$  and,  $x|_{t_1}^{t_2} := \{x(t_1), \dots, x(t_2)\}$ ,  $t_1 < t_2$ .

### B.3.1 Tuning-based Performance: An Example (Continued)

Consider the example of Section B.1. Consistently with the adopted notation, let  $t_* := 80$  s, and  $t_+ := 100$  s. Before  $t_+$ , the supervisor switches among the three pre-designed candidate controller, and selects  $\mathcal{C}_2$ . Accordingly, the tuning algorithm starts at time  $t_*$  by minimizing the loss function  $\Lambda(\alpha, t_*)$  based on recorded data  $z^{t_*}$  and reference model  $W_2(d)$  corresponding to the reference-loop  $(\mathcal{M}_2/\mathcal{C}_2)$ , where model and controller have the following transfer functions

$$\begin{aligned} M_2(d) &= \frac{0.0014d(1 + 3.533d)(1 + 0.256d)}{(1 - 0.905d)(1 - 1.820d + 0.905d^2)}, \\ C_2(d) &= \frac{0.428(1 - 0.8411d)}{1 - d}. \end{aligned} \tag{B.20}$$

## Appendix B. Performance-oriented Controller Tuning: Some Remarks

The controller to be designed is chosen to be of the form

$$C(\alpha, d) = \alpha^a + \frac{\alpha^b}{1-d} \quad (\text{B.21})$$

initialized from  $\alpha_0 = [\alpha_0^a \ \alpha_0^b] := \hat{\alpha}_2 = [0.360 \ 0.068]'$ . The left side of Figure B.2 shows that the loss function  $\Lambda(\alpha, t_*)$  approaches zero quite rapidly, with corresponding parameters vector  $\alpha_* = [0.240 \ 0.045]$  (right side of Figure B.2). Accordingly, a fourth reference-loop, ( $\mathcal{M}_4/\mathcal{C}_4$ ), is built with

$$C_4(d) := \frac{0.285(1 - 0.8411d)}{1 - d} \quad (\text{B.22})$$

and  $\mathcal{M}_4$  obtained from (B.15),

$$M_4(d) := \frac{0.0021d(1 + 3.533d)(1 + 0.256d)}{(1 - 0.905d)(1 - 1.820d + 0.905d^2)}. \quad (\text{B.23})$$

At time  $t_+$ , all test functionals are reset and  $\Pi_4$  is inserted into the switching logic. As shown in Fig. B.3,  $\mathcal{C}_4$  is soon switched on as the final controller, the behavior of ( $\mathcal{P}/\mathcal{C}_4$ ) being pretty close to the one dictated by the desired behavior represented by  $W_2(d)$  (in fact,  $\mathcal{M}_4$  matches almost perfectly with the discrete-time process corresponding to  $\theta = 1.5$ ).

## B.4 Concluding Remarks and Open Problems

Controlling an uncertain process by means of a finite family of pre-designed controllers, managed by a supervisory unit, has evident advantages with respect to the classical continuous adaptive control in terms of speed of adaptation of the control action. However, the discrete nature of the control need not guarantee high performance in correspondence of all process configurations, most of all in case of large process uncertainty. Although a first solution to improve the performance could be obtained by increasing the number of the candidate controllers, computational aspects may force the designer to work with a limited candidate set. To this end, in this appendix a novel, provably correct, adaptive switching control scheme has been introduced, wherein the use of pre-designed controllers is combined with a data-based controller design procedure. By on-line generating a new candidate controller, the modified switching scheme proves to compare favourably to a pure switching-based mechanism, thus resulting of practical relevance for on-line implementation of highly performing adaptive control systems. Positive features of this tuning mechanism are the following: i) Switching and tuning mechanisms run in a separate way, supervisor

## *Appendix B. Performance-oriented Controller Tuning: Some Remarks*

keeps the complete management of the process at each time and interaction between the two schemes occurs only at the time the new candidate controller is added to the controller family; ii) Tuning mechanism does not influence the properties of the switching scheme (see Theorem 3.4.1); iii) The experimental load, typically cumbersome in data-driven controller tuning mechanisms, is reduced at the minimum thanks to the use of the virtual reference tool. However, some questions regarding technical aspects of the algorithm are still open: i) The minimization procedure needs not to alter the unstable part of the initial controller, thus imposing the use of constrained optimization algorithms; ii) Final switching time is not detectable so, an automatic mechanism for activating the tuning procedure could be useful to reduce the waiting times due to pre-scheduled activation rules. Referring to the example, indeed, we can see that the tuning algorithm could start few seconds after the power-on time of the control system, rather than at the time 80 s (as pre-scheduled by the designer), see Figures B.1 and B.3.

# Appendix C

## Proofs

Hereafter, the operator  $d$  and the time  $t$  will be omitted, where possible, for sake of simplicity. All the results are generalized to the case of non-square systems, that is for systems with  $m$  inputs, *i.e.*  $u \in \mathbb{R}^m$ , and  $p$  outputs, *i.e.*  $y \in \mathbb{R}^p$ , all polynomial matrices having hence consistent dimensions.

Before proceeding, we present the following result.

**Lemma C.0.1** Let  $\Psi_{i/i} := R_i D_i + S_i N_i$ , whose determinant equals that of (3.20). Then, the following relationships hold

$$Y_i \Xi_{i/i}^{-1} A_i = D_i \Psi_{i/i}^{-1} S_i, \quad (\text{C.1})$$

$$X_i \Xi_{i/i}^{-1} B_i = N_i \Psi_{i/i}^{-1} R_i. \quad (\text{C.2})$$

□

**Proof of Lemma C.0.1.** Consider first (C.1), and notice that

$$\begin{aligned} S_i A_i^{-1} \Xi_{i/i} &= S_i A_i^{-1} (A_i X_i + B_i Y_i) \\ &= S_i X_i + S_i N_i D_i^{-1} Y_i \\ &= R_i Y_i + (\Psi_{i/i} - R_i D_i) D_i^{-1} Y_i \\ &= \Psi_{i/i} D_i^{-1} Y_i, \end{aligned}$$

Appendix C. Proofs

where the third equality follows from  $S_i X_i = R_i Y_i$  and the definition of  $\Psi_{i/i}$ . In turns,

$$\begin{aligned} S_i A_i^{-1} \Xi_{i/i} &= \Psi_{i/i} D_i^{-1} Y_i \Rightarrow \\ \Psi_{i/i}^{-1} S_i A_i^{-1} &= D_i^{-1} Y_i \Xi_{i/i}^{-1} \Rightarrow \\ D_i \Psi_{i/i}^{-1} S_i &= Y_i \Xi_{i/i}^{-1} A_i. \end{aligned}$$

Likewise,

$$\begin{aligned} \Xi_{i/i} X_i^{-1} N_i &= (A_i X_i + B_i Y_i) X_i^{-1} N_i \\ &= A_i N_i + B_i R_i^{-1} S_i N_i \\ &= B_i D_i + B_i R_i^{-1} (\Psi_{i/i} - R_i D_i) \\ &= B_i R_i^{-1} \Psi_{i/i}, \end{aligned}$$

where the third equality follows from  $B_i D_i = A_i N_i$  and the definition of  $\Psi_{i/i}$ . Hence,

$$\begin{aligned} \Xi_{i/i} X_i^{-1} N_i &= B_i R_i^{-1} \Psi_{i/i} \Rightarrow \\ X_i^{-1} N_i \Psi_{i/i}^{-1} &= \Xi_{i/i}^{-1} B_i R_i^{-1} \Rightarrow \\ N_i \Psi_{i/i}^{-1} R_i &= X_i \Xi_{i/i}^{-1} B_i. \end{aligned}$$

□

**Proof of Lemma 3.3.1.** It follows from

$$\begin{aligned} \Xi_{\theta/i}^{-1} - \Xi_{i/i}^{-1} &= \Xi_{\theta/i}^{-1} (I_p - \Xi_{\theta/i} \Xi_{i/i}^{-1}) \\ &= \Xi_{\theta/i}^{-1} (\Xi_{i/i} - \Xi_{\theta/i}) \Xi_{i/i}^{-1} \\ &= \Xi_{\theta/i}^{-1} \begin{bmatrix} \Delta_{B_i}(\theta) & \Delta_{A_i}(\theta) \end{bmatrix} \begin{bmatrix} -Y_i \\ X_i \end{bmatrix} \Xi_{i/i}^{-1}. \end{aligned}$$

□

**Proof of Lemma 3.5.1.** For reasons of generality, hereafter we refer to Figure A.3, instead of Figure 3.2. Accordingly, since  $u_i$  and  $y_i$  in (A.10)<sup>1</sup> can be obtained as

$$u_i = D_i \Psi_{i/i}^{-1} w_i, \quad y_i = N_i \Psi_{i/i}^{-1} w_i,$$

---

<sup>1</sup>Notice that, in the square case and  $v_i$  well-defined, figures A.3 and 3.2 are equivalent and so,  $u_i \equiv u_{i/i}$  and  $y_i \equiv y_{i/i}$ .

Appendix C. Proofs

then, by using (C.1) and (C.2), one has

$$\begin{aligned}
u - u_i &= u - D_i \Psi_{i/i}^{-1} w_i \\
&= u - D_i \Psi_{i/i}^{-1} (R_i u + S_i y) \\
&= (I_m - D_i \Psi_{i/i}^{-1} R_i) u - D_i \Psi_{i/i}^{-1} S_i y \\
&= (D_i - D_i \Psi_{i/i}^{-1} R_i D_i) D_i^{-1} u - Y_i \Xi_{i/i}^{-1} A_i y \\
&= (D_i - D_i \Psi_{i/i}^{-1} (\Psi_{i/i} - S_i N_i)) D_i^{-1} u - Y_i \Xi_{i/i}^{-1} A_i y \\
&= D_i \Psi_{i/i}^{-1} S_i A_i^{-1} B_i u - Y_i \Xi_{i/i}^{-1} A_i y \\
&= Y_i \Xi_{i/i}^{-1} B_i u - Y_i \Xi_{i/i}^{-1} A_i y \\
&= -Y_i \Xi_{i/i}^{-1} (A_i y - B_i u),
\end{aligned}$$

and with similar algebra,  $y - y_i = X_i \Xi_{i/i}^{-1} (A_i y - B_i u)$ . Thereby, one get

$$\begin{bmatrix} u - u_i \\ y - y_i \end{bmatrix} = \begin{bmatrix} -Y_i \\ X_i \end{bmatrix} \Xi_{i/i}^{-1} \varepsilon,$$

and so, (3.37) follows from the second one of (3.17) and by supposing zero plant initial conditions as in (3.3).  $\square$

**Proof of Theorem 3.4.1.** As in the proof of Lemma 3.5.1, we consider  $z_i$  in place of  $z_{i/i}$ . According to that, the transfer matrix of the system mapping  $z - \tilde{z}_i$  to  $\tilde{z}_i$  coincides with  $Q_{\theta/i} \Delta_{\theta/i}$ , (3.25) holding also in the non-square case. Therefore, under feasibility condition **a1**, Assumption **hsl<sub>2</sub>** is satisfied. Moreover, Assumption **hsl<sub>1</sub>** is automatically satisfied because of the maximum operator in (A.9). Thus, Lemma 3.1.1 holds, and controller switching always stops in a finite time for every reference sequence  $r \in \mathcal{S}$ . By Lemma 3.1.1, the test functional  $\Lambda_f^{1/2}$  related to the final switched-on controller  $\mathcal{C}_f$  is bounded, *viz.* there exists a positive real  $\kappa$  such that

$$\Lambda_f^{1/2}(t) \leq \kappa, \quad \forall t \in \mathbb{Z}_+. \tag{C.3}$$

Then, by triangular inequality, one has

$$\|z^t\| \leq \kappa \|(z - \tilde{z}_f)^t\| + \|\tilde{z}_f^t\| \leq (1 + \kappa) \|(z - \tilde{z}_f)^t\|.$$

### Appendix C. Proofs

Recalling (3.25), one finds that

$$\begin{aligned}
z - \tilde{z}_f &= z - Q_{f/f} \Delta_{\theta/f} z(t) \\
&= z - \begin{bmatrix} -Y_f \\ X_f \end{bmatrix} \Xi_{f/f}^{-1} (A_f y - B_f u) \\
&= z - \begin{bmatrix} -Y_f \\ X_f \end{bmatrix} \Xi_{f/f}^{-1} A_f (y - N_f D_f^{-1} u). \tag{C.4}
\end{aligned}$$

The first  $m$  rows of (C.4) yield

$$\begin{aligned}
u + Y_f \Xi_{f/f}^{-1} A_f (y - N_f D_f^{-1} u) &= D_f \Psi_{f/f}^{-1} S_f y + (I_m - D_f \Psi_{f/f}^{-1} S_f N_f D_f^{-1}) u \\
&= D_f \Psi_{f/f}^{-1} S_f y + [I_m - D_f \Psi_{f/f}^{-1} (\Psi_{f/f} - R_f D_f) D_f^{-1}] u \\
&= D_f \Psi_{f/f}^{-1} S_f y + D_f \Psi_{f/f}^{-1} R_f u \\
&= D_f \Psi_{f/f}^{-1} \begin{bmatrix} R_f & S_f \end{bmatrix} z, \tag{C.5}
\end{aligned}$$

where the first inequality follows from (C.1). Likewise, the last  $p$  rows of (C.4) yield

$$y - X_f \Xi_{f/f}^{-1} A_f (y - N_f D_f^{-1} u) = (I_p - X_f \Xi_{f/f}^{-1} A_f) y + X_f \Xi_{f/f}^{-1} B_f u,$$

as  $A_f N_f = B_f D_f$ . From (C.2) we get  $X_f \Xi_{f/f}^{-1} B_f = N_f \Psi_{f/f}^{-1} R_f$ . Moreover,

$$\begin{aligned}
I_p - X_f \Xi_{f/f}^{-1} A_f &= X_f \Xi_{f/f}^{-1} A_f (A_f^{-1} \Xi_{f/f} X_f^{-1} - I_p) \\
&= X_f \Xi_{f/f}^{-1} A_f [A_f^{-1} (A_f X_f + B_f Y_f) X_f^{-1} - I_p] \\
&= X_f \Xi_{f/f}^{-1} B_f (Y_f X_f^{-1}) \\
&= N_f \Psi_{f/f}^{-1} R_f (R_f^{-1} S_f),
\end{aligned}$$

which finally yields

$$y - X_f \Xi_{f/f}^{-1} A_f (y - N_f D_f^{-1} u) = N_f \Psi_{f/f}^{-1} \begin{bmatrix} R_f & S_f \end{bmatrix} z. \tag{C.6}$$

Combining (C.5) and (C.6), (C.4) can be therefore rewritten as

$$z - \tilde{z}_f = \begin{bmatrix} D_f \\ N_f \end{bmatrix} \Psi_{f/f}^{-1} \begin{bmatrix} R_f & S_f \end{bmatrix} z. \tag{C.7}$$

Further, regardless of the state the controller  $\mathcal{C}_f$  is in at time  $t^*$ , one has  $R_f u(t) + S_f y(t) = S_f r(t)$  for  $t > t^* + n_{c_f}$  with  $n_{c_f} = \max\{\deg S_f, \deg R_f\}$ . This, along with the fact that determinant of  $\Psi_{f/f}$  is strictly Schur, implies that

$$\|(z - \tilde{z}_f)^t\| \leq \alpha \|r^t\| + \delta \tag{C.8}$$

### Appendix C. Proofs

for some positive reals  $\alpha$  and  $\delta$ . Hence, input-output  $l_2$ -stability follows at once.

Consider next that the HSL (3.8) and the test functionals (A.9)- (A.10) (or (3.15)- (3.16)) assure that the value of  $\Pi_i(t)$ , every time that the controller  $\mathcal{C}_i$  is switched-on, increases at least by  $h$ . Under a model distribution  $\mathcal{M}(\bar{\beta})$ , there always exists a stabilizing controller, say  $\mathcal{C}_s$ , such that  $\Pi_s(t) \leq \bar{\beta}^2$ . Hence, each index can be switched-on at most  $\lceil \bar{\beta}^2/h \rceil$  times since in the negative, its test functional would exceed the upper-bound of  $\Pi_s(\cdot)$ , contradicting (3.8).  $\square$

#### Proof of Lemma 3.4.1.

Suppose that there are finitely many switching times and let  $\mathcal{C}_f$  be the final switched-on controller. According to Definition 3.2.1, cost detectability of the pair  $(\Pi, \mathcal{C})$  holds provided that  $\Pi_f(t)$  is bounded as  $t \rightarrow \infty$  if and only if there exist finite nonnegative reals  $a_i$ ,  $i = 1, 2$ , such that (3.9) holds.

(*if*):  $\Pi_f(t)$  is bounded implies that (3.9) holds for some finite nonnegative reals  $a_i$ ,  $i = 1, 2$ . See proof of Theorem 3.4.1 from C.3 to C.8.

(*only if*): (3.9) holding for some finite nonnegative reals  $a_i$ ,  $i = 1, 2$  implies that  $\Pi_f(t)$  is bounded. Suppose that (3.9) holds, then

$$\Lambda_f(t) = \frac{\|\tilde{z}_f^t\|}{\|(z - \tilde{z}_f)^t\|} \leq 1 + \frac{\|z^t\|}{\|(z - \tilde{z}_f)^t\|} \leq 1 + \frac{a_1 + a_2 \|r^t\|}{\|(z - \tilde{z}_f)^t\|} \quad (\text{C.9})$$

Note that the denominator in (C.9) is monotonically non-decreasing and so, the rightmost term of (C.9) diverges only if  $\|r^t\|$  diverges as  $t \rightarrow \infty$ . Thus, to have  $\Lambda_f(t)$  bounded as  $t \rightarrow \infty$ , it is only needed to show that the rightmost term of (C.9) remains bounded as  $\|r^t\| \rightarrow \infty$ . To see this, notice that, based on (C.7), after an opportune time  $t^*$  one has

$$z - \tilde{z}_f = \begin{bmatrix} D_f \\ N_f \end{bmatrix} \Psi_{f/f}^{-1} S_f r, \quad (\text{C.10})$$

which implies

$$\|(z - \tilde{z}_f)^t\| \geq \delta \min_{\omega \in [-\pi, \pi]} \lambda_{\min} \left( \begin{bmatrix} D_f \\ N_f \end{bmatrix} \Psi_{f/f}^{-1} S_f \right) \|r^t\| = \kappa \|r^t\|, \quad (\text{C.11})$$

where the positive real  $\delta \in (0, 1]$  accounts for the truncation effects on the  $l_2$ -norm and  $\lambda_{\min}(M)$  stands for the least singular value of the polynomial matrix  $M(d)$ . Further,  $\kappa > 0$



Appendix C. Proofs

as  $S_f$  has no root on the unit circle,  $N_f$  and  $D_f$  having strictly Schur greatest common right divisor (g.c.r.d.). Hence, recalling (C.9), boundedness of  $\Pi_f(t)$  as  $t \rightarrow \infty$  follows at once.  $\square$

**Proof of Theorem 3.4.2.**

With obvious meaning of symbols, we refer to  $\zeta_i$  in place of  $\zeta i/i$  (and so  $\tilde{\zeta}_i$  in place of  $\tilde{\zeta} i/i$ ) to account for the non-square case. Hence, exploiting the results of Theorem 3.4.1 we obtain that switching stops onto some candidate controller  $\mathcal{C}_f$ , and  $\Lambda_f^{1/2}(t) \leq \kappa_1$  for some positive real  $\kappa_1$ . By virtue of the design conditions **a4** and **a5**,  $\zeta_f(\cdot)$  converges to zero, and, hence,  $\|\zeta_f^t\| \leq \kappa_2$  for some positive real  $\kappa_2$ <sup>2</sup>. By triangular inequality, we obtain

$$\|\zeta^t\| \leq \kappa_1 (1 + \kappa_2) =: \kappa \quad (\text{C.12})$$

from which we conclude that  $\zeta(\cdot)$  converges to zero. This proves the offset-free tracking property.

As for input-output  $l_2$ -stability, notice first that (C.12) implies

$$\text{i) } \|y^t\| \leq \kappa + \|r^t\|;$$

$$\text{ii) } \|\eta^t\| \leq \kappa.$$

By Bezout identity, **a3** implies the existence of two polynomial matrices  $J_1(\theta)$  and  $J_2(\theta)$  such that

$$\Phi J_1(\theta) + J_2(\theta) B(\theta) = I \quad (\text{C.13})$$

Multiplying both the sides of (C.13) by  $u$ , we get  $J_1(\theta) \eta + J_2(\theta) A(\theta) y = u$ . By combining the last equality with i) and ii), we obtain the desired result.  $\square$

---

<sup>2</sup>Notice that, in the general case of non-square systems, necessary condition for asymptotic tracking is that  $m \geq p$ .

**PART II**  
**Control Transfer**

## Chapter 4

# Performance-Oriented Transfer for Model-based Switching Schemes

In adaptive switching control, most of the attention has been devoted to the study of strategies for on-line controller selection -see [Lib03] for a rather recent survey on the topic. On the other hand, very few schemes have been proposed to properly handle the transitions between controllers. In different contexts, the issue of how to transfer between controllers has received a lot of attention from the research community over the last decades. More specifically, there have been numerous approaches aimed at minimizing or reducing the bumps in the control signal after switching, namely *bumpless transfer* [AW96, TW00, ZT02, ZT05, CS06]. In the literature, such approaches are mainly motivated by the goal of ensuring smooth control transitions between stabilizing controllers. However, similarly to fault-tolerant control, adaptive switching control is mainly concerned with the case where the process dynamics can vary and produce abrupt and significant performance degradations of the feedback loop, indeed suddenly unstable closed-loops. In such a context, the primary goal of controller switching is to promptly recover an adequate input/output process behavior, not to assure smooth control transitions. Approaches aimed at enhancing the closed-loop performance (for example, improving tracking output performance), rather than assuring smooth control transitions, have been proposed in the literature, and they are usually referred to as *conditioning* techniques [HKH87, PVHW88, YQK10]. Their main positive feature is the simple design procedure as well as the moderate computational burden, the latter being an important factor for real-time implementation when the number

of controllers is large. Actually, also the bumpless transfer approach in [TW00] could be regarded as a conditioning technique. It indeed reduces to the Hanus's conditioning scheme under particular assumptions and conditions. However, the key aspect of conditioning is the process-independent formulation of the control transfer problem (indeed, they are also referred to as *self-conditioning* techniques). Although such a feature may look appealing from a conceptual point of view, it has to be expected that definite performance improvements can be effectively achieved only if a set of models approximating the process uncertainty is available and suitably exploited. Note that, in adaptive switching control, the main motivation for resorting to multiple models architectures is indeed essentially identical, see [ABLM01, BBMT10] for a detailed discussion of this point.

More technically, the “bump phenomenon” is known to be directly related to the initial value of the output of the off-line controller to be switched on as compared to that of the on-line controller at the switching instant. Clearly, when these two output signals are equal or very close, “almost continuity” of the signal at the process input is achieved, thereby allowing a smooth transition where undesirable transients are avoided or minimized. It has been recognized that the bump phenomenon originating from the mismatch between controllers outputs can be translated into conditions on the controllers states. Indeed, controllers being dynamical systems, their state must have the correct value when a (closed loop mode) switching occurs, and if this is not the case, the corresponding control loops experience undesirable and harmful switching transients.

This chapter deals with a model-based control transfer approach which has been thought to be well suited for ASC schemes, along with both set-point regulation and tracking problems [BMMT]. The solution is realized via shared-state multicontroller architecture, described in Section 4.2, equipped with a suitable controller state reset map, as in classical initial value compensation / controller state resetting schemes [Joh00, PHGne]. The reinitialization of the common state is active at each switch-on time and depends *affinely*, by a pre-computed set of constant gains, on the same closed-loop data as the ones in input to the supervisor, thus not requiring additional information. Sections 4.3 and 4.4 describe how to obtain such a set of gains by solving *off-line* performance-oriented control problems suitably defined. More specifically, the candidate feedback-gain matrices are the ones resulting from the steady-state response of the feedback loop made up by the switched-on controller

and the related process model. Accordingly, the multicontroller state is reinitialized so as to minimize the discrepancy between actual and steady-state closed-loop behaviors. The sense of the minimization is specified in Section 4.3 wherein an optimal reinitialization is achievable for the process, as it is supposed to be coincident with one of the available nominal models. Moreover, since ASC schemes are usually concerned with the case where the process uncertainty can not be completely represented by the model distribution, namely  $\Theta$  is a continuum or a discrete with too high cardinality, in Section 4.4 we discuss how the optimal solution can be suitably “robustified” so as to still provide explicit, though suboptimal, solutions, where only a finite number feedback-gain matrices is allowed such to allow the designer to trade off performance vs. memory savings and/or computational complexity. In Section 4.5 a numerical example is carried out which aims at showing the benefits of the optimal / robust solutions and also, a comparison with a pre-existing conditioning technique is discussed in Section 4.5.1. Before proceeding, Section 4.1 resumes the overall problem.

## 4.1 Overall Problem

The control framework is the same as the one described in Chapter 2. Hereafter, the interest refers to better characterize the multicontroller architecture and, more in general, how managing the transfer of the control action among controllers.

Since, in general, it is desired both to stabilize the process  $\mathcal{P}(\theta)$  and also to cause its output to track a prescribed reference trajectory, let the references vector  $r(t) \in \mathbb{R}^p$  be given by the autonomous LTI exosystem

$$\left. \begin{aligned} \eta(t+1) &= E \eta(t) \\ r(t) &= L \eta(t) \end{aligned} \right\} \quad (4.1)$$

such to satisfy the following assumption.

**a6.** The matrix  $E$  has eigenvalues on the unit circle with algebraic multiplicity one.

**Remark 4.1.1** Assumption **a6** addresses the problem of output regulation (sometimes known as *generalized tracking problem*), which can be found discussed more in detail in [IMS03]. In broad terms, such assumption refers to a subset of all the bounded sequences, namely, the ones generated by a linear model with simple eigenvalues on the unit circle.

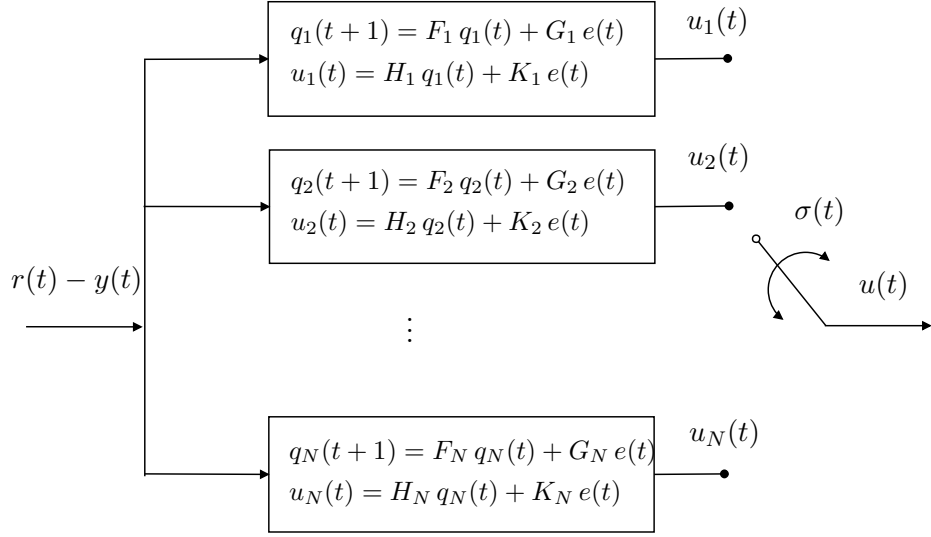


**Figure 4.1:** Multi-system controller realization.

Notice that the autonomous system in (4.1) can be represented in terms of autonomous difference equations through the polynomial matrix  $\Phi(d)$ , as defined in (3.31). Then, by assuming condition **a3** of Section 3.4.1 holds, controllers exist such to guarantee asymptotic tracking. Also, the family of candidate controllers can be designed according to the conditions **a4** and **a5**.

Next section accounts for how implementing the multicontroller system.

## 4.2 State-shared multicontroller implementation

The switching scheme developed in Chapter 3 hinges upon the multicontroller  $\mathcal{C}_{\sigma(\cdot)}$  in (3.5). As shown in Figure 3.1, the classical approach to implement  $\mathcal{C}_{\sigma(\cdot)}$  consists in placing each of the *latent* controllers under separate feedbacks, as a typical *multi-system architecture* [AW97]. In broad terms, at every time, the supervisor selects one of the controllers in  $\mathcal{C}$ , while the other ones operate in stand-by mode driven by the signal  $(r - y)$ . This take inevitably to precondition their state vectors, namely  $q_i$ ,  $i \in \overleftarrow{N}$ , before the switch-on time. The multicontroller resulting from a multi-system architecture is depicted in Figure 4.1, where  $\{F_i, G_i, H_i, K_i\}$  represents a state-space realization of the  $i$ -th controller  $\mathcal{C}_i$ ,  $i \in \overleftarrow{N}$ .

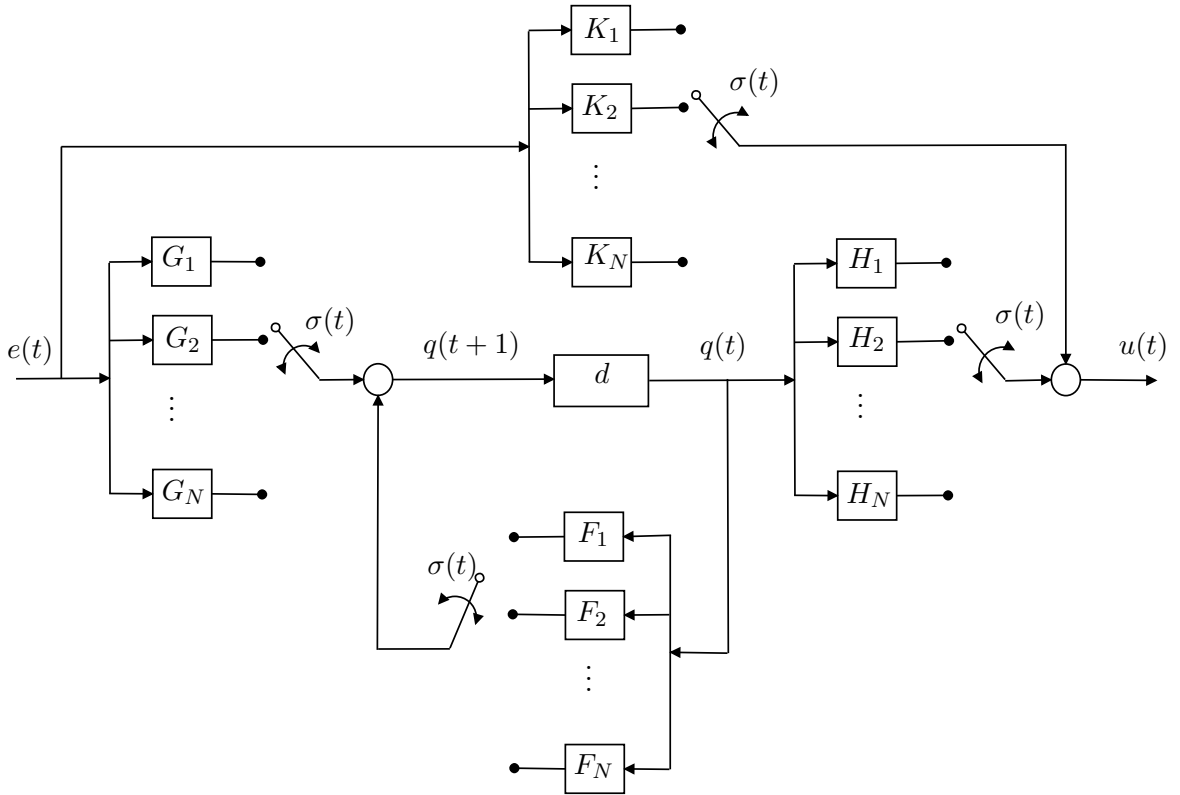


**Figure 4.2:** Hybrid linear controller realization.

As it is possible to see, the reason why the multi-system architecture is impractical is twofold: first, it is advisable to simplify the implementation by avoiding to run the  $N$  controllers  $\mathcal{C}_i$ ; even more importantly, in order to make computations numerically possible, it is required that each controller – whether or not in charge of the process – run in a stable fashion, *i.e.*  $F_i$ 's have to be strictly Schur matrices. Also, as widely discussed in [YQK07], multi-system architecture suggests to derive bumpless / conditioning transfer schemes, see [GA96, TW00, GL95, ZT02, ZT05], where the state of each idle controller is forced to evolve in an appropriate way, usually to achieve some optimal goals, by appending the controller with additional circuitry. Clearly, such solutions become cumbersome and hard to implement when the number of controller is large.

A more convenient way to implement the multicontroller  $\mathcal{C}_{\sigma(\cdot)}$ , whose idea is illustrated in Figure 4.2, consists in realizing a *hybrid linear system* as the following

$$\left. \begin{aligned} q(t+1) &= F_{\sigma(t)} q(t) + G_{\sigma(t)} e(t) \\ u(t) &= H_{\sigma(t)} q(t) + K_{\sigma(t)} e(t) \end{aligned} \right\} \quad (4.2)$$

which has the peculiarity to share a state vector  $q(t)$  and, the control transfer reduces to switch a number of feedback gain matrices according to the switching sequence  $\sigma(t)$ , dictated by the supervisory unit. Architecture as in (4.2), known also as *state-sharing* multirealizations [Mor95, SAB06], are commonly used for supervisory control of sampled-data systems [BBMT10, BMST10, CHP04, ZMF00] since, though not reflecting optimal-oriented features, possess a number of desirable properties. First, they allow the use of unstable candidate controllers, since there is no need to implement each candidate controller as a single dynamical system; second, they need of low computational load, the computational cost being invariant to the number of candidate controllers.

In the present case, where the controllers are available by an input-output description, each one being defined through MFDs as in (2.4), a possible state vector can be defined as follows

$$q(t) := [e(t-1)' \ \cdots \ e(t-n_c)' \ u(t-1)' \ \cdots \ u(t-n_c)']', \quad (4.3)$$

where  $e(t) := r(t) - y(t)$  is the tracking error,  $n_c := \max_{i \in \overline{N}} \{\deg S_i, \deg R_i\}$ , with  $\deg M$  standing for the highest degree of all the entries of  $M(d)$ . Accordingly, the output of the multicontroller can be thought as the one of a linear regression obtained by

$$\mathcal{C}_{\sigma(t)}(e)(t) := [\mathcal{S}_{\sigma(t)1} \ \cdots \ \mathcal{S}_{\sigma(t)n_c} \ -\mathcal{R}_{\sigma(t)1} \ \cdots \ -\mathcal{R}_{\sigma(t)n_c}] q(t) + \mathcal{S}_{\sigma(t)0} e(t), \quad (4.4)$$



which has an equivalent realization in the state-space form provided that the matrices  $F_i$ ,  $G_i$ ,  $H_i$  and  $K_i$  assume the form

$$\left. \begin{array}{l}
 F_i = \left[ \begin{array}{c|c|c|c}
 0_p & \cdots & 0_p & 0_p \\
 \hline
 & & & 0_p \\
 & I_{(n_c-1)p} & & \vdots \\
 & & & 0_p \\
 \hline
 \mathcal{S}_{i1} & \cdots & \mathcal{S}_{i(n_c-1)} & \mathcal{S}_{in_c} \\
 \hline
 & & & -\mathcal{R}_{i2} \cdots -\mathcal{R}_{i(n_c-1)} \\
 & & & -\mathcal{R}_{in_c} \\
 \hline
 & & & 0_p \\
 & & & \vdots \\
 & & & 0_p \\
 \hline
 \mathcal{S}_{i1} & \cdots & \mathcal{S}_{i(n_c-1)} & \mathcal{S}_{in_c} \\
 \hline
 & & & -\mathcal{R}_{i2} \cdots -\mathcal{R}_{i(n_c-1)} \\
 & & & -\mathcal{R}_{in_c}
 \end{array} \right] &
 G_i = \left[ \begin{array}{c}
 I_p \\
 0_p \\
 \vdots \\
 0_p \\
 \hline
 \mathcal{S}_{i0} \\
 \hline
 0_p \\
 \vdots \\
 0_p \\
 \hline
 \mathcal{S}_{i0}
 \end{array} \right] \\
 H_i = \left[ \begin{array}{c|c|c|c}
 0_p & \cdots & 0_p & 0_p \\
 \hline
 & & & 0_p \\
 & I_{(n_c-1)p} & & \vdots \\
 & & & 0_p \\
 \hline
 \mathcal{S}_{i1} & \cdots & \mathcal{S}_{i(n_c-1)} & \mathcal{S}_{in_c} \\
 \hline
 & & & -\mathcal{R}_{i2} \cdots -\mathcal{R}_{i(n_c-1)} \\
 & & & -\mathcal{R}_{in_c} \\
 \hline
 & & & 0_p \\
 & & & \vdots \\
 & & & 0_p \\
 \hline
 \mathcal{S}_{i1} & \cdots & \mathcal{S}_{i(n_c-1)} & \mathcal{S}_{in_c} \\
 \hline
 & & & -\mathcal{R}_{i2} \cdots -\mathcal{R}_{i(n_c-1)} \\
 & & & -\mathcal{R}_{in_c}
 \end{array} \right] &
 K_i = \left[ \begin{array}{c}
 I_p \\
 0_p \\
 \vdots \\
 0_p \\
 \hline
 \mathcal{S}_{i0} \\
 \hline
 0_p \\
 \vdots \\
 0_p \\
 \hline
 \mathcal{S}_{i0}
 \end{array} \right]
 \end{array} \right\} \quad (4.5)$$

with  $i \in \overleftarrow{N}$ .

**Remark 4.2.1** In case  $n_{s_i} := \deg S_i < n_c$  and/or  $n_{r_i} := \deg R_i < n_c$  for some  $i$ , implementation (4.5) is obtained by simply setting  $\mathcal{S}_{in_c-j} = 0$ ,  $j = 0, \dots, (n_c - n_{s_i} - 1)$  and, consistently,  $\mathcal{R}_{in_c-k} = 0$ ,  $k = 0, \dots, (n_c - n_{r_i} - 1)$ .

**Remark 4.2.2** Multicontroller scheme similar to (4.2) have been proposed in [BMM99, TWY07]. A different approach is also adopted in [BF08], where the controller state is reset to zero at each switching time. However, such techniques do not follow any performance-oriented strategy for the control transfer.

**Remark 4.2.3** Notice that the state-space realization (4.5) provides an equivalent description, in terms of input-output behavior, of the left MFD of the controller  $\mathcal{C}_i$ , see (2.4). Given a family  $\mathcal{C}$  of stabilizable and detectable controllers  $\mathcal{C}_i$  as defined in (2.4), *i.e.* such that  $R_i(d)$  and  $S_i(d)$  have strictly Schur g.l.c.d., then the state-space representations  $\{F_i, G_i, H_i, K_i\}$ ,  $i \in \overleftarrow{N}$ , are stabilizable and detectable as well. In particular, the eigenvalues of  $F_i$  contain the roots of the determinant of  $R_i(z)$ , with  $z = d^{-1}$  here assumed to be the unit forward shift operator, and extra unobservable eigenvalues in  $z = 0$ . If  $R_i(d)$  and  $S_i(d)$  are coprime, then  $(F_i, G_i)$  is reachable [Mos95].

Prompted by these observations, the goal is to propose a performance-oriented approach for the control transfer which, while optimizing an engineering significant performance index, preserve all desirable features of the hybrid linear architectures described

above. More specifically, we propose a model-based approach to the control transfer, which exploits the nominal models available to the supervisory unit and aims at resetting the state of the multicontroller so as to optimize (in a sense to be defined) the closed-loop transient response by using the available input-output process data, along with the state of the exosystem in (4.1).

### 4.3 Optimal conditioning

In this section the best possible scenario is first considered. Let the process  $\mathcal{P}(\theta)$  coincide with the one of the nominal models, namely  $\mathcal{P}(\theta) = \mathcal{M}_i$  and, at the time  $t_s$ , the supervisory unit switches-on the corresponding controller  $\mathcal{C}_i$ , so that  $\mathcal{C}_i$  is placed in feedback with the process after  $t_s$ .

To cope with this situation where the input-output process data are available <sup>1</sup>, an equivalent description, in terms of input-output behavior, of the process MFDs defined in (2.2) can be derived. Along the same lines as before, the input-output process behavior can be represented by the following state-space system

$$\left. \begin{aligned} x(t+1) &= \mathcal{A}_i x(t) + \mathcal{B}_i u(t) \\ y(t) &= \mathcal{C}_i x(t) \end{aligned} \right\} \quad (4.6)$$

where the state vector assumes of the form

$$x(t) := [u(t-1)' \ \cdots \ u(t-n_p)' \ y(t-1)' \ \cdots \ y(t-n_p)']' \quad (4.7)$$

---

<sup>1</sup>This is an usual situation in adaptive/fault-tolerant control, the process state being not accessible in many applications.

with  $n_p := \max_{i \in \overleftarrow{N}} \{\deg A_i, \deg B_i\}$  and, accordingly, the dynamics matrices are as follows

$$\left. \begin{array}{l}
 \mathcal{A}_i = \left[ \begin{array}{c|c|c|c}
 0_p & \cdots & 0_p & 0_p \\
 \hline
 & & & 0_p \\
 & I_{(n_p-1)p} & & \vdots \\
 & & & 0_p \\
 \hline
 \mathcal{B}_{i1} & \cdots & \mathcal{B}_{i(n_p-1)} & \mathcal{B}_{in_p} \\
 \hline
 & & -\mathcal{A}_{i2} & \cdots & -\mathcal{A}_{i(n_p-1)} & -\mathcal{A}_{in_p} \\
 \hline
 & & & & & 0_p \\
 & 0_{(n_p-1)p} & & & I_{(n_p-1)p} & \vdots \\
 & & & & & 0_p
 \end{array} \right] & \mathcal{B}_i = \left[ \begin{array}{c}
 I_p \\
 \hline
 0_p \\
 \vdots \\
 \hline
 0_p \\
 \hline
 0_p \\
 \hline
 0_p \\
 \vdots \\
 \hline
 0_p
 \end{array} \right] \\
 \mathcal{C}_i = \left[ \mathcal{B}_{i1} \cdots \mathcal{B}_{i(n_p-1)} \mid \mathcal{B}_{in_p} \mid -\mathcal{A}_{i2} \cdots -\mathcal{A}_{i(n_p-1)} \mid -\mathcal{A}_{in_p} \right]
 \end{array} \right\} \quad (4.8)$$

**Remark 4.3.1** Same considerations as in Remark 4.2.1 can be done also for state-space realization in (4.8).

The solution, which will be developed in the sequel, consists in resetting the multicontroller state in (4.2) at switching time  $t_s$  in such a way that the future behavior of the current closed-loop  $(\mathcal{P}(\theta)/\mathcal{C}_i)$ , where the process  $\mathcal{P}(\theta)$  is supposed to be coincident with the model  $\mathcal{M}_i$ , be as close as possible, in a sense to be specified, to the desired offset-free steady-state behavior of the loop  $(\mathcal{M}_i/\mathcal{C}_i)$ .

Let

$$w(t) := \begin{bmatrix} x(t) \\ q(t) \end{bmatrix}, \quad \text{and} \quad z(t) := \begin{bmatrix} u(t) \\ e(t) \end{bmatrix} \quad (4.9)$$

denote, respectively, the state and the output vectors of the closed-loop switched system  $(\mathcal{P}(\theta)/\mathcal{C}_{\sigma(\cdot)})$ , defined in (3.5). Then, the time evolution of such vectors starting from the switching time  $t_s$  can be described by the following state-space system

$$\left. \begin{array}{l}
 w(t+1) = \mathcal{A}_i^{cl} w(t) + \mathcal{B}_i^{cl} r(t) \\
 z(t) = \mathcal{C}_i^{cl} w(t) + \mathcal{D}_i^{cl} r(t) \\
 w(t_s) = \begin{bmatrix} x(t_s) \\ q(t_s) \end{bmatrix}
 \end{array} \right\} \quad (4.10)$$

where  $t \in \mathbb{Z}_{t_s} := \{t_s, t_s + 1, \dots\}$  and, the matrices  $\mathcal{A}_i^{cl}$ ,  $\mathcal{B}_i^{cl}$ ,  $\mathcal{C}_i^{cl}$  and  $\mathcal{D}_i^{cl}$ , characterizing the closed-loop behavior, assume the form

$$\left[ \begin{array}{c|c} \mathcal{A}_i^{cl} & \mathcal{B}_i^{cl} \\ \hline \mathcal{C}_i^{cl} & \mathcal{D}_i^{cl} \end{array} \right] := \left[ \begin{array}{cc|c} \mathcal{A}_i - \mathcal{B}_i K_i \mathcal{C}_i & \mathcal{B}_i H_i & \mathcal{B}_i K_i \\ -G_i \mathcal{C}_i & F_i & G_i \\ \hline -K_i \mathcal{C}_i & H_i & K_i \\ -\mathcal{C}_i & 0 & I \end{array} \right] \quad (4.11)$$

As known, see [IMS03], the controller  $\mathcal{C}_i$  solves the output regulation problem <sup>2</sup>, for each initial condition  $(x(t_s), q(t_s), \eta(t_s))$ , if and only if the Sylvester equation

$$\mathcal{A}_i^{cl} \begin{bmatrix} X_i \\ Q_i \end{bmatrix} + \mathcal{B}_i^{cl} L = \begin{bmatrix} X_i \\ Q_i \end{bmatrix} E \quad (4.12)$$

admits an unique solution  $[X_i' \ Q_i']'$  such that

$$0_p = -\mathcal{C}_i X_i + L \quad (4.13)$$

holds. In (4.12), uniqueness of  $[X_i' \ Q_i']'$  stems from the fact that the spectra (consisting in set of eigenvalues) of  $\mathcal{A}_i^{cl}$  and  $E$  are disjoint by hypothesis,  $\mathcal{A}_i^{cl}$  being a stability matrix by construction (*cf.* Assumption **a5**) and  $E$  having all the eigenvalues on the unit circle (*cf.* Assumption **a6**) [OS62].

Define

$$\tilde{x}(t) := x(t) - X_i \eta(t), \quad \text{and} \quad \tilde{q}(t) := q(t) - Q_i \eta(t) \quad (4.14)$$

and, accordingly, consider

$$\tilde{w}(t) := \begin{bmatrix} \tilde{x}(t) \\ \tilde{q}(t) \end{bmatrix}. \quad (4.15)$$

---

<sup>2</sup>Given the system (4.6) with exosystem (4.1), the controller  $\mathcal{C}_i$ , with state-space realization  $\{F_i, G_i, H_i, K_i\}$ , is such that:

- (a) the closed-loop system (4.10) is asymptotically stable;
- (b) for every initial conditions  $(x(t_s), q(t_s), \eta(t_s))$

$$\lim_{t \rightarrow \infty} e(t) = 0$$

holds.

Then, in the new coordinates, the state equation in (4.10) becomes

$$\left. \begin{aligned} \tilde{w}(t+1) &= \mathcal{A}_i^{cl} \tilde{w}(t) \\ \tilde{w}(t_s) &= \begin{bmatrix} x(t_s) - X_i \eta(t_s) \\ q(t_s) - Q_i \eta(t_s) \end{bmatrix} \end{aligned} \right\} \quad (4.16)$$

Since  $A_i^{cl}$  is a stability matrix, one has that

$$\lim_{t \rightarrow \infty} \tilde{w}(t) = 0 \quad (4.17)$$

for every initial condition  $(x(t_s), q(t_s), \eta(t_s))$ . This corresponds to have process and controller states  $x(t)$  and  $q(t)$  converging, as  $t \rightarrow \infty$ , at the steady-state solutions  $\bar{x}(t) := X_i \eta(t)$  and  $\bar{q}(t) := Q_i \eta(t)$ , respectively, which values depend on the state of the exosystem at the time  $t_s$  as follows <sup>3</sup>

$$\left. \begin{aligned} \bar{x}(t) &= X_i E^{t-t_s} \eta(t_s) \\ \bar{q}(t) &= Q_i E^{t-t_s} \eta(t_s) \end{aligned} \right\} \quad (4.20)$$

Accordingly, the output vector of the closed-loop system  $z(t)$  converge to its steady-state value

$$\bar{z}(t) := \begin{bmatrix} \bar{u}(t) \\ \bar{e}(t) \end{bmatrix}, \quad (4.21)$$

which components are given by

$$\left. \begin{aligned} \bar{u}(t) &:= (K_i (-\mathcal{C}_i X_i + L) + H_i Q_i) \eta(t) \\ \bar{e}(t) &:= -(\mathcal{C}_i X_i - L) \eta(t) \end{aligned} \right\} \quad (4.22)$$

and, under the condition (4.13) <sup>4</sup>, one has

$$\left. \begin{aligned} \bar{u}(t) &= U_i \eta(t) = U_i E^{t-t_s} \eta(t_s) \\ \bar{e}(t) &= 0 \end{aligned} \right\} \quad (4.23)$$

---

<sup>3</sup>Steady-state solutions (4.20) derive from the condition (4.12), which expresses the existence of an invariant subspace for the closed-loop system

$$\left. \begin{aligned} \eta(t+1) &= E \eta(t) \\ w(t+1) &= \mathcal{A}_i^{cl} w(t) + \mathcal{B}_i^{cl} L r(t) \end{aligned} \right\} \quad (4.18)$$

having the form

$$\mathcal{V} = \left\{ (\eta, w) \mid w = \begin{bmatrix} X_i \\ Q_i \end{bmatrix} \eta \right\}, \quad (4.19)$$

and on which the restriction reduces to  $\eta(t+1) = E \eta(t)$  [IMS03].

<sup>4</sup>Note that condition (4.13) expresses the fact that the steady-state tracking error  $\bar{e}$  in (4.22) is zero at each point of the invariant subspace  $\mathcal{V}$ , defined in (4.19). Asymptotic tracking, namely  $\bar{e}(t) = 0$ , is actually

where  $U_i := H_i Q_i$ .

Thus, process / controller initial conditions  $(x(t_s), q(t_s))$  do not affect the regime behavior of (4.16); on the contrary, they determine its transient behavior  $\widehat{w}(t) = \mathcal{A}_i^{cl t - t_s} w(t_s)$ . Hereafter, the attention will be however focused on  $q(t_s)$ , which is the only free assignable variable, process and exosystem being not-manipulable dynamics systems. Indeed, the idea is the one to operate on the specific choice of  $q(t_s)$  in order to manage the transient behavior of closed-loop system  $(\mathcal{P}(\theta)/\mathcal{C}_i)$  after switching.

A suitable variable to account for the discrepancy, at time  $t$ , between the actual behavior from the steady-state (regime) behavior can be the following

$$\tilde{z}(t) := z(t) - \bar{z}(t) = \begin{bmatrix} u(t) - U_i \eta(t) \\ e(t) \end{bmatrix}. \quad (4.24)$$

Denote by  $(\tilde{w}(t, \xi), \tilde{z}(t, \xi))$  the solution pair resulting from (4.16) and (4.24) when the controller initial state  $q(t_s)$  is set to be equal to  $\xi$ . Also define

$$q^\circ(t_s) := F_{\sigma(t_s-1)} q(t_s - 1) + G_{\sigma(t_s-1)} e(t_s - 1) \quad (4.25)$$

which, in essence, coincides with the state of the multi-controller  $\mathcal{C}_{\sigma(\cdot)}$  in (4.2) at the time  $t_s$  in case no particular action (like state reset map) is applied when a switching occurs.

The performance index for control transfer to be minimized is as follows,

$$q(t_s) = \arg \min_{\xi} f(\xi), \quad (4.26a)$$

$$f(\xi) := \sum_{k=t_s}^{\infty} |\tilde{z}(k, \xi)|_{\Psi}^2 + |\xi - q^\circ(t_s)|_{\Omega}^2, \quad (4.26b)$$

where  $\Psi$  and  $\Omega$  are symmetric non-negative definite matrices,  $[\Psi \ \Omega] \neq 0$ , and  $|x|_{\Psi}^2 := x' \Psi x$ .

---

achieved if and only if the unique solution of (4.12) satisfies (4.13): (*if*) let initial condition  $(w(t_s), \eta(t_s))$  of (4.18) be in  $\mathcal{V}$ , then the corresponding trajectory  $\{(w(t), \eta(t)), \ t \geq t_s\}$  remains in  $\mathcal{V}$  and yields a copy of the trajectory of the exosystem  $\{\eta(t), \ t \geq t_s\}$ , which do not converge to  $(0, 0, 0)$  because the exosystem is neutrally stable (assumption **a6**). Thus, the only way of having asymptotic tracking is that  $\bar{e}(t)$ , as a function of  $\bar{w}(t)$ , is zero at any point of  $\mathcal{V}$ ; (*only if*) let initial condition  $(w(t_s), \eta(t_s))$  of (4.18) be outside  $\mathcal{V}$ , all trajectories of (4.18) converge, as  $t \rightarrow \infty$ , to  $\mathcal{V}$ , and hence yield a tracking error which asymptotically decays to zero. According to that, the steady-state process input turns out to be  $\bar{u}(t) = H_i Q_i \eta(t)$  and it is possible to show, that it coincides with the feed-forward control action capable of keeping  $e(t)$  identically at zero if the initial condition of (4.6), namely,  $x(t_s)$ , is set equal to  $X_i \eta(t_s)$  [IMS03].

**Remark 4.3.2** Appropriate choices of weighting matrices can be used to trade off high regulation performance vs. smooth control output signals. Indeed, the second term in the right-hand-side of (4.26) accounts for the discrepancy between  $\xi$  and the multi-controller state which would be obtained with no reinitialization procedure. A practical motivation for the presence of this term is that in model-based architectures the choice of  $\sigma(t_s)$  is often based on the outcome of a process-model *estimation* process. Since the smaller  $\Omega$  is, the more aggressive the control action turn out to be, the choice of  $\Omega$  should reflect the confidence in the switching decision strategy.

Let  $\mathcal{L}_i$  be the symmetric non-negative definite solution of the Lyapunov equation

$$(\mathcal{A}_i^{cl})' \mathcal{L}_i \mathcal{A}_i^{cl} + (\mathcal{C}_i^{cl})' \Psi \mathcal{C}_i^{cl} = \mathcal{L}_i, \quad (4.27)$$

which always exists unique being  $\mathcal{A}_i^{cl}$  a stability matrix. Let us partition  $\mathcal{L}_i$  as follows

$$\mathcal{L}_i = \left[ \begin{array}{c|c} \mathcal{L}_{1i} & \mathcal{L}_{2i} \\ \hline \mathcal{L}'_{2i} & \mathcal{L}_{3i} \end{array} \right], \quad (4.28)$$

the dimensions of blocks  $\mathcal{L}_{1i}$ ,  $\mathcal{L}_{2i}$  and  $\mathcal{L}_{3i}$  being in accordance with the ones in (4.11).

The main result of this section can be stated.

**Proposition 4.3.1** Let Assumption **a6** holds. Further, assume that  $\mathcal{A}_i^{cl}$  is a stability matrix and that the unique solution  $[X_i' Q_i']'$  of (4.12) satisfies (4.13). Then, the optimal solution  $q(t_s)$  of (4.26) always exists and satisfies

$$(\mathcal{L}_{3i} + \Omega) q(t_s) = \left[ \begin{array}{ccc} -\mathcal{L}'_{2i} & (\mathcal{L}_{3i} Q_i + \mathcal{L}'_{2i} X_i) & \Omega \end{array} \right] \left[ \begin{array}{c} x(t_s) \\ \eta(t_s) \\ q^\circ(t_s) \end{array} \right], \quad (4.29)$$

where  $\mathcal{L}_i$  is as in (4.27).

*Proof.* Consider the following state-space system

$$\left. \begin{array}{l} \tilde{w}(t+1, \xi) = \mathcal{A}_i^{cl} \tilde{w}(t, \xi) \\ \tilde{z}(t, \xi) = \mathcal{C}_i^{cl} \tilde{w}(t, \xi) \\ \tilde{w}(t_s, \xi) = \left[ \begin{array}{c} x(t_s) - X_i \eta(t_s) \\ \xi - Q_i \eta(t_s) \end{array} \right] \end{array} \right\} \quad (4.30)$$

for  $t \in \mathbb{Z}_{t_s}$ , which time evolution depends on the initial controller state  $\xi$ . Then, one has

$$\sum_{k=t_s}^{\infty} |\tilde{z}(k, \xi)|_{\Psi}^2 = \sum_{k=t_s}^{\infty} |\tilde{w}(k, \xi)|_{\Psi_i}^2 = |\tilde{w}(t_s, \xi)|_{\mathcal{L}_i}^2 \quad (4.31)$$

where  $\Psi_i := (\mathcal{C}_i^{cl})' \Psi \mathcal{C}_i^{cl}$  and  $\mathcal{L}_i$  is as in (4.27). Thus the objective function  $f(\xi)$  in (4.26b) can be rewritten as

$$f(\xi) = \begin{bmatrix} x(t_s) - X_i \eta(t_s) \\ Q_i \eta(t_s) - q^\circ(t_s) \\ \xi - Q_i \eta(t_s) \end{bmatrix}' \left[ \begin{array}{cc|c} \mathcal{L}_{1i} & 0 & \mathcal{L}_{2i} \\ 0 & \Omega & \Omega \\ \hline \mathcal{L}'_{2i} & \Omega & \mathcal{L}_{3i} + \Omega \end{array} \right] \begin{bmatrix} x(t_s) - X_i \eta(t_s) \\ Q_i \eta(t_s) - q^\circ(t_s) \\ \xi - Q_i \eta(t_s) \end{bmatrix} \quad (4.32)$$

and the result follows by equating to zero the gradient of (4.32) with respect to  $\xi$ . Note that (4.29) always admits a solution since  $\text{im}([\mathcal{L}'_{2i} \ \Omega]) \subseteq \text{im}([\mathcal{L}_{3i} \ \Omega])$ .  $\square$

Note that the solution of (4.29) is in general not unique. In fact, unless the couple  $(H_i, F_i)$  is observable, the matrix  $\mathcal{L}_{3i}$ , related to the Observability Gramian of the realization  $\{F_i, G_i, H_i, K_i\}$ <sup>5</sup>, turns out to be singular. However, all such solutions would yield the same input-output behavior. So, a particular solution of (4.29) is given by

$$q(t_s) = \Upsilon_i v(t_s), \quad (4.33)$$

where

$$\Upsilon_i = \begin{bmatrix} V_i & P_i & T_i \end{bmatrix}, \quad (4.34)$$

$$v(t_s) = \begin{bmatrix} x(t_s)' & \eta(t_s)' & q^\circ(t_s)' \end{bmatrix}', \quad (4.35)$$

with

$$\left. \begin{array}{l} V_i := -(\mathcal{L}_{3i} + \Omega)^\dagger \mathcal{L}'_{2i} \\ P_i := (I - T_i)Q_i - V_i X_i \\ T_i := (\mathcal{L}_{3i} + \Omega)^\dagger \Omega \end{array} \right\} \quad (4.36)$$

$M^\dagger$  denoting the Moore-Penrose inverse of the matrix  $M$ . Accordingly, the related optimal cost becomes

$$f(q(t_s)) = v(t_s)' \mathcal{G}'_i \Delta_i \mathcal{G}_i v(t_s), \quad (4.37)$$

---

<sup>5</sup>More specifically, one has

$$\mathcal{L}_{3i} = \sum_{k=t_s}^{\infty} (F_i^k)' H_i' \Psi H_i (F_i^k).$$



where

$$\Delta_i := \begin{bmatrix} \mathcal{L}_{1i} & 0 & \mathcal{L}_{2i} \\ 0 & \Omega & \Omega \\ \mathcal{L}'_{2i} & \Omega & \mathcal{L}_{3i} + \Omega \end{bmatrix}, \quad \text{and} \quad \mathcal{G}_i := \begin{bmatrix} I & -X_i & 0 \\ 0 & Q_i & -I \\ V_i & P_i - Q_i & T_i \end{bmatrix}.$$

Eventually, the proposed solution for the conditioning of the control transfer amounts to set the multi-controller  $\mathcal{C}_{\sigma(\cdot)}$  as in the following

$$\left. \begin{aligned} q(t) &= \begin{cases} \Upsilon_{\sigma(t)} v(t), & \text{if } \sigma(t) \neq \sigma(t-1) \\ q^\circ(t), & \text{otherwise} \end{cases} \\ u(t) &= H_{\sigma(t)} q(t) + K_{\sigma(t)} e(t) \\ q^\circ(t+1) &= F_{\sigma(t)} q(t) + G_{\sigma(t)} e(t) \end{aligned} \right\} \quad (4.38)$$

which results the same as (4.2) with an additional state reset map at the times of switching, namely at all  $t$ 's such that  $\sigma(t) \neq \sigma(t-1)$ .

**Remark 4.3.3** In case the state realization of the family of candidate controllers is as in (4.5), then the vector state  $q^\circ$  to be used in (4.38) is defined as follows

$$q^\circ(t) := [e(t-1)' \ \cdots \ e(t-n_c)' \ u(t-1)' \ \cdots \ u(t-n_c)']'. \quad (4.39)$$

**Remark 4.3.4** Note that  $q(t_s)$  in (4.33) depends *affinely* on the closed-loop data sequence  $v(t_s)$ , while the gain matrices  $V_i$ ,  $P_i$  and  $T_i$  can be pre-computed off-line for each reference-loop  $(\mathcal{M}_i/\mathcal{C}_i) \in \mathcal{F}$ . As a result, the new multi-controller can still be implemented as a hybrid linear system, see (4.38), with an additional computational cost only consisting of solving a matrix-vector product at each switching time. However, it has to be noted that (4.29) does not represent the optimal solution to the problem of minimizing the closed-loop transients after switching. It only yields the optimal controller state reset map. More general solutions for a similar problem have been considered in [TW00, ZT05]. Such solutions require the adoption of additional dynamic compensators, which must be active at all times, *i.e.* before, at and after switching. This kind of approach is hence typically not amenable to hybrid linear implementations and, it would be suitable for multi-system implementations even if, in such a case, the total computational cost usually became cumbersome as the number of candidate controllers would increase. Thereby, although potentially suboptimal with

respect to multi-system based approaches, where additional compensators run in parallel to the on/off-line controllers (to achieve the conditioning of the controllers states), the proposed solution turns out to be very low in computational load, thus simplifying the implementation for real-time operations.

### 4.3.1 Time-Weighted cost

Since the goal consists on reducing as much as possible the transient effects, the first samples of the sequence  $\tilde{z}_i(\xi)|_{t_s}^\infty$  may be more weighted into the cost (4.26b). In this respect, given  $\gamma \in (0, 1]$ , in place of  $\sum_{k=t_s}^\infty |\tilde{z}(k, \xi)|_\Psi^2$ , one can substitute an  $\gamma$ -exponentially weighted  $l_2$ -norm as follows:

$$\sum_{k=t_s}^\infty \gamma^{2(k-t_s)} |\tilde{z}(k, \xi)|_\Psi^2 . \quad (4.40)$$

By defining the new vector  $\tilde{w}_\gamma(t, \xi) := \gamma^{(t-t_s)} \tilde{w}(t, \xi)$ , one has that (4.30) becomes

$$\left. \begin{aligned} \tilde{w}_\gamma(t+1, \xi) &= \gamma \mathcal{A}_i^{cl} \tilde{w}_\gamma(t, \xi) \\ \gamma^{(t-t_s)} \tilde{z}(t, \xi) &= \mathcal{C}_i^{cl} \tilde{w}_\gamma(t, \xi) \\ \tilde{w}_\gamma(t_s, \xi) &= \tilde{w}(t_s, \xi) \end{aligned} \right\} \quad (4.41)$$

with  $t \in \mathbb{Z}_{t_s}$  and, the solution to the problem (4.26) continues to be provided by (4.29) where the matrix  $\mathcal{L}_i$ , see (4.28), turns out to be computed through the Lyapunov equation as follows

$$(\mathcal{A}_i^{cl})' \gamma \mathcal{L}_i \gamma \mathcal{A}_i^{cl} + (\mathcal{C}_i^{cl})' \Psi \mathcal{C}_i^{cl} = \mathcal{L}_i . \quad (4.42)$$

## 4.4 Robust Conditioning

The foregoing developments consider the ideal case of exact-match of the process with one of the nominal models. Such a case applies to situations where the process can take on a finite number of possible configurations and so, if the supervisory unit selects the right controller, the state reset obtained by (4.33) yields the best transient in terms of the cost (4.26b). However, although this is a subject of interest in the study of the so-called switched systems, in many practical situations, like adaptive/fault tolerant control problems, the exact-match between process and model is not realistic. Indeed, if the process does not belong to the model distribution  $\mathcal{M}$  (see (2.7)), the use of the state reset (4.33) turns out to return a suboptimal solution. This scenario occurs when each controller takes

care of more than one process configuration. Hereafter, let us assume that a finite cover for  $\Theta$  exists as follows

$$\Theta \subset \bigcup_{i=1}^N \Theta_i, \quad (4.43)$$

where  $\Theta_i$  is the region associated to  $\mathcal{C}_i$ , *i.e.* such that the closed-loop system  $(\mathcal{P}(\theta)/\mathcal{C}_i)$  is internally stable for all  $\theta \in \Theta_i$ . In this case, the supervisor allows only to restrict the uncertainty region where the process could be in. Indeed, it may be impossible, if  $\Theta$  is a continuum, or not convenient, if  $\Theta$  is a discrete with too high cardinality, to store in the computer memory one nominal model for each process parameter  $\theta$ , along with (in case) the related controller.

The idea to deal with the control transfer in case of large process uncertainty consists in optimizing the choice of the gain matrices for the state reset map directly with respect to the uncertainty subsets, namely for each controller  $\mathcal{C}_i$  we will consider the corresponding  $\Theta_i$ . Hence, in this section the scenario is the following. Given the process  $\mathcal{P}(\theta)$  with  $\theta \in \Theta_i$ , at the time  $t_s$ , the supervisory unit switches-on the corresponding controller  $\mathcal{C}_i$ , which is placed in feedback with the process after the switching <sup>6</sup>.

By the arguments of Section 4.3, for any  $\theta \in \Theta_i$ , the optimal multi-controller state resetting is given by the vector

$$q(t_s) = \Upsilon_i(\theta) v(t_s) \quad (4.44)$$

with  $\Upsilon_i(\theta) = [V_i(\theta)' \ P_i(\theta)' \ T_i(\theta)']'$ , which matrix components result from (4.36), solved with respect to the closed-loop  $(\mathcal{P}(\theta)/\mathcal{C}_i)$ . Hence, the cost achieves the optimal value

$$f(\Upsilon_i(\theta) v(t_s)) = v(t_s)' \mathcal{G}_i(\theta)' \Delta_i(\theta) \mathcal{G}_i(\theta) v(t_s), \quad (4.45)$$

where

$$\Delta_i(\theta) := \begin{bmatrix} \mathcal{L}_{1i}(\theta) & 0 & \mathcal{L}_{2i}(\theta) \\ 0 & \Omega & \Omega \\ \mathcal{L}_{2i}(\theta)' & \Omega & \mathcal{L}_{3i}(\theta) + \Omega \end{bmatrix}, \quad \text{and} \quad \mathcal{G}_i(\theta) := \begin{bmatrix} I & -X_i(\theta) & 0 \\ 0 & Q_i(\theta) & -I \\ V_i(\theta) & P_i(\theta) - Q_i(\theta) & T_i(\theta) \end{bmatrix},$$

with  $[X_i(\theta)' \ Q_i(\theta)']'$  and  $\mathcal{L}_i(\theta)$  being solutions of (4.12)-(4.13) and (4.27), respectively, both solved with respect to  $(\mathcal{P}(\theta)/\mathcal{C}_i)$ .

---

<sup>6</sup>Given a set  $\Theta_i$ , sufficient conditions exist on  $\mathcal{P}(\theta)$  under which  $\mathcal{C}_i$  solves the output regulation problem for any value of  $\theta \in \Theta_i$ . In turns, the result stems from a sort of “robustification” of conditions (4.12) and (4.13). The interested reader is referred to [IMS03].

**Remark 4.4.1** Since  $\mathcal{L}_i(\theta)$ , where

$$\mathcal{L}_i(\theta) = \left[ \begin{array}{c|c} \mathcal{L}_{1i}(\theta) & \mathcal{L}_{2i}(\theta) \\ \hline \mathcal{L}_{2i}(\theta)' & \mathcal{L}_{3i}(\theta) \end{array} \right],$$

if it exists, is related to the Observability Gramian of the closed-loop system  $(\mathcal{P}(\theta)/\mathcal{C}_i)$  and  $\Omega$  is symmetric and non-negative definite, then it is possible to show that, by construction, also  $\Delta_i(\theta)$  continues to be symmetric non-negative definite. Accordingly the cost as in (4.44) is non-negative, *i.e.*  $f(\Upsilon_i(\theta) v(t_s)) \geq 0$  for each  $\theta \in \Theta_i$  and finite-value vector  $v(t_s)$ .

More realistically, consider a reinitialization gain matrix  $\tilde{\Upsilon}_i := \begin{bmatrix} \tilde{V}_i & \tilde{P}_i & \tilde{T}_i \end{bmatrix}$  which is common for all  $\theta \in \Theta_i$ . Then, the cost related to the actual process  $\mathcal{P}(\theta)$  resulting from the state resetting by the vector  $\tilde{\Upsilon}_i v(t_s)$  turns out to be

$$f(\tilde{\Upsilon}_i v(t_s)) = v(t_s)' \tilde{\mathcal{G}}_i(\theta)' \Delta_i(\theta) \tilde{\mathcal{G}}_i(\theta) v(t_s), \quad (4.46)$$

with

$$\tilde{\mathcal{G}}_i(\theta) := \begin{bmatrix} I & -X_i(\theta) & 0 \\ 0 & Q_i(\theta) & -I \\ \tilde{V}_i & \tilde{P}_i - Q_i(\theta) & \tilde{T}_i \end{bmatrix}. \quad (4.47)$$

**Remark 4.4.2** As widely discussed in the Section 4.3, the choice of  $q(t_s)$  does not affect the regime behavior of the system  $(\mathcal{P}(\theta)/\mathcal{C}_i)$ , provided that  $\mathcal{C}_i$  solves the output regulation problem. According to that, one has  $f(\tilde{\Upsilon}_i v(t_s)) < \infty$  for any possible choice of  $\tilde{\Upsilon}_i$ .

The use of  $\tilde{\Upsilon}_i$  in place of  $\Upsilon_i(\theta)$  takes to a degradation on the transient performance after the switching. Indeed, one has that

$$f(\tilde{\Upsilon}_i v(t_s)) \geq f(\Upsilon_i(\theta) v(t_s)) \quad (4.48)$$

holds for each  $\theta \in \Theta_i$  and finite-value vector  $v(t_s)$ ,  $\Upsilon_i(\theta) v(t_s)$  being the optimal solution. Let us define the performance loss function  $l_i(\cdot)$  related to  $\Theta_i$ , due to replacing  $\Upsilon_i(\theta)$  with  $\tilde{\Upsilon}_i$ , as follows

$$l_i(\theta) := f(\tilde{\Upsilon}_i v(t_s)) - f(\Upsilon_i(\theta) v(t_s)) \quad (4.49)$$

which has the feature to be non-negative definite and upper-bounded for each  $\theta \in \Theta_i$ , *i.e.*  $\infty > l_i(\theta) \geq 0$  with  $\theta \in \Theta_i$ . By simple algebra, we can write

$$l_i(\theta) = v(t_s)' \mathcal{D}_i(\theta) v(t_s) \quad (4.50)$$

where

$$\mathcal{D}_i(\theta) := \tilde{\mathcal{G}}_i(\theta)' \Delta_i(\theta) \tilde{\mathcal{G}}_i(\theta) - \mathcal{F}_i(\theta), \quad \text{and} \quad \mathcal{F}_i(\theta) := \mathcal{G}_i(\theta)' \Delta_i(\theta) \mathcal{G}_i(\theta), \quad (4.51)$$

and so we obtain

$$l_i(\theta) \leq \lambda_{\max}(\mathcal{D}_i(\theta)) \|v(t_s)\|^2, \quad \theta \in \Theta_i, \quad (4.52)$$

with  $\lambda_{\max}(M)$  standing for the maximum eigenvalue of  $M$ ,  $\mathcal{D}_i(\theta)$  being a real symmetric matrix. Accordingly, in order to reduce as much as possible the performance degradation  $l_i(\theta)$ , the reinitialization gain matrix related to  $\Theta_i$  can be determined via the following optimization problem

$$\Upsilon_i(\Theta_i) = \arg \inf_{\Upsilon_i} \gamma_i, \quad \text{subject to} \quad (4.53a)$$

$$\left. \begin{array}{l} \lambda_{\max}(\mathcal{D}_i(\theta)) < \gamma_i, \quad \forall \theta \in \Theta_i \\ \gamma_i > 0 \end{array} \right\} \quad (4.53b)$$

and the robust solution of (4.26) turns out to be obtained as

$$q(t_s) = \Upsilon_i(\Theta_i) v(t_s). \quad (4.54)$$

Note that the first condition in (4.53b) can be equivalently set as follows

$$\gamma_i I + \mathcal{F}_i(\theta) - \tilde{\mathcal{G}}_i(\theta)' \Delta_i(\theta) \tilde{\mathcal{G}}_i(\theta) \succ 0, \quad \theta \in \Theta_i. \quad (4.55)$$

**Remark 4.4.3** Condition (4.55) derives from the following arguments. Given (4.52) and the first of (4.53b), one have that

$$v(t_s)' \mathcal{D}_i(\theta) v(t_s) \leq v(t_s)' (\lambda_{\max}(\mathcal{D}_i(\theta)) I) v(t_s) < v(t_s)' (\gamma_i I) v(t_s)$$

holds for all  $\theta \in \Theta_i$  and finite-value vectors  $v(t_s)$ , accordingly  $v(t_s)' (\mathcal{D}(\theta) - \gamma_i I) v(t_s) < 0$ . Then  $(\mathcal{D}(\theta) - \gamma_i I) \prec 0$  holds for all  $\theta \in \Theta_i$ .

Notice that, by means of standard manipulations, the first condition in (4.53b) can be expressed as a Linear Matrix Inequality (LMI) constraint with respect to  $\tilde{V}_i$ ,  $\tilde{P}_i$ ,  $\tilde{T}_i$  and the optimization problem (4.53) can be formulated as follows

$$\Upsilon_i(\Theta_i) = \arg \inf_{\tilde{\Upsilon}_i} \gamma_i, \quad \text{subject to} \quad (4.56a)$$

$$\left[ \begin{array}{cc|c} \gamma_i I + \mathcal{F}_i(\theta) & \tilde{\mathcal{G}}_i(\theta)' \mathcal{H}(\theta)' & 0 \\ \mathcal{H}(\theta) \tilde{\mathcal{G}}_i(\theta) & I & \\ \hline & 0 & \gamma_i \end{array} \right] \succ 0, \quad \forall \theta \in \Theta_i, \quad (4.56b)$$

with  $\mathcal{H}_i(\theta) := (\Delta_i(\theta))^{1/2}$ . More specifically, condition (4.56b) is a direct consequence of the Schur complement <sup>7</sup>.

**Remark 4.4.4** The variant proposed in this section enjoys the same positive features of the basic scheme of Section 4.3, since  $\Upsilon_i(\Theta_i)$  can be pre-computed off-line for each candidate controller  $\mathcal{C}_i \in \mathcal{C}$ . In particular,  $\tilde{\mathcal{G}}_i(\theta)$  depends *affinely* on the design parameters  $\tilde{V}_i, \tilde{P}_i, \tilde{T}_i$  (cf. (4.47)) and hence, (4.56) is a Linear Matrix Inequality (LMI) with respect to such design parameters for each  $\theta$ . While solution of (4.56) is straightforward when  $\Theta_i$  is discrete, viable approaches exist in the literature for dealing also with a continuum of LMI constraints. For instance, approximation schemes such as the one in [CC06] prove relevant in this regard.

## 4.5 An Example

In order to show the effectiveness of the proposed method for the control transfer problem, consider the following hybrid linear process

$$\left. \begin{aligned} \dot{\chi}(t) &= \bar{A}_j \chi(t) + \bar{B}_j u(t) \\ y(t) &= \bar{C} \chi(t) \end{aligned} \right\} \quad (4.57)$$

made up by 5 regimes, where each triple  $\{\bar{A}_j, \bar{B}_j, \bar{C}\}$  (corresponding to a single regime) is the discrete-time version (by means of an input zero-order holder with sampling time equal

<sup>7</sup>*Schur complement* [BEFB94]. Suppose  $Q$  and  $R$  are symmetric matrices. Then, the condition

$$\left[ \begin{array}{cc} Q & S \\ S' & R \end{array} \right] \succ 0$$

is equivalent to

$$R \succ 0 \quad \text{and} \quad Q - S R^\dagger S' \succ 0.$$

regime $j$	airspeed (knots)	$\alpha_j$	$\beta_j$	$\delta_j$
1	50-75	0.06635	0.1198	0.9770
2	75-100	0.2	0.5	1.9
3	100-125	0.285	0.9	2.73
4	125-150	0.3681	1.42	3.5446
5	150-175	0.5045	2.526	5.112

**Table 4.1:** Parameters values at different airspeed ranges.

to 0.1 s) of a continuous-time linear system with state-space representation  $\{\bar{A}_i^{ct}, \bar{B}_i^{ct}, \bar{C}^{ct}\}$  as follows

$$\bar{A}_j^{ct} = \begin{bmatrix} -0.0366 & 0.0271 & 0.0188 & -0.455 \\ 0.0482 & -1.0100 & 0.0024 & -4.02 \\ 0.1000 & \alpha_j & -0.7070 & \beta_j \\ 0 & 0 & 1 & 0 \end{bmatrix} \quad \bar{B}_j^{ct} = \begin{bmatrix} 0.422 & 0.176 \\ \delta_j & -7.590 \\ -5.520 & 4.490 \\ 0 & 0 \end{bmatrix}$$

$$\bar{C}^{ct} = \begin{bmatrix} 1 & 0 & 0 & 0 \\ 0 & 0 & 0 & 1 \end{bmatrix}$$

which value is specified in Table 4.1. Accordingly, the process uncertainty is a discrete

$$\Theta = \{\theta_1, \dots, \theta_5\},$$

where  $\theta_j = [\alpha_j \ \beta_j \ \delta_j]'$  indicates the parameters vector.

In particular, the process is a 2-inputs/2-outputs system which represents a linear approximation of the longitudinal and vertical dynamics of a helicopter moving at different longitudinal airspeeds: The state  $\chi(t)$  is a four components vector made up by longitudinal velocity  $\chi_1(t)$  [kt], vertical velocity  $\chi_2(t)$  [kt], pitch rate  $\chi_3(t)$  [deg/s] and, pitch angle  $\chi_4(t)$  [deg]. The aim is to control the longitudinal velocity  $y_1(t)$  and pitch angle  $y_2(t)$  by means of collective pitch  $u_1(t)$  and longitudinal cyclic pitch  $u_2(t)$  of the rotor blades. More technical details can be found in [AW97] and [NB97]. In the following, all simulations consider the process to be fixed at a pre-specified regime and, also, represent an unit step of the longitudinal velocity, while the pitch angle is kept unchanged. Then, a switch from the initial controller to the right one in the pre-designed family is supposed to be performed, once it is correctly detected, by a high-level supervision unit.

process configuration	from $\mathcal{C}_2$ to $\mathcal{C}_1$			from $\mathcal{C}_1$ to $\mathcal{C}_2$	
	$\mathcal{P}(\theta_1)$	$\mathcal{P}(\theta_2)$	$\mathcal{P}(\theta_3)$	$\mathcal{P}(\theta_4)$	$\mathcal{P}(\theta_5)$
non conditioning	3905	1837	1268	1622	5349
optimal conditioning	519	103	75	307	311
robust conditioning	295	91	113	232	311

**Table 4.2:** Values of the cost  $f(q(t_s))$  for each possible simulation scenario in case the switching occurs at  $t_s = 5$  s. Legend: Non state conditioning ( $q(t_s) = q^\circ(t_s)$ ), optimal state conditioning ( $q(t_s) = \Upsilon_i v(t_s)$ ), robust state conditioning ( $q(t_s) = \Upsilon_i(\Theta_i) v(t_s)$ ), index  $i$  indicating the switched-on stabilizing controller. In all cases  $\Psi = I_4$  and  $\Omega = 0.1 I_{2n_c}$ .

Consistently with the previous chapters,  $\mathcal{P}(\theta_j)$  indicates the process dynamics associated to the  $j$ -th discrete-time regime. In the present case, two optimal discrete-time controllers  $\mathcal{C}_i$ ,  $i = 1, 2$ , with integral action have been designed in accordance with the performance criterion

$$\sum_{k=0}^{\infty} |e(k)|^2 + |\nu(k)|^2,$$

where  $\nu(k) := u(k) - u(k-1)$ . The first controller,  $\mathcal{C}_1$ , has been designed in correspondence of  $\mathcal{P}(\theta_3)$  and stabilizes regimes 1-4:  $\Theta_1 = \{\theta_1, \dots, \theta_4\}$ . The second one,  $\mathcal{C}_2$ , refers to  $\mathcal{P}(\theta_5)$  and stabilizes regime 5 only:  $\Theta_2 = \theta_5$ . This simple scenario aims at representing a situation wherein, although the process can assume a finite number of possible configurations, a lower number of controllers is assumed to be sufficient to guarantee high control performance.

MFDs as in (2.4) and (2.6) are suitably obtained both for controllers and for related nominal models, namely  $\mathcal{M}_1 = \mathcal{P}(\theta_3)$  and  $\mathcal{M}_2 = \mathcal{P}(\theta_5)$ , respectively. The implementation adopted to realize the multicontroller is the state-sharing one as in (4.2). Eventually, for controller  $\mathcal{C}_1$ , both the optimal state reset map related to the model  $\mathcal{M}_1$ , namely the gain matrix  $\Upsilon_1$  obtained by (4.26), and the robust variant related to the uncertainty subset  $\Theta_1$ , namely  $\Upsilon_1(\Theta_1)$  obtained by (4.53), have been pre-designed. As for  $\mathcal{C}_2$ , the optimal state reset map,  $\Upsilon_2$  by (4.26), related to  $\mathcal{M}_2$  has been computed.

#### *Optimal / robust state conditioning*

In the left side of Figure 4.3, the process is supposed to be  $\mathcal{P}(\theta_3)$  and the controller  $\mathcal{C}_2$  to be connected in feedback with the process at the initial time  $t = 0$  s. A high-level



supervision unit (which is immaterial to specify for the present purposes) switches the multicontroller from  $\mathcal{C}_2$  to  $\mathcal{C}_1$  at  $t_s = 5$  s. As expected, in a model-matching case the optimal state resetting given by  $\Upsilon_1 v(t_s)$ , as in (4.33)-(4.36), provides the best transient with respect to the ones obtained by the robust one  $\Upsilon_1(\Theta_1) v(t_s)$ , where  $\Upsilon_1(\Theta_1)$  is obtained by solving (4.56), and non state reinitialization  $q^\circ(t_s)$  as in (4.25), see Table 4.2 for the related cost values. Note that, contrarily to the classical multicontroller implementation yielding a huge bump on the process outputs, by the two state reset maps it is possible to produce a jump on the control actions such to reduce the picks on the outputs, so allowing to promptly recover the regime behavior charactering the final control loop ( $\mathcal{P}(\theta_3)/\mathcal{C}_1$ ). Indeed, multicontroller implementation (4.2), with common state as in (4.3), preconditions its state so as to maintain continuity of the controller output signal <sup>8</sup>, with consequent performance degradation of the closed loop behavior.

The right side of Figure 4.3 depicts results for the case wherein the process is  $\mathcal{P}(\theta_4)$  and the setup is as before. In this case, a model-mismatching case, the best transient is provided, contrarily to the previous case, by the robust state reset map  $\Upsilon_1(\Theta_1) v(t_s)$  as in (4.54), see Table 4.2 for the cost values.

Eventually, the multicontroller architecture as in (4.38) with optimal / robust state conditioning prove to compare favorably with respect to the state-sharing architecture with no controller state resetting (4.2). Table 4.2 sums up all the possible scenarios.

#### 4.5.1 State reset map vs. dynamic compensation

This section aims at briefly showing the differences between the implementation by hybrid linear controller with state reset map, as described in (4.38), and the multisystem implementation of Figure 4.1, where each controller is equipped with a dedicated dynamic compensator.

In particular, we consider the architecture proposed in [ZT05] which aims at recovering as soon as possible a predefined “target” response in a  $l_2$  sense. The approach is

---

<sup>8</sup>Obviously, the concept of continuity of a signal makes sense only for continuous-time systems but does not extend to discrete-time devices as our controllers, simply because it is difficult to talk about continuity in time of some variable on a discrete time setting. Here, the concept of “continuity” has to be meant with the acceptance of a minimum jump of the signal value between two consecutive sampling instants.

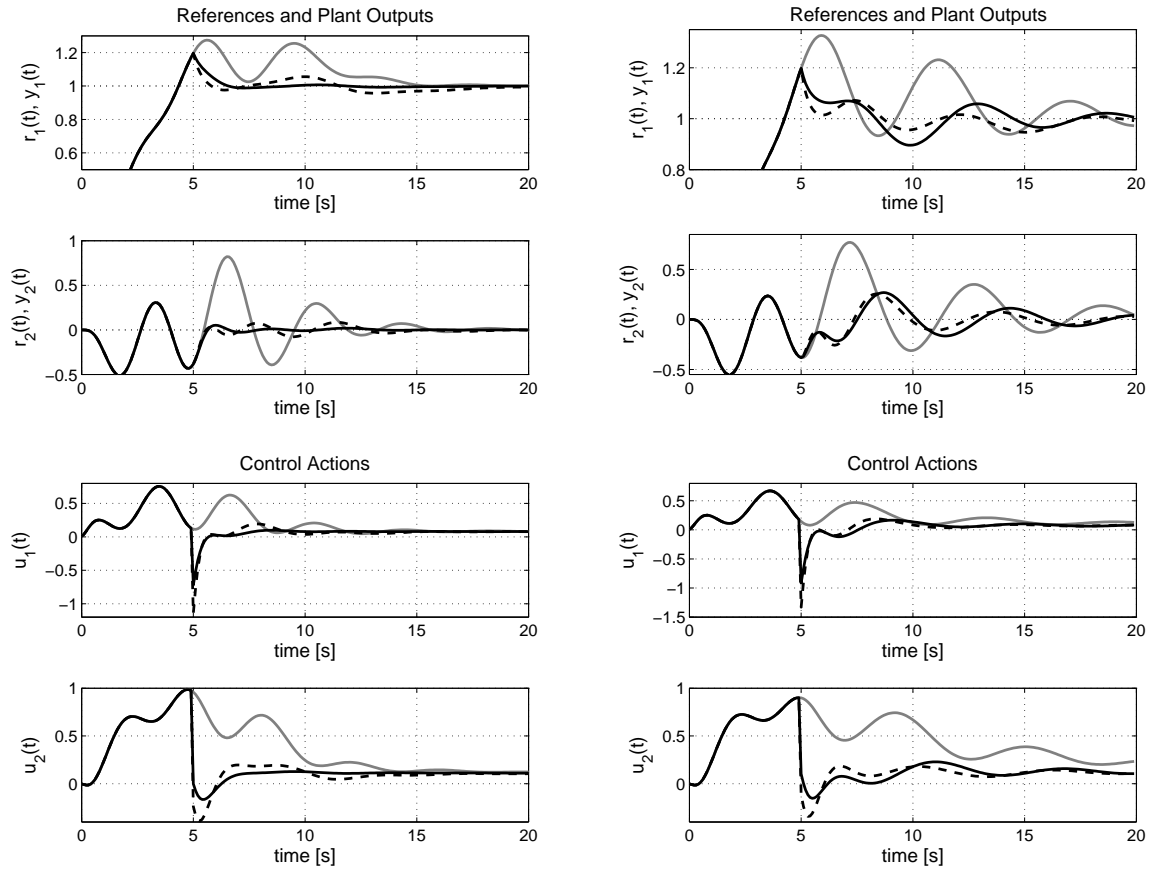


**Figure 4.3:** Controller transition from  $\mathcal{C}_2$  to  $\mathcal{C}_1$  at  $t = 5$  s. Left: process configuration corresponding to  $\mathcal{P}(\theta_3)$ . Right: process configuration corresponding to  $\mathcal{P}(\theta_4)$ . In both cases  $\Psi = I_4$  and  $\Omega = 0.1 I_{2n_c}$ . Legend: Non state conditioning (solid grey), optimal state conditioning (solid black), robust state conditioning (dash black).

accordingly a typical conditioned transfer technique, even if authors in [ZT05] refer to as bumpless transfer technique. The control scheme is appropriately rearranged for the specific study case here considered <sup>9</sup>. More specifically, the dynamic compensator is as follows

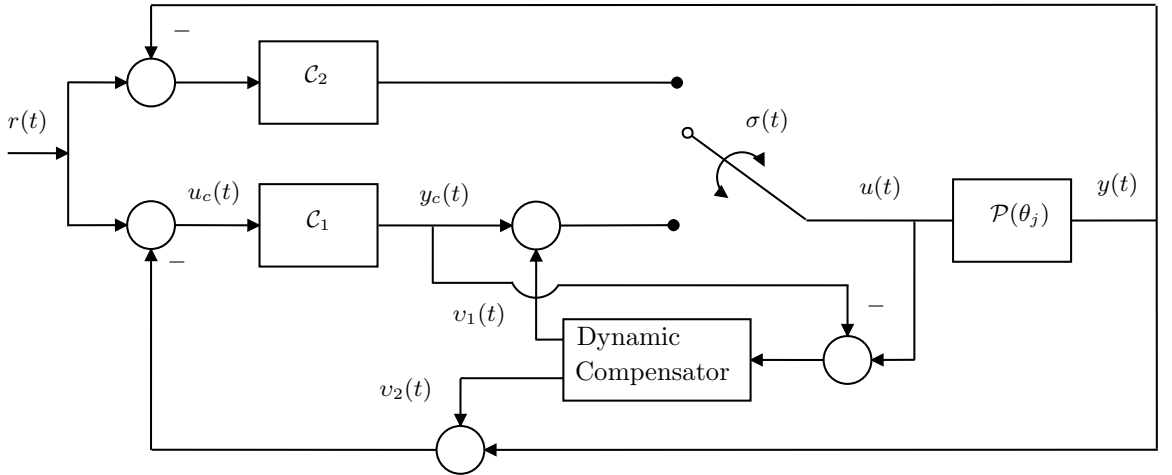
$$\left. \begin{aligned} x_e(t+1) &= \bar{A}_3 x_e(t) + \bar{B}_3 (u(t) - y_c(t)) \\ v_1(t) &= \Phi_1 x_e(t) \\ v_2(t) &= -\bar{C} x_e \end{aligned} \right\} \quad (4.58)$$

where, consistently with the notation adopted in the previous section, the triple  $\{\bar{A}_3, \bar{B}_3, \bar{C}\}$  corresponds to the state-space realization of the nominal model  $\mathcal{M}_1$ , this technique being a model-based conditioned transfer. The time evolution of the state vector  $x_e(t)$  is piloted by the difference signal between the process input and the off-line controller output  $\mathcal{C}_1$ , while the two outputs,  $v_1(t)$  and  $v_2(t)$ , pre-condition both the input and the output of the off-line controller before the latter one be inserted in feedback with the process. The matrix  $\Phi_1$  is devoted to pre-condition the output of controller  $\mathcal{C}_1$  and aims at minimizing a non-negative real gain  $\gamma$  such that

$$\sum_{k=t_s}^{\infty} |\mu(k) - \mu_T(k)|^2 \leq \gamma |\chi(t_s) - \chi_T(t_s)|, \quad (4.59)$$

where  $\mu(t) = C_\mu \chi(t) + D_\mu u(t)$  is the performance output and  $\mu_T(t) = C_\mu \chi_T(t) + D_\mu u(t)$  is its target value, obtained by the target value  $\chi_T(t)$  of the model state  $\chi(t)$ . In [ZT05], it is

<sup>9</sup>Scheme of the adopted multi-system controller implementation with dynamic compensator:



shown that  $\chi_T(t)$  corresponds to the steady-state value at  $t$  of the state of process model (in this particular application  $\mathcal{M}_1$ )<sup>10</sup>. In particular, the value of  $\Phi_1$  is a priori determined by the state-space realizations of nominal model and controller. The interested reader is referred to [ZT05] for more details concerning the solution of the problem (4.59).

Hereafter, some simulations are carried out in order to compare the approach based on state reset map, proposed in the previous sections, and the one obtained through the use of additional dynamic compensator as in (4.58).

As first scenario, consider the case wherein the process is in the third regime  $\mathcal{P}(\theta_3)$  (model-matching case) and, a switching occurs between the (initial) controller  $\mathcal{C}_2$  and  $\mathcal{C}_1$  at time 15 s. The weight matrices of criterion (4.26) are set as follows:  $\Psi = [0_2; I_2]$  and  $\Omega = 0_{2n_c}$ . Criterion (4.59) is set by imposing  $C_\mu = [0_{4 \times 2}; \bar{C}]$  and  $D_\mu = [0_2; 0_2]$ . These particular choices allow to have the same objective for both procedures. According to the arguments of Remark 4.3.4, the left side of Figure 4.4 shows that the dynamic compensation provides a prompter transient on the process output than a simple state reinitialization however, as predictable, it needs of a strong control action, which can be undesirable in case the process inputs be subject to some saturation constraint. Notice that, this scenario corresponds to have “control action-free” objectives, the difference between process output and its regime value being the only term to be minimized. In the right side of Figure 4.4 (where the simulation setup keeps the same) switching occurs at 5 s. In this case, the optimal state reset map given by (4.33) provides a better transient with respect to the dynamic compensator, the latter one being sensible to the switching time with respect to the power-on time of the control loop. Indeed, dynamic compensator needs of a certain time horizon to correctly precondition the state of the off-line controller.

A second scenario is depicted in Figure 4.5, where the process is in the first regime  $\mathcal{P}(\theta_1)$  (model-mismatching case). In this case, it is considered the robust state reset map (4.54) as state reinitialization to carry out the comparison. Notice that, at the most of the knowledge of the author, the approach in [ZT05] does not have a robust variant. Indeed, in a case of process/model-mismatching, the transient behavior given by the dynamic compensator deteriorates compared with the model-matching case, such device being designed

---

<sup>10</sup>Note that, in [ZT05] authors implicitly assume that the process state be accessible. On the contrary, dynamic compensator as in (4.58) can be however obtained by making use of model state-space realizations as specified in (4.8).

to be used by supposing to know the exact model of the process. Accordingly, the transient yielded by the robust state reset turns out to be comparable at the first output and prompter at the second one, while the inputs keep two order of magnitude smaller than the ones produced by the dynamic compensator.

As final scenario, consider newly the simulation presented in the first scenario wherein at present we set  $C_\mu = [0_{4 \times 2}; \tilde{C}]$ ,  $D_\mu = [I_2; 0_2]$  and, also,  $\Psi = I_4$  and  $\Omega = 0_{2n_c}$  in order to weight the control action in both cases (note that, so doing, there is no exact correspondence between the two related objectives). Figure 4.6 shows how the control action provided by the dynamic compensator considerably reduces its magnitude with respect to the previous two scenarios and transient behavior by the two approaches turns out to be very close.

## 4.6 Concluding Remarks

This chapter discusses the control transfer problem in model-based switching schemes. Two different architectures for implementing the multicontroller have been compared: the multi-system- based realization and the hybrid linear realization. From the comparison, it arises that the latter one proves to be more suitable in cases where the number of controllers is high, its computational being independent of the number of controllers. Also, it allows to manage with unstable controllers. By a hybrid linear controller architecture, controllers can share their states and, accordingly, only one (common) state vector turns out to be operative at each time. The idea to condition the control transfer consists so in solving a problem of optimal / robust reset of the multicontroller state at each time of switching. The aim is to provide the optimal transient with respect to a pre-specified performance index in case of exact matching between process and nominal model. A robust variant is also proposed for more general cases, where the process uncertainty does not coincide with the models distribution. The state reinitialization is obtained through a linear map and gains characterizing such a map can be a priori computed starting from available models and controllers. Hence, computational burden of the resulting hybrid linear controller with state reset map does not increase with respect to the original implementation, thus proving to be suitable to be applied in case of a large number of controllers. A simulative example has been also carried out to show the effectiveness of the method and to

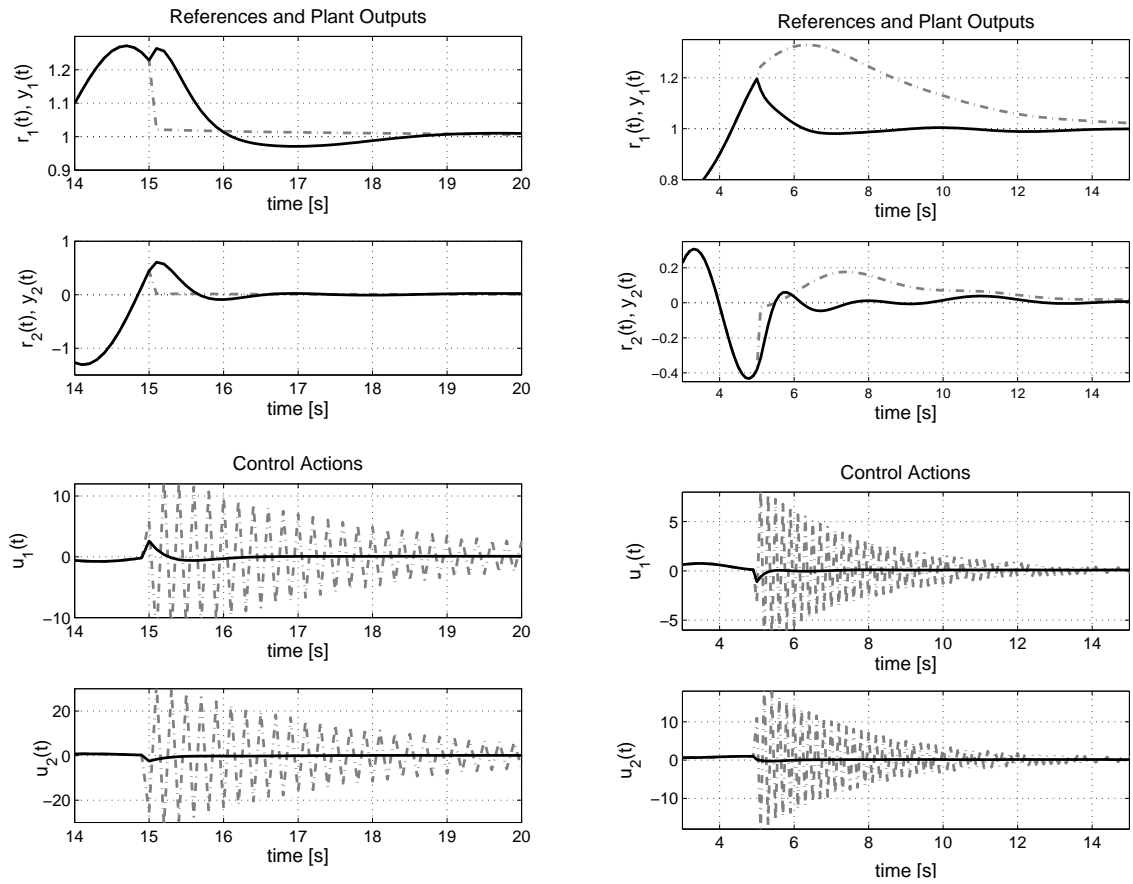


**Figure 4.4:** Process configuration corresponding to  $\mathcal{P}(\theta_3)$  and controller transition from  $\mathcal{C}_2$  to  $\mathcal{C}_1$ . Left: Switching at  $t = 15$  s. Right: Switching at  $t = 5$  s. Legend: Optimal state conditioning (solid black), dynamic compensation (dash dot grey).

compare its features compared with the ones of a multi-system implementation equipped with additional dynamic compensator for the manage of control transfer.

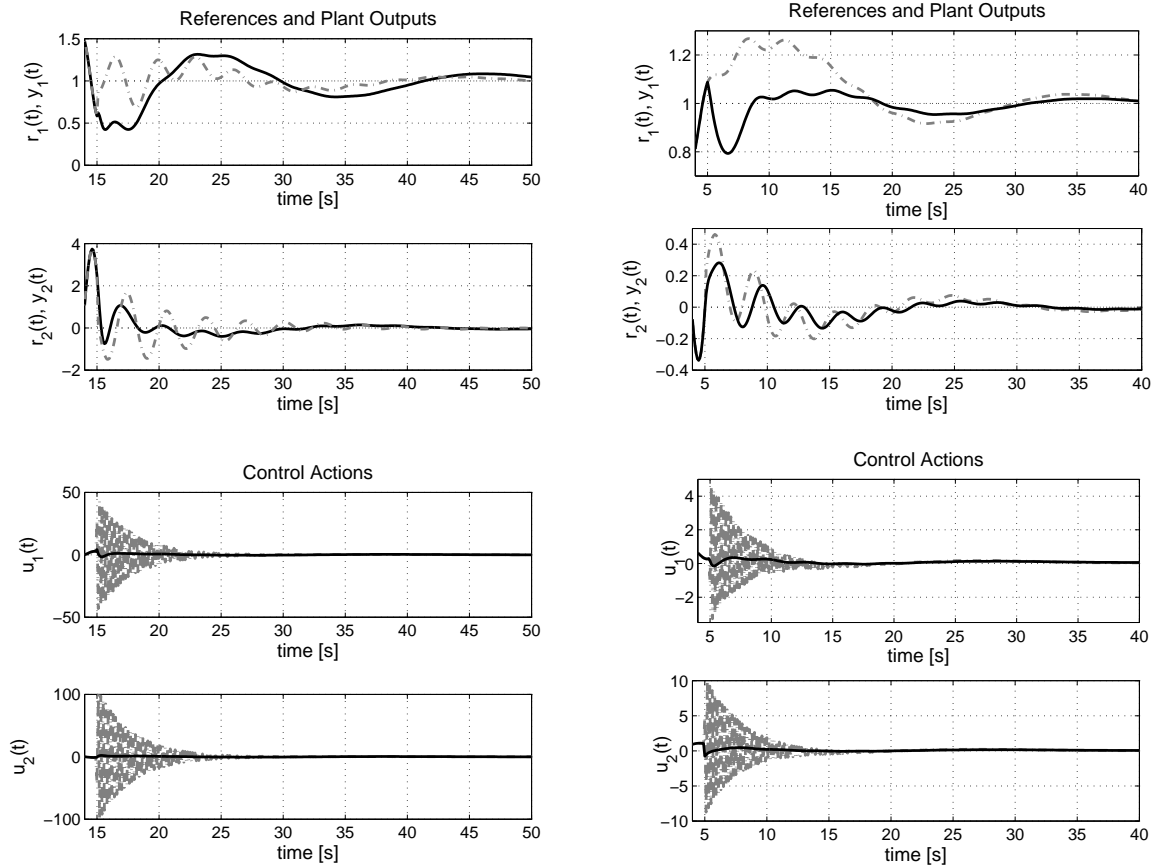


**Figure 4.5:** Process configuration corresponding to  $\mathcal{P}(\theta_1)$  and controller transition from  $\mathcal{C}_2$  to  $\mathcal{C}_1$ . Left: Switching at  $t = 15$  s. Right: Switching at  $t = 5$  s. Legend: Robust state conditioning (solid black), dynamic compensation (dash dot grey).

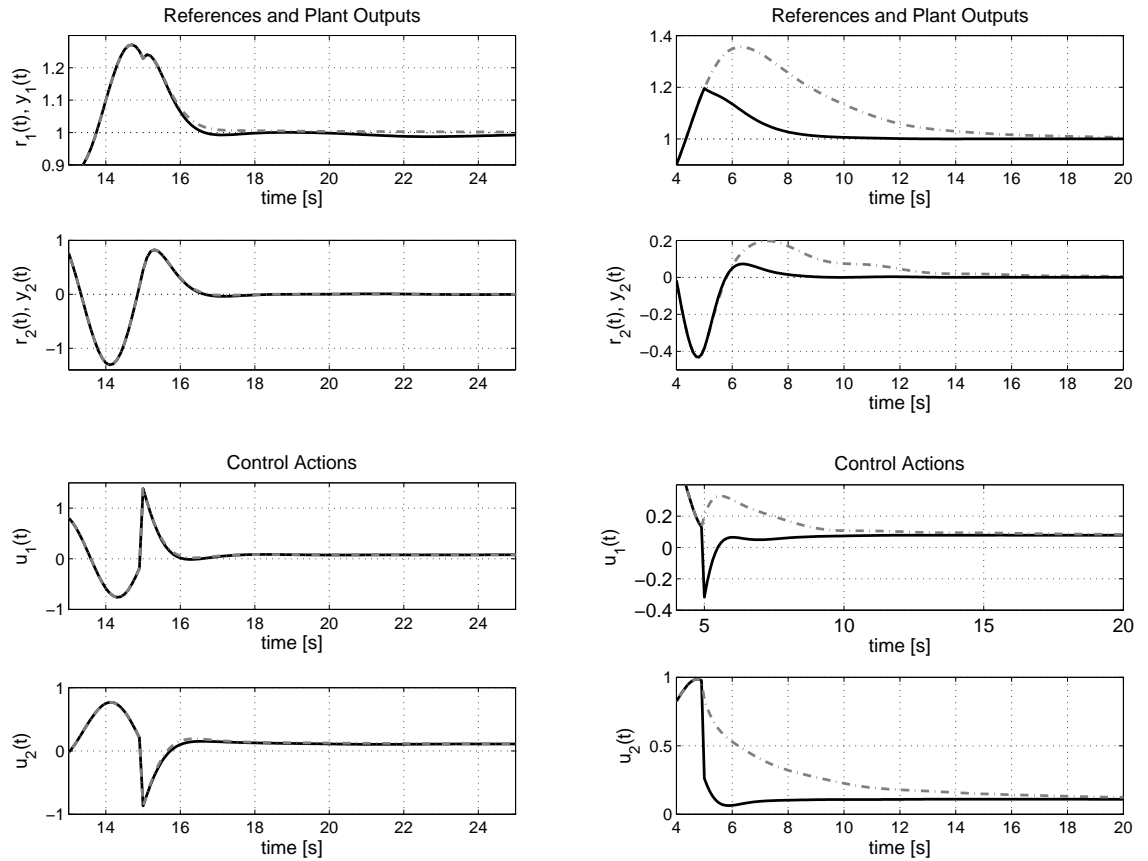


**Figure 4.6:** Process configuration corresponding to  $\mathcal{P}(\theta_3)$  and controller transition from  $\mathcal{C}_2$  to  $\mathcal{C}_1$  (weight on the control actions). Left: Switching at  $t = 15$  s. Right: Switching at  $t = 5$  s. Legend: Optimal state conditioning (solid black), dynamic compensation (dash dot grey).



**PART III**  
**Simulative Example**

## Chapter 5

# A Four Carts Example

Since simulation of adaptive control systems are often useful for performance evaluation, this chapter focuses on a dynamic system which has been designed as extension to the multivariable case of the benchmark problem proposed in [BW92] and also, it is used in [BBM<sup>+</sup>12, MCC01] in the context of switching supervisory control. In the sequel, first the controller selecting rule presented in Chapter 3 and the conditioning solutions of Chapter 4 are sequentially tested by separate experiments. Then, a general control scheme which exploits both techniques is considered in order to show possible performance improvements.

Consider the process represented in Figure 5.1, made up by four carts mechanically coupled by springs and dampers, where the control problem consists in positioning the external carts by applying manipulable forces to the internal ones. The resulting system is square with 2 inputs and 2 outputs and, the continuous-time state-space representation is as follows

$$\left. \begin{aligned} \dot{x}(\tau) &= \bar{A}^{ct}(\theta) x(\tau) + \bar{B}^{ct} u(\tau) \\ y(\tau) &= \bar{C}^{ct} x(\tau) \end{aligned} \right\} \quad (5.1)$$

where  $\tau$  indicates the continuous time,  $u(\tau) \in \mathbb{R}^2$  and  $y(\tau) \in \mathbb{R}^2$  are the vectors containing the forces on the internal carts and the positions of the external ones respectively,  $x(\tau) \in \mathbb{R}^8$

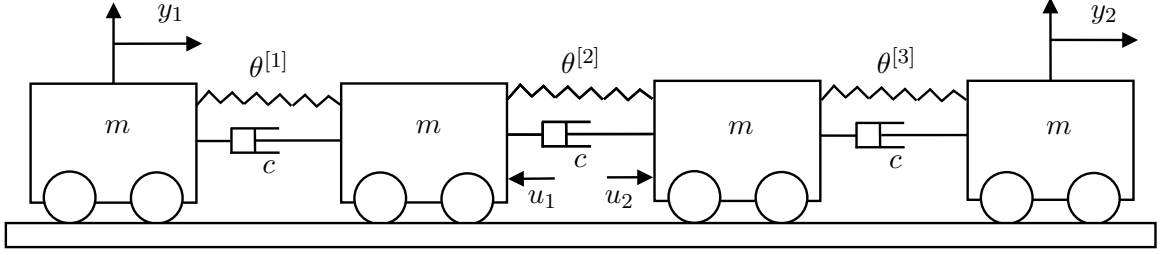


**Figure 5.1:** Four carts plant.

is the state vector containing positions and velocities of the four carts and

$$\bar{A}^{ct}(\theta) = \begin{bmatrix} 0 & 0 & 0 & 0 & 1 & 0 & 0 & 0 \\ 0 & 0 & 0 & 0 & 0 & 1 & 0 & 0 \\ 0 & 0 & 0 & 0 & 0 & 0 & 1 & 0 \\ 0 & 0 & 0 & 0 & 0 & 0 & 0 & 1 \\ -\frac{\theta^{[1]}}{m} & \frac{\theta^{[1]}}{m} & 0 & 0 & -\frac{c}{m} & \frac{c}{m} & 0 & 0 \\ \frac{\theta^{[1]}}{m} & -\frac{(\theta^{[1]}+\theta^{[2]})}{m} & \frac{\theta^{[2]}}{m} & 0 & \frac{c}{m} & -\frac{2c}{m} & -\frac{c}{m} & 0 \\ 0 & \frac{\theta^{[2]}}{m} & -\frac{(\theta^{[2]}+\theta^{[3]})}{m} & \frac{\theta^{[3]}}{m} & 0 & \frac{c}{m} & -\frac{2c}{m} & -\frac{c}{m} \\ 0 & 0 & \frac{\theta^{[3]}}{m} & -\frac{\theta^{[3]}}{m} & 0 & 0 & \frac{c}{m} & \frac{c}{m} \end{bmatrix} \quad \bar{B}^{ct} = \begin{bmatrix} 0 & 0 \\ 0 & 0 \\ 0 & 0 \\ 0 & 0 \\ 0 & 0 \\ -\frac{1}{m} & 0 \\ 0 & \frac{1}{m} \\ 0 & 0 \end{bmatrix}$$

$$\bar{C}^{ct} = \begin{bmatrix} 1 & 0 & 0 & 0 & 0 & 0 & 0 & 0 \\ 0 & 0 & 0 & 1 & 0 & 0 & 0 & 0 \end{bmatrix}$$

Each cart has mass  $m$  equal to 1 Kg and the dampers have a viscous damping coefficient  $c$  equal to 0.1 Ns/m, while the vector

$$\theta = \begin{bmatrix} \theta^{[1]} \\ \theta^{[2]} \\ \theta^{[3]} \end{bmatrix} \quad (5.2)$$

with  $\theta^{[i]} \in \mathbb{R}$ ,  $i = 1, 2, 3$ , denotes the value of stiffness of the three springs.

*Control scheme setting.* The supervisor  $\mathcal{S}$  adopts the switching rule described in Chapter 3, so, the controller index  $\sigma$  is selected in accordance with the HSL (3.8) with test functionals (3.15)-(3.16). Given a family of discrete-time controllers as in (2.4), the multicontroller  $\mathcal{C}_{\sigma(\cdot)}$  is a discrete-time device realized by a hybrid linear architecture as in (4.2), with common

state given by

$$q(t) := [e(t-1)' \cdots e(t-n_c)' u(t-1)' \cdots u(t-n_c)']', \quad (5.3)$$

where  $e(t) := r(t) - y(t)$ ,  $n_c := \max_{i \in \overline{N}} \{\deg S_i, \deg R_i\}$ , with  $\deg M$  standing for to the highest degree of all the entries of  $M(d)$ . Eventually, assume zero plant initial condition and zero noises and disturbances.

Hereafter, two different scenarios are taken in account.

## 5.1 First Scenario: Monodimensional Uncertainty

Consider the case where only the spring connecting the carts on the left has an uncertain stiffness parameter  $\theta^{[1]} \in \Theta$ , where

$$\Theta = [0.1, 1.2] \text{ N/m}, \quad (5.4)$$

while the other springs are assumed to have a known stiffness coefficient  $\theta^{[2]} = \theta^{[3]} = 0.7$  N/m. For this scenario, three different one-degree-of-freedom continuous-time LTI controllers have been designed in order to guarantee stability and performance requirements on the whole uncertain interval  $\Theta$ , defined in (5.4). The three controllers  $\mathcal{C}_i$ ,  $i = 1, 2, 3$ , have been designed with integral action in accordance to the following performance criterion

$$\int_{-\infty}^{\infty} |e(\tau)|_{\Psi_{e_i}}^2 + |\nu(\tau)|_{\Psi_{\nu_i}}^2,$$

where  $\nu(\tau) := s u(\tau)$ , where, here,  $s$  indicates the Laplace operator. The weight matrices are as follows:  $\Psi_{e_i} = \psi_{e_i} I_2$ , with  $\psi_e = \{10, 1, 0.1\}$  and,  $\Psi_{\nu_i} = I_2$ ,  $i = 1, 2, 3$ . Such controllers have been designed relatively to nominal models  $\mathcal{M}_i = \mathcal{P}(\theta_i)$  corresponding to three stiffness representative values:

- $\theta_1^{[1]} = 0.25$  N/m;
- $\theta_2^{[1]} = 0.50$  N/m;
- $\theta_3^{[1]} = 1.00$  N/m.

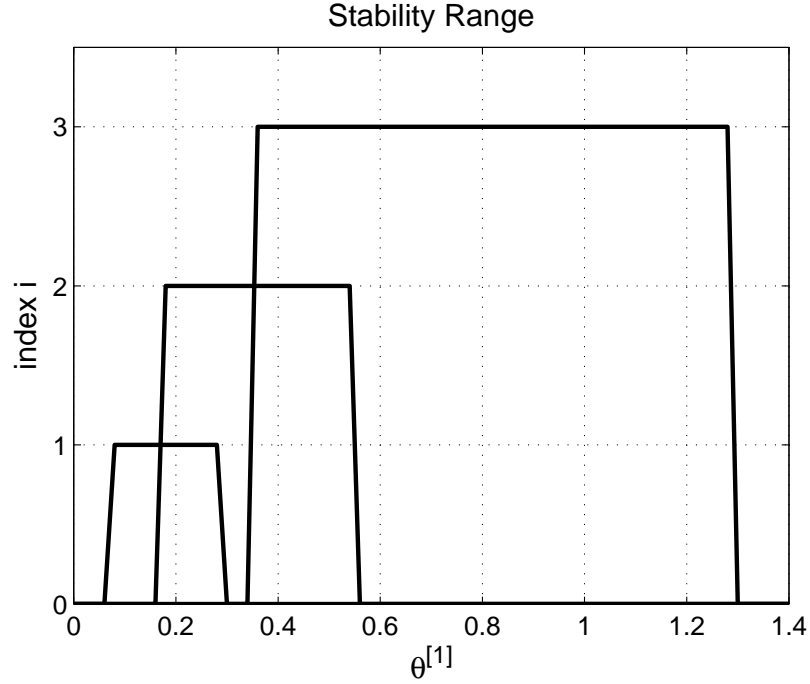


**Figure 5.2:** Monodimensional uncertainty. Stability ranges of the three controllers:  $\Theta_1^{[1]} = (0.08, 0.28)$  N/m,  $\Theta_2^{[1]} = (0.18, 0.54)$  N/m,  $\Theta_3^{[1]} = (0.36, 1.28)$  N/m.

Then, nominal models and related controllers are discretized by means of an input zero-order holder with sampling time equal to 0.1 s. Figure 5.2 shows the subintervals  $\Theta_i^{[1]}$ ,  $i \in \overleftarrow{3}$ , wherein each controller  $\mathcal{C}_i$  guarantees internal stability. Note that

$$\Theta = \bigcup_{i=1}^3 \Theta_i^{[1]}.$$

In the following simulations, the reference signals  $r_1(\tau) \in \mathbb{R}$  and  $r_2(\tau) \in \mathbb{R}$ , to be tracked from the positions of the external carts, are assumed to be set-points equal to 1 m and -2 m with respect to an equilibrium position  $(r_1, r_2)_{\text{eq}} = (0, 0)$ . Further, the hysteresis constant  $h$  is set equal to 0.1.

First, focus only on the supervision rule, the multicontroller being assumed without state reset map. In this case, Table 5.1 reports simulation results related to different stiffness values of the uncertain spring. Such simulations ranges on the overall uncertainty

$\theta^{[1]}$	Switching Logic			Process Behavior	
	Initial index	Final index	Final time	Max. values of $ y_1 $ and $ y_2 $	Max. values of $ u_1 $ and $ u_2 $
0.10	3	1	3.40 s	2.38 and 6.11	6.46 and 6.72
0.15	2	1	7.60 s	1.64 and 3.34	2.77 and 3.20
0.20	3	2	3.30 s	3.83 and 5.46	6.36 and 7.30
0.27	3	1	3.40 s	4.95 and 6.27	6.33 and 8.35
0.35	3	2	54.0 s	63.4 and 89.0	40.5 and 47.2
0.40	1	2	8.80 s	2.84 and 3.72	2.99 and 2.77
0.45	3	2	7.40 s	4.35 and 4.07	4.63 and 4.90
0.60	1	3	45.6 s	7.56 and 9.95	7.02 and 6.72
0.65	1	3	20.6 s	4.38 and 6.53	4.56 and 5.29
0.75	2	3	21.6 s	2.25 and 3.05	2.81 and 2.77
0.80	1	3	4.00 s	2.01 and 3.15	2.37 and 2.48
0.90	1	3	3.40 s	2.20 and 3.13	2.23 and 2.48
1.20	2	3	6.20 s	1.99 and 2.55	2.27 and 2.28

**Table 5.1:** Monodimensional uncertainty. Simulation results obtained by switching among 3 controllers with non state conditioning.

interval, and show how the switching sequence always ends in finite time on the more adequate controller, *i.e.* the one guaranteeing internal stability with respect to the process configuration. Note that, in most cases, such controller is associated to the nominal model closer to the process realization. However, the selection turns out to be stability-based: indeed, for  $\theta^{[1]} = 0.35$ , the nominal model closer to the process is the first one, *i.e.*  $\mathcal{M}_1$ , nonetheless, the final choice falls upon  $\mathcal{C}_2$ ,  $\mathcal{C}_1$  being destabilizing; same considerations hold for  $\theta^{[1]} = 0.60$  and  $\theta^{[1]} = 0.65$ .

Consider now the multicontroller. At present, assume that a (not specified) high-level supervision unit determines the mode of the multicontroller, according to a pre-scheduled switching sequence. The aim is to evaluate the possible improvement on transient behavior after the switching by means of the conditioning techniques of Chapter 4. To this

end, Figure 5.3 compares the values of the cost (4.26b) with respect to the process uncertainty  $\theta$  for the following solutions: non state conditioning (solid grey), optimal state conditioning (solid black) and, robust solution conditioning (dash black). More specifically, the figure refers to a case wherein the switching is scheduled 3 s after the power-on time of the control system. As it is possible to see, the proposed approaches yields a huge improvement compared with the case of no state-resetting. Of course, the multicontroller is always assumed to switch on the stabilizing controller. In particular, for each case represented in figure, it is possible to detect a neighbourhood of the nominal point (corresponding to the nominal model), wherein the optimal state reset map provides the best solution. On the contrary, far from the nominal points, the robust solution turns out to produce the best values, this being in accordance to the continuous nature of the process uncertainty. The robust solution, in particular, is obtained by solving the optimization problem as in (4.56) on a “discrete scenario”, see [CC06], namely, by sampling the uncertainty  $\Theta$  from  $\theta_{\min} = 0.1$  with a sampling step  $\Delta\theta = 0.002$ , simulations having shown that such uncertainty sampling provides a satisfactory trade-off between computational load and performance improvements. Eventually, Figure 5.4 depicts the three solutions for two particular values of the uncertainty.

The way how conditioning / bumpless techniques influence the closed loop behavior of the adaptive supervisory control schemes is, in general, unpredictable. Indeed, in general, although architectures dedicated to control transfer aim at improving the transients of a control system at the time of switching, stability / performance characteristics of the resulting switching scheme can be subjected to dramatic consequences. However, the switching scheme adopted in Chapter 3, combined with state reset map proposed in Chapter 4 is such that the stability property of the original switching scheme keeps unchanged. Indeed, stability only depends on the preliminary feasibility condition **a1** and also, the idea of resetting the multicontroller state allows not to alter the stability properties of the switched control system, the latter being a favourable feature for a control transfer device. However, this could not prevent / avoid undesired transients due to possible malfunctioning of the supervision rule. In this respect, Figure 5.5 shows the ASC scheme behavior in case of switching rule be combined with the robust state conditioning as in (4.54), for two different process configurations. As it can be seen in Figure 5.6, such solution takes to an improvement of the closed loop dynamics, compared with the one obtained by using

Chapter 5. A Four Carts Example

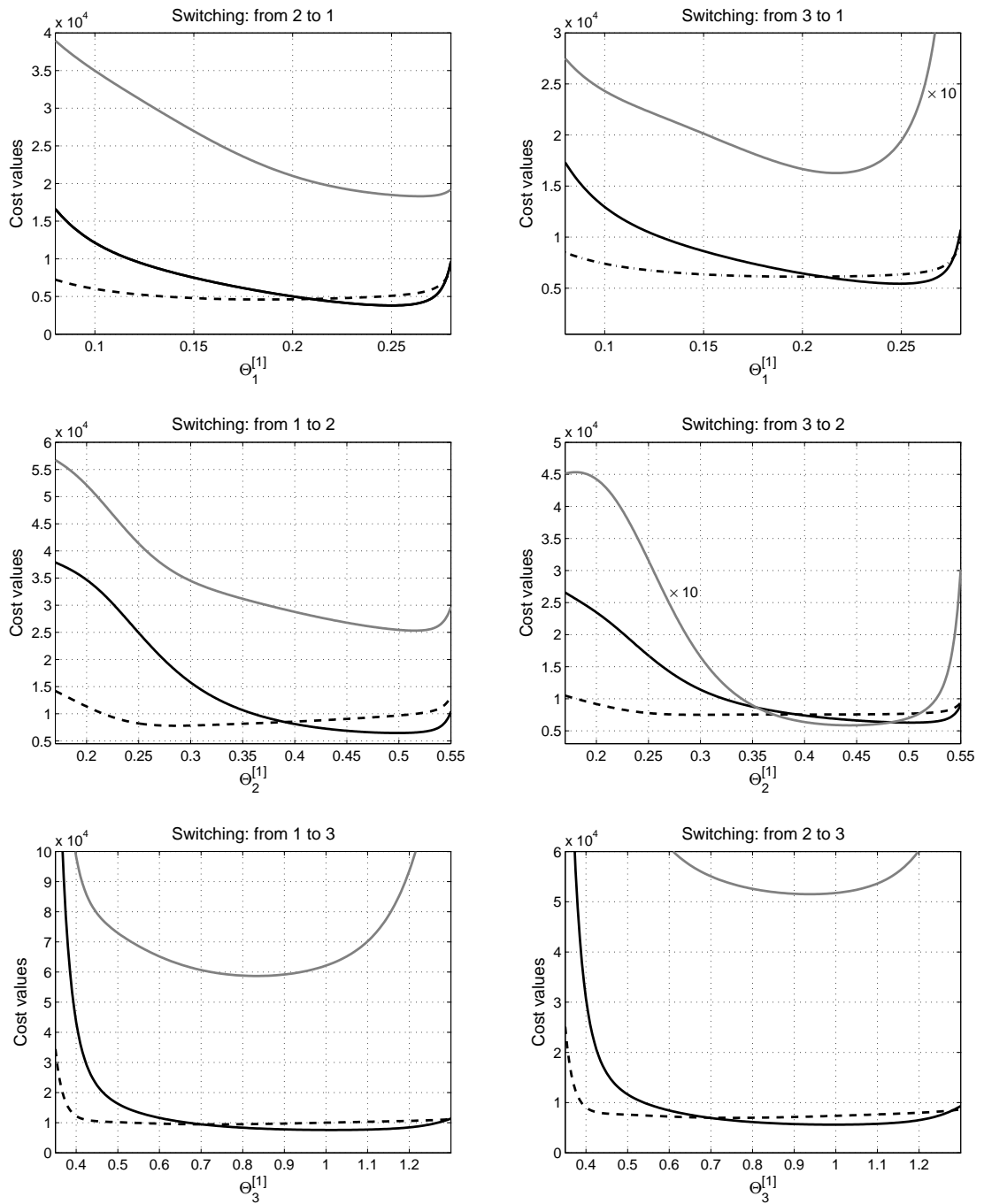


**Figure 5.3:** Monodimensional uncertainty. Values of the cost (4.26b) for each possible process configuration / control transfer in case the switching occurs at 3 s ( $\Psi = \text{diag}(I_2, 10^3 I_2)$ ,  $\Omega = 0_{2n_c}$ ). Legend: Non state conditioning (solid grey), optimal state conditioning (solid black), robust state conditioning (dash black) –  $\times 10$  indicates that the values of the curve have to be multiplied by 10.



Chapter 5. A Four Carts Example

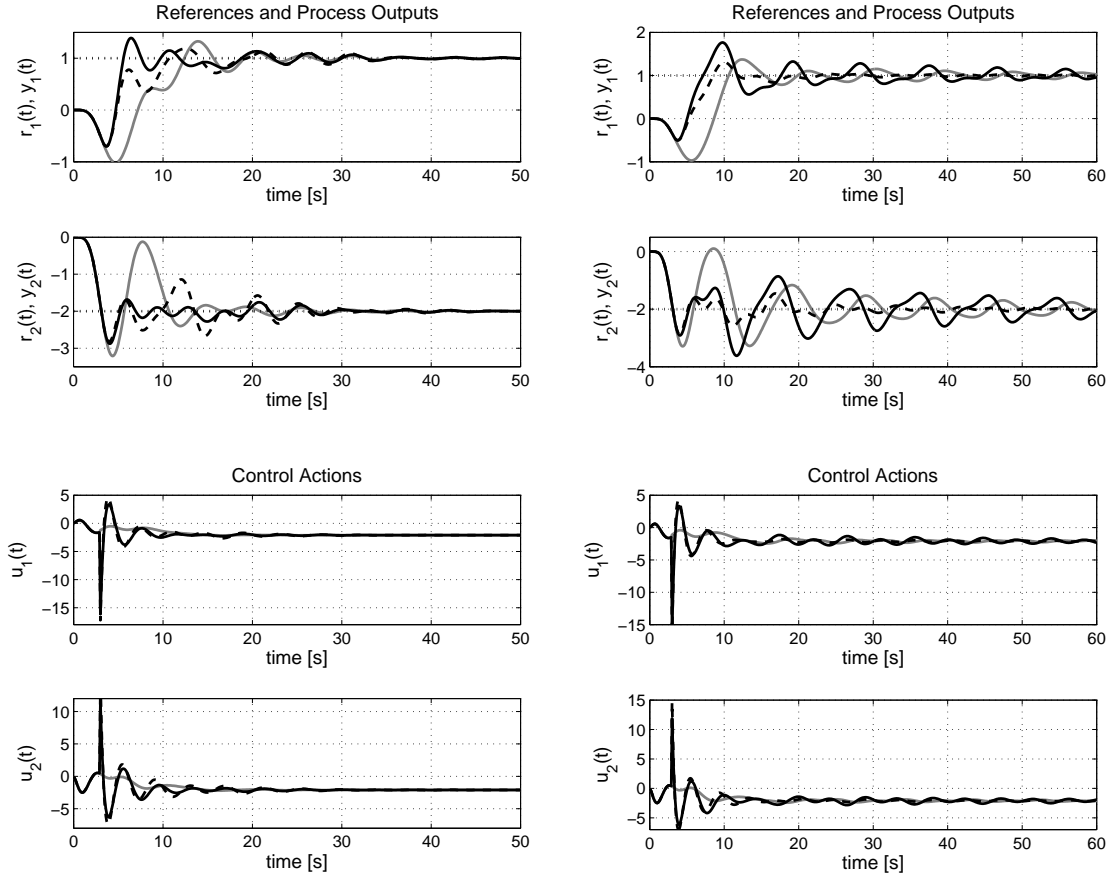


**Figure 5.4:** Monodimensional uncertainty. Switching from  $\mathcal{C}_1$  to  $\mathcal{C}_2$  at  $t_s = 3$  s ( $\Psi = \text{diag}(I_2, 10^3 I_2)$ ,  $\Omega = 0_{2n_c}$ ). Left: Process configuration corresponding to  $\theta^{[1]} = 0.50$ . Right: Process configuration corresponding to  $\theta^{[1]} = 0.25$ . Legend: Non state conditioning (solid grey), optimal state conditioning (solid black), robust state conditioning (dash black).

non state conditioning (4.25). In both cases,  $\Psi = \text{diag}(I_2, 10^3 I_2)$  and the weight matrix  $\Omega$  has been set equal to  $0.001 I_{2n_c}$ , the latter one being dictated by the desire to provide an aggressive control actions at times of switching in order to track as soon as possible the reference signals. As previously anticipated in Remark 4.3.2, in the adaptive control context, however, this could be not always the best choice and so, the setting of weight matrices can be sometimes critical. To show that, Figure 5.7 depicts one of the cases of Table 5.1, which corresponds to consider the process in  $\theta^{[1]} = 0.6$  and  $C_1$  as initial controller. Notice that, in case non state resetting be pre-imposed, the switching rule needs long time to select the right controller (nonetheless, this does not yield high magnitude of signals). Then, suppose to reinitialize the multicontroller state by the robust reset map. So doing, we see that the choice of the weight matrices turns out to affect the closed loop behavior: smaller  $\Omega$  is, more long the process outputs keeps around the reference signals, thus increasing the time needed to the supervisor to detect an unstable trend and recognize the right controller (the values of weight matrices are specified in the figure). So, we can conclude that the values of resetting weight matrices, namely  $\Psi$  and  $\Omega$ , have to be suitably chosen in base of the confidence in the decision ability of the switching rule.

## 5.2 Second Scenario: Bidimensional Uncertainty

Consider now a more complex case, which requires a larger number of controllers to satisfy the feasibility assumption **a1**. Specifically, assume that both the external springs have the uncertainty on the stiffness value, namely,  $\theta^{[1]} \in [0.18, 1.6]$  N/m and  $\theta^{[3]} \in [0.18, 1.6]$  N/m, while the internal spring takes on a known constant value  $\theta^{[2]} = 0.7$  N/m. Accordingly, the uncertainty set corresponds to

$$\Theta = [0.18, 1.6] \times [0.18, 1.6] \text{ N/m}. \quad (5.5)$$

In this case, we need of nine candidate controllers to guarantee feasibility condition **a1**, where the plant configurations corresponding to nine nominal models are indicated in Figure 5.8, along with the stability ranges of the corresponding controllers. Hence, given  $M_i(s) = A_i^{-1}(s)B_i(s)$  (with  $s$  the Laplace operator),  $i \in \overleftarrow{\mathfrak{I}}$ , denoting the continuous-time left MFD of the process model with stiffness  $\theta_i$ , the corresponding one-degree-of-freedom continuous-time controller with right MFD  $C_i(s) = Y_i(s)X_i(s)^{-1}$  can be selected among all stabilizing controllers  $\tilde{C}(s) = \tilde{Y}(s)\tilde{X}^{-1}(s)$  in accordance with the following weighted  $H_\infty$

Chapter 5. A Four Carts Example

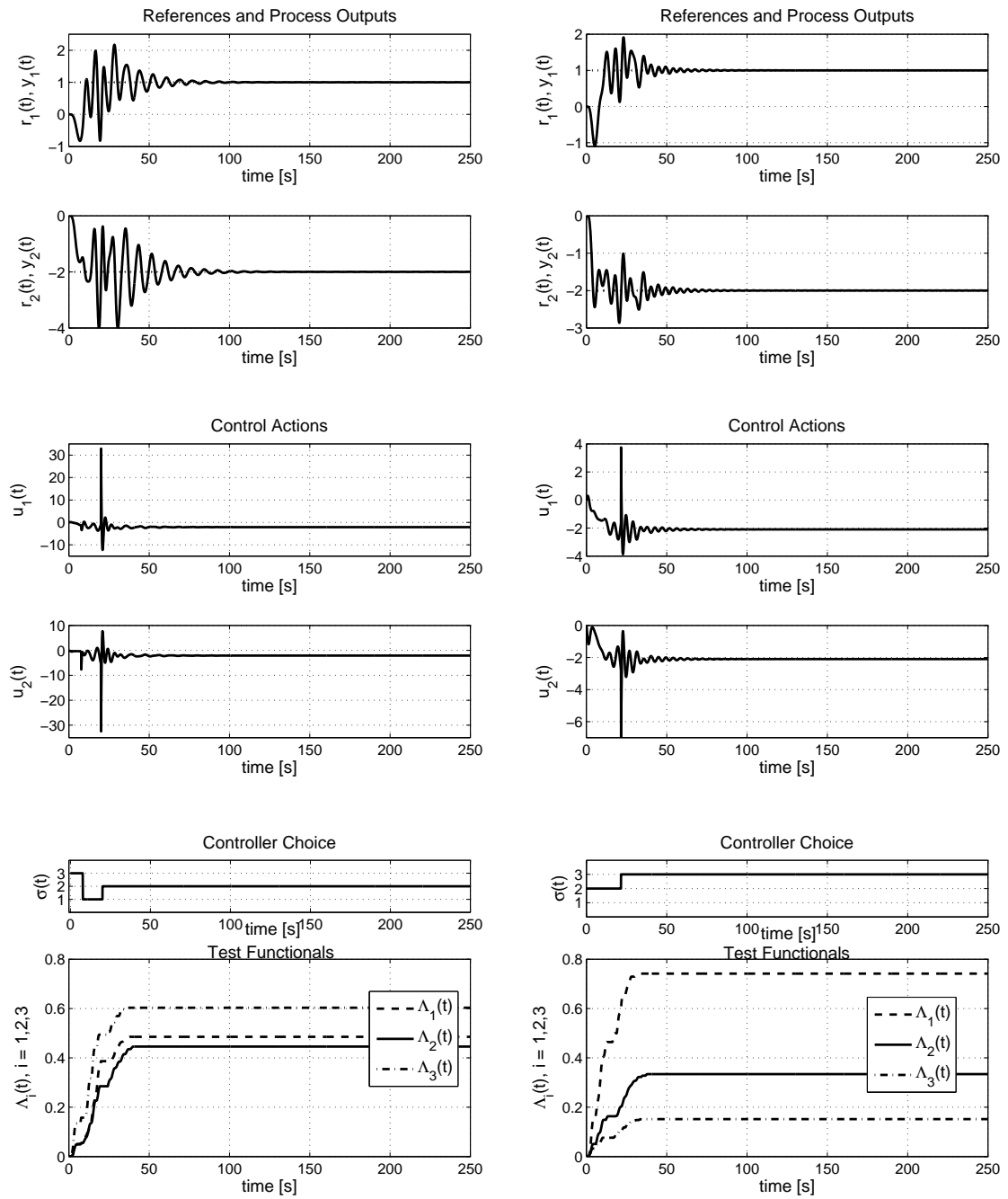


**Figure 5.5:** Monodimensional uncertainty. Response of the switching control scheme with robust state conditioning. Left: Process configuration corresponding to  $\theta^{[1]} = 0.35$  and  $\sigma(0) = 3$ ; Right: Process configuration corresponding to  $\theta^{[1]} = 0.75$  and  $\sigma(0) = 2$ .

Chapter 5. A Four Carts Example

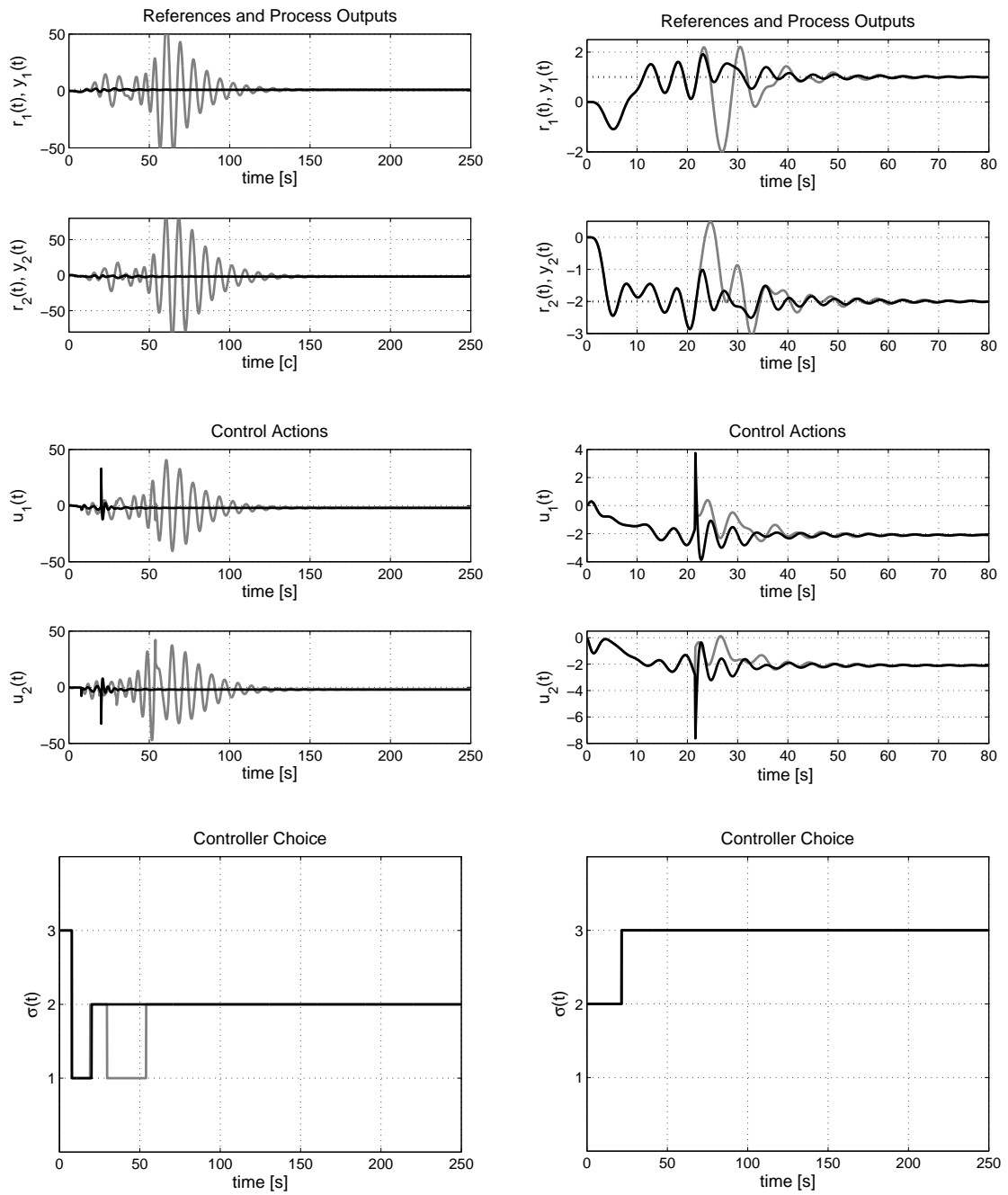


**Figure 5.6:** Monodimensional uncertainty. Response of the switching control scheme with non / robust state conditioning. Left: Process configuration corresponding to  $\theta^{[1]} = 0.35$  and  $\sigma(0) = 3$ ; Right: Process configuration corresponding to  $\theta^{[1]} = 0.75$  and  $\sigma(0) = 2$ . Legend: Non state conditioning (grey), robust state conditioning (black)

Chapter 5. A Four Carts Example

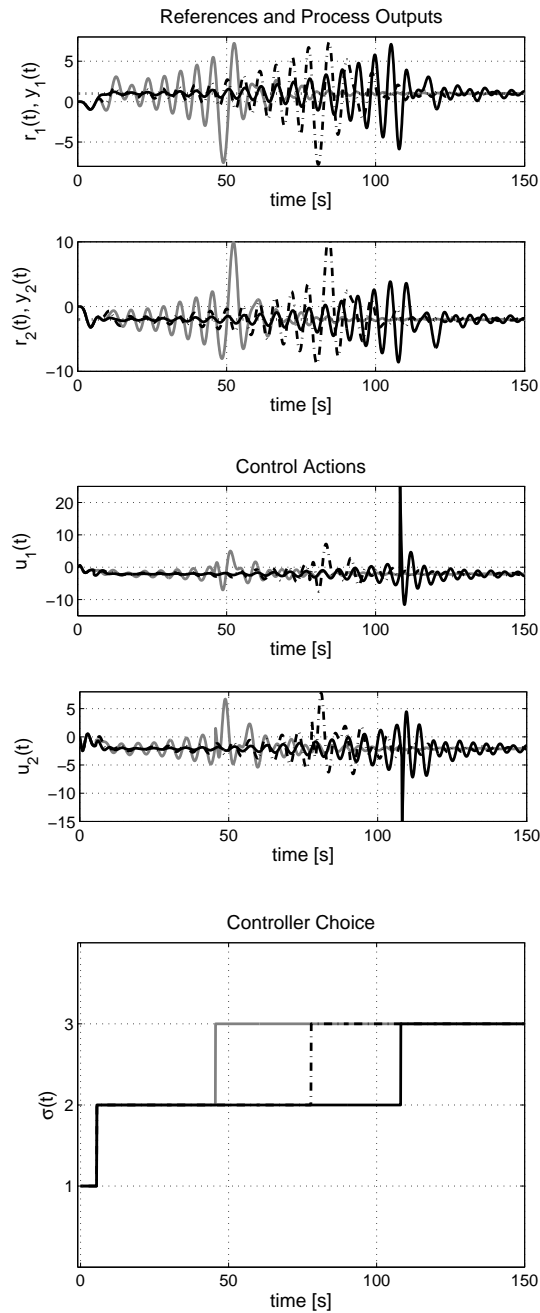


**Figure 5.7:** Monodimensional uncertainty. Response of the switching control scheme with no / robust state conditioning and different choices of the weight matrix  $\Omega$ . Process configuration corresponding to  $\theta^{[1]} = 0.60$  and  $\sigma(0) = 1$ . Legend: Non state resetting (solid grey); robust state resetting with  $\Omega = 0.001 I_{2n_c}$  (solid black) and,  $\Omega = 10 I_{2n_c}$  (dash-dot black).

Chapter 5. A Four Carts Example

mixed-sensitivity criterion [Kwa91]:

$$C_i(s) = \arg \inf_{\tilde{C}} \sup_{\omega} \bar{\sigma}[\Phi_{W_i}(j\omega)],$$

where  $\bar{\sigma}$  denotes maximum singular value and  $\Phi_{W_i}(s)$  the  $W$ -weighted mixed sensitivity matrix

$$\Phi_{W_i}(s) = \begin{bmatrix} \{\Psi_i^u\}^{-1/2} W_i(s) \tilde{Y}(s) \\ \{\Psi_i^y\}^{-1/2} W_i(s) \tilde{X}(s) \end{bmatrix} \tilde{\Xi}_i^{-1}(s) A_i(s),$$

with  $\tilde{\Xi}_i(s) := A_i(s)\tilde{X}(s) + B_i(s)\tilde{Y}(s)$ . Then, models and controllers have been discretized by means of an input zero-order holder with sampling time equal to 0.1 s. The use of a control design technique different from the previous section is motivated by the desire to show how the supervisor / multicontroller architectures do not depend on the adopted controller family, as well as a robust control design is resulted to be the most adequate technique to be applied to a so large process uncertainty. The results indicated in Table 5.2 show the

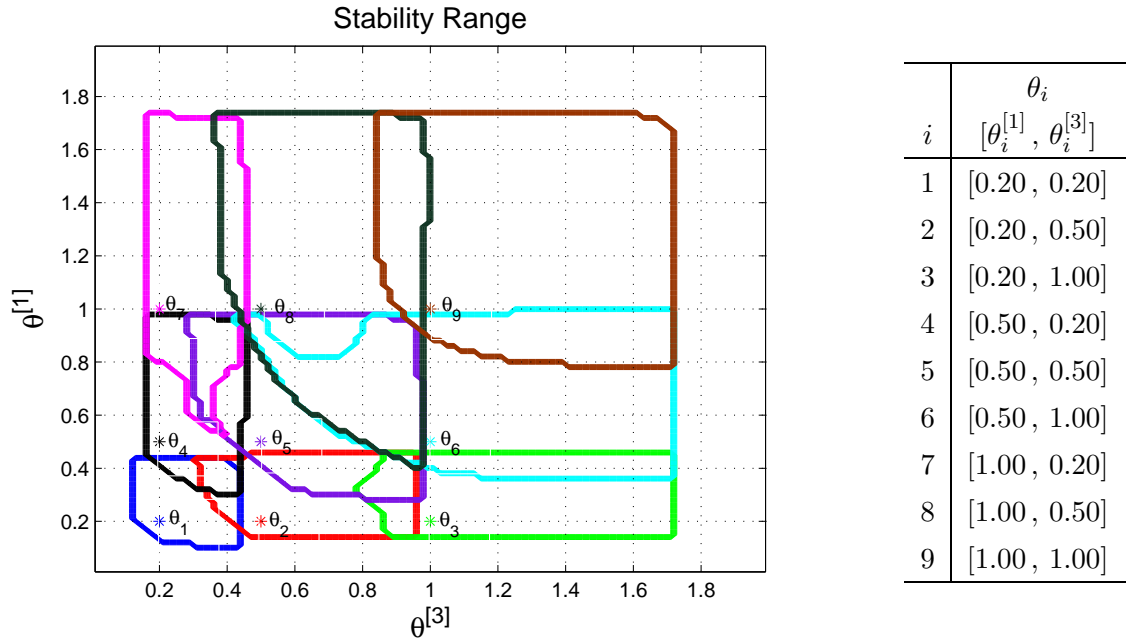


**Figure 5.8:** Bidimensional uncertainty. Left: Stability ranges of the nine controllers, which are obtained by setting  $W_i(s) = 0.01/(s+0.01) I_2$ ,  $\Psi_i^y = I_2$  and  $\Psi_i^u = 10^{-3} I_2$ ,  $i = 1, 2, \dots, 9$ . Right: Values corresponding to the nominal models.

behavior of the switched control system in response to two square waves,  $r_1(\tau)$  and  $r_2(\tau)$ ,

of amplitudes and periods equal to  $\pm 2.5$  m and 150 s, and  $\pm 1.5$  m and 100 s, respectively. Simulations are carried out with a switching control scheme where the hysteresis constant  $h$  is set equal 0.05 and, the multicontroller is equipped with the robust state reset map (4.54) (where,  $\Psi = \text{diag}(I_2, 10^3 I_2)$ ,  $\Omega = 0.001 I_{2n_c}$  and, the discrete scenario is obtained by sampling the uncertainty using a squared grid, each cell having side equal to 0.01). The table considers a set of process configurations supposed to be representative for the whole uncertainty, while Figure 5.9 depicts two of the most critical scenarios, as reported in Table 5.2. Consistent with intuition, the most critical cases are those involving process parameters close to the boundary regions of destabilizing controllers. Nonetheless, from the performance point of view, the closed-loop behavior always remains satisfactory, the process inputs-outputs always being kept at a moderate level.

### 5.3 Concluding Remarks

This chapter has been devoted to the analysis of a numerical example, which has allowed us to test the effectiveness both of the controller selecting rule, described in Chapter 3, and of the multicontroller state conditioning techniques, discussed in Chapter 4. From simulations we conclude that: i) the switching logic is always able to detect unstable trends and to stop on a stabilizing controller, provided that condition **a1** be satisfied; ii) the optimal / robust conditioning of the multicontroller state improves the transient behavior after switching for each process configuration (note that, the process varies continuously with the uncertain parameters); iii) stability property of the switching scheme keeps unchanged for each (finite) reinitialization of the state of the multicontroller, in particular, the weight matrices characterizing the state reset map have to be appropriately chosen, based on the confidence in the switching decision ability.

$[\theta^{[1]} \ \theta^{[3]}]$	Switching Logic			Process Behavior	
	Initial index	Final index	Final time	Max. values of $ y_1 $ and $ y_2 $	Max. values of $ u_1 $ and $ u_2 $
[0.25, 0.30]	6	1	0.90 s	2.57 and 1.56	7.63 and 5.70
[0.30, 1.30]	8	3	0.70 s	2.51 and 1.66	7.61 and 7.71
[0.60, 0.20]	2	4	0.80 s	2.50 and 1.53	14.39 and 5.68
[0.40, 1.20]	1	6	0.70 s	2.53 and 1.61	14.34 and 9.17
[0.70, 0.70]	5	8	2.70 s	2.62 and 1.65	6.07 and 5.14
[1.00, 0.65]	9	8	48.70 s	3.29 and 2.51	12.90 and 27.23
[0.90, 1.40]	1	9	0.60 s	2.55 and 1.52	14.62 and 10.03
[1.25, 1.30]	3	9	0.60 s	2.54 and 1.55	15.52 and 4.45
[1.40, 0.60]	4	8	0.70 s	2.55 and 1.58	8.34 and 10.30
[0.35, 0.40]	7	2	135.7 s	3.96 and 3.27	10.59 and 29.68
[0.30, 0.85]	8	3	0.70 s	2.51 and 1.73	7.60 and 6.32
[0.50, 0.90]	9	6	0.80 s	2.52 and 1.50	6.59 and 4.50
[1.40, 0.30]	3	7	0.60 s	2.59 and 1.52	16.91 and 5.70
[0.55, 0.55]	1	5	0.60 s	2.52 and 1.54	13.23 and 8.95
[0.80, 0.35]	1	5	101.5 s	3.67 and 2.45	55.96 and 14.76

**Table 5.2:** Bidimensional uncertainty. Simulation results obtained by switching among 9 controllers with robust state conditioning.



Chapter 5. A Four Carts Example

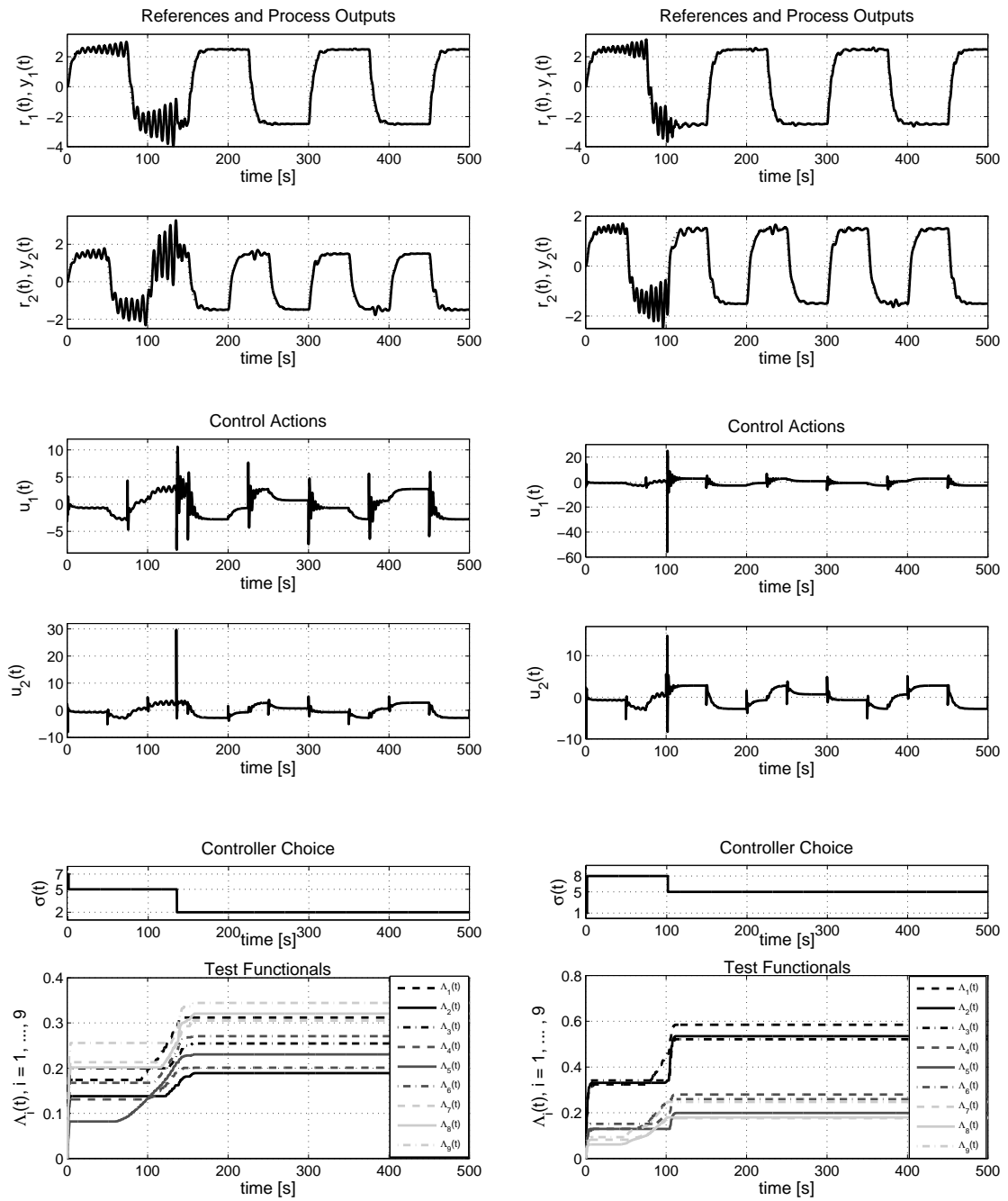


**Figure 5.9:** Bidimensional uncertainty. Response of the switching control scheme with robust state conditioning. Left: Process configuration corresponding to  $[\theta^{[1]}, \theta^{[3]}] = [0.35, 0.40]$  and  $\sigma(0) = 7$ ; Right: Process configuration corresponding to  $[\theta^{[1]}, \theta^{[3]}] = [0.80, 0.35]$  and  $\sigma(0) = 1$ .

# Conclusions

In this thesis adaptive switching control schemes have been tackled and, solutions have been proposed to respond to the questions of how selecting the right controller and then, how transferring the control action.

Part I has been devoted to the controller selection strategy in case of multivariable systems. The selection is carried out with respect to a finite family of pre-fixed controllers with the possible addition of one adaptive controller. In particular, Chapter 3 has been focused on the problem of controlling uncertain squared systems by means of an ASC scheme which exploits pre-fixed controllers. Selection is carried out by comparing test functionals suitably chosen to evaluate the suitability of each controller to be connected in feedback with the process. In such a chapter the Multi-Model Unfalsified ASC approach, introduced in [BBMT10] for handling SISO systems, has been extended to square systems. The case of non-square systems has been separately treated in Appendix A. In general, it has been shown that, by suitably redefining the test functionals, the same stability and performance features of the SISO systems carry over to the generic multivariable case with no additional assumptions on the process to be controlled. More specifically, under the only reasonable requirements to have a stabilizing controller for each process configuration, a stable behavior of the switched system with response to a generic bounded reference signal is guaranteed. In addition, a simple variant of the basic test functional has been proposed such to ensure, along with stability, the offset-free tracking with respect to signals originated by LTI exosystems. Appendix B has dealt with the problem to increase performance by means of the combination of the ASC scheme with an adaptive mechanism which aims at suitably tuning an additional controller to be compared with the pre-fixed family. The proposed mechanism for the on-line generation of new controller has proven to be an interesting solution for different reasons: i) It runs separately with the switching scheme, which continues to have the

complete management of the process, and interaction between the two schemes occurs only at the time the new controller is added to the controller family; ii) It does not influence the characteristics of the switching scheme; iii) The experimental load, typically cumbersome in data-driven controller tuning mechanisms, is reduced at the minimum, thanks to the use of the virtual reference tool. However, some questions regarding technical aspects of the algorithm continue to be open.

Part II has discussed the control transfer problem to model-based switching schemes. Chapter 4 has compared two different architectures for implementing the multicontroller into an ASC scheme: the multi-system-based realization and the hybrid linear realization. By the comparison, the latter one has proved to be more suitable in cases where the number of controllers is high, its computational cost being independent of the number of controllers. Also, it allows to manage with unstable controllers. By a hybrid linear architecture, controllers can share their states and, accordingly, only one (common) state vector turns out to be operative at each time. The idea to improve the transient performance at each switching time has been the one to condition the control transfer by suitably resetting the state of the multicontroller. In particular, the state reinitialization has been obtained through a linear map where related gains can be a priori computed with respect to process uncertainty and available controllers. Hence, computational burden of the resulting hybrid linear controller with state reset map does not increase with respect to the original implementation, thus proving to be suitable to be applied in case of a large number of controllers.

In Part III, a numerical example has been considered in order to test the effectiveness both of the controller selecting rule, described in Chapter 3, and of the multicontroller state conditioning techniques, discussed in Chapter 4. From simulations of Chapter 5 it has been possible to see that: i) The switching logic detects unstable trends and stops on a stabilizing controller, provided that it exist; ii) By the conditioning of the multicontroller state, the transient behavior improves performance after switching; iii) Stability property of the switching scheme keeps unchanged by conditioning the state of the multicontroller.

# Bibliography

- [ABB<sup>+</sup>11] G. Agapito, S. Baldi, G. Battistelli, D. Mari, E. Mosca, and A. Riccardi. Automatic tuning of the internal position control of an adaptive secondary mirror. *European Journal of Control*, 3:273–289, 2011.
- [ABD<sup>+</sup>01] B. D. O. Anderson, T. S. Brinsmead, F. De Bruye, J. Hespanha, D. Liberzon, and A. S. Morse. Multiple model adaptive control, part 2: switching. *Int. J. Robust Nonlinear Control*, 11(5):479–496, 2001.
- [ABLM01] B. D. O. Anderson, T. S. Brinsmead, D. Liberzon, and A. S. Morse. Multiple model adaptive control with safe switching. *Int. J. Adaptive Control Signal Proc.*, 15:445–470, 2001.
- [ABM<sup>+</sup>12] G. Agapito, G. Battistelli, D. Mari, D. Selvi, A. Tesi, and P. Tesi. Frequency based design of modal controllers for adaptive optics systems. *Optics Express*, 20, 2012.
- [AD08] B.D.O. Anderson and A. Dehghani. Challenges of adaptive control-past, permanent and future. *Annual Reviews in Control*, 32:123–135, 2008.
- [APH98] K.G. Astrom, H. Panagopoulos, and T. Hagglund. Design of pi controllers based on non-convex optimization. *Automatica*, 34:585–601, 1998.
- [AW96] A.B. Arehart and W.A. Wolovich. Bumpless switching controllers. *Proc. 35th Conference on Decision and Control, Kobe, Japan*, 1996.
- [AW97] A.B. Arehart and W.A. Wolovich. Bumpless switching in hybrid systems. In P. Antsaklis, W. Kohn, and S. Sastry, editors, *Hybrid Systems IV: Lecture Notes in Computer Science 1273*, pages 1–17. Springer, 1997.

- [BBM<sup>+</sup>11a] S. Baldi, G. Battistelli, D. Mari, E. Mosca, and P. Tesi. Multi-model adaptive switching control for uncertain multivariable systems. In *Proc. of the 50<sup>th</sup> IEEE Conf. on Decision and Control and European Control Conference (CDC-ECC)*, Dec. 2011.
- [BBM<sup>+</sup>11b] S. Baldi, G. Battistelli, D. Mari, E. Mosca, and P. Tesi. Multi-model adaptive switching control with fine controller tuning. In *Proc. of the 18<sup>th</sup> IFAC World Congress*, Sept. 2011.
- [BBM<sup>+</sup>12] S. Baldi, G. Battistelli, D. Mari, E. Mosca, and P. Tesi. Multi-model switching control of uncertain multivariable systems. *International Journal of Adaptive Control and Signal Processing*, 26:705–722, 2012.
- [BBMT10] S. Baldi, G. Battistelli, E. Mosca, and P. Tesi. Multi-model unfalsified adaptive switching supervisory control. *Automatica*, 46:249–259, 2010.
- [BBMT11] S. Baldi, G. Battistelli, E. Mosca, and P. Tesi. Multi-model unfalsified adaptive switching control. test functionals for stability and performance. *International Journal of Adaptive Control and Signal Processing*, 25:595–612, 2011.
- [BEFB94] S. Boyd, L. El Ghaoui, E. Feron, and V. Balakrishnan. *Linear Matrix Inequalities in System and Control Theory*, volume 15 of *Studies in Applied Mathematics*. SIAM, Philadelphia, PA, June 1994.
- [Ber96] D. P. Bertsekas. *Constrained Optimization and Lagrange Multiplier Methods*. Athena Scientific, Belmont, Massachusetts, 1996.
- [BF08] D. Buchstaller and M. French. Gain bounds for multiple model switched adaptive control of general mimo lti systems. *Proc. 47th Conference on Decision and Control, Cancun, Mexico*, 2008.
- [BG97] M. Bodson and J.E. Groszkiewicz. Multivariable adaptive algorithms for reconfigurable flight control. *IEEE Trans. on Control System Technology*, 5:217–229, 1997.
- [BMM99] D. Borrelli, A. S. Morse, and E. Mosca. Discrete-time supervisory control of families of 2-dof linear set-point controllers. *IEEE Trans. on Aut. Contr.*, 44:178–181, 1999.

- [BMMT] G. Battistelli, D. Mari, E. Mosca, and P. Tesi. Performance-oriented transfer for switching control. preliminary accepted to *Automatica*.
- [BMST10] G. Battistelli, E. Mosca, M. G. Safonov, and P. Tesi. Stability of unfalsified adaptive switching control in noisy environments. *IEEE Transactions on Automatic Control*, 55:2424–2429, 2010.
- [BW92] D. Bernstein and B. Wie. Benchmark problems for robust control design. *Journal of Guidance and Control*, 15:1057–1059, 1992.
- [CC06] G.C. Calafiore and M. C. Campi. The scenario approach to robust control design. *IEEE Trans. on Aut. Contr.*, 51:742–753, 2006.
- [CD99] M. H. Chang and E. J. Davison. Adaptive switching control of lti mimo systems using a family of controllers approach. *Automatica*, 35:453–465, 1999.
- [CHP04] M. Campi, J.P. Hespanha, and M. Prandini. Cautious hierarchical switching control of stochastic linear systems. *Int. J. Adaptive Control Signal Proc.*, 18:319–333, 2004.
- [CN94] K. Ciliz and K. S. Narendra. Multiple model based adaptive control of robotic manipulators. *Proc. 33rd IEEE Conf. on Decision and Control*, pages 1305–1310, 1994.
- [CS06] S. Y. Cheong and M. G. Safonov. Improved bumpless transfer with slow-fast controller decomposition. *Proc. 2009 American Control Conference, St. Louis, USA*, 2006.
- [DAL07] A. Dehghani, B. D. O. Anderson, and A. Lanzon. Unfalsified adaptive control: a new controller implementation and some remarks. *Proc. of the European Control Conference, Kos, Greece*, 2007.
- [DFT90] J. Doyle, B. Francis, and A. Tannenbaum. *Feedback Control Theory*. Macmillan Publishing Co., 1990.
- [DG75] E. J. Davison and A. Goldengerg. Robust control of a general servomechanism problem: the servo compensator. *Automatica*, 11:461–471, 1975.

- [DLVL09] A. Dehghani, A. Lecchini-Visitini, and B.D.O. Lanzon, A. Anderson. Validating controllers for internal stability utilizing closed-loop data. *IEEE Trans. on Automatic Control*, 54:2719–2725, 2009.
- [FAP06] S. Fekri, M. Athans, and A. Pascoal. Issues, progress and new results in robust adaptive control. *Int. J. Adapt. Control Signal Process.*, 20:519–579, 2006.
- [FB86] M. Fu and B. Barmish. Adaptive stabilization of linear systems via switching control. *IEEE Trans. on Automatic Control*, 31:1097–1109, 1986.
- [FW76] B. A. Francis and W. M. Wonham. The internal model principle of control theory. *Automatica*, 12:457–465, 1976.
- [GA96] S. F. Graebe and A.L.B. Ahlèn. Dynamic transfer among alternative controllers and its relation to antiwindup controller design. *IEEE Trans. on Control System Technology*, 4:92–96, 1996.
- [Gev93] M. Gevers. Towards a joint design of identification and control. In H.T.J. Trentelman and J.C. Willems, editors, *Essay on control: Perspectives in the theory and its applications*, pages 111–151. Basel: Birkhauser, 1993.
- [GL95] M. Green and D.J.N. Limebeer. *Linear Robust Control*. Pearson Education, Inc., 1995.
- [HGGL98] H. Hjalmarsson, M. Gevers, S. Gunnarsson, and O. Lequin. Iterative feedback tuning: theory and applications. *IEEE Control System Magazine*, 18(4):26–41, 1998.
- [HIKH09] N. Hirose, M. Iwasaki, M. Kawafuku, and Hirai H. Initial value compensation using additional input for semi-closed control systems. *IEEE Trans. on Industrial Electronics*, 56(3):635–641, 2009.
- [HKH87] R. Hanus, M. Kinneart, and J. L. Henrotte. Conditioning technique, a general anti-windup and bumpless transfer method. *Automatica*, 23(6):729–739, 1987.
- [HLe01] J.P. Hespanha and D. Liberzon editors. Switching and logic in adaptive control. *Special issue in Int. J. Adaptive Control Signal Proc.*, 2001.

- [HLM03a] J. P. Hespanha, D. Liberzon, and A. S. Morse. Hysteresis-based switching algorithms for supervisory control of uncertain systems. *Automatica*, 39:263–272, 2003.
- [HLM03b] J. P. Hespanha, D. Liberzon, and A. S. Morse. Overcoming the limitations of adaptive control by means of logic-based switching. *Systems & Control Letters*, 49:49–95, 2003.
- [HM98] Y. Huang and W.C. Messner. A novel robust time-optimal algorithm for servo systems with bias disturbance. *IEEE Trans. on Magnetics*, 34(1):7–12, 1998.
- [IMS03] A. Isidori, L. Marconi, and A. Serrani. *Robust Autonomous Guidance. An Internal Model Approach (Advances in Industrial Control)*. Springer Verlag, 2003.
- [IS96] P. A. Ioannou and J. Sun. *Robust Adaptive Control*. Prentice Hall, 1996.
- [Joh00] M. Johansson. Optimal initial value compensation for fast settling times in mode-switching control systems. In *Proc. of the 39<sup>th</sup> IEEE Conf. on Decision and Control*, Dec. 2000.
- [KSe01] R.L. Kosut and M.G. Safonov editors. Adaptive control, with confidence. *Special issue in Int. J. Adaptive Control Signal Proc.*, 2001.
- [Kwa91] H. Kwakernaak. The polynomial approach to  $\mathcal{H}_\infty$  optimal regulation. In E. Mosca and L. Pandolfi, editors, *Control Theory, Lecture Notes in Mathematics*, volume 1496, pages 141–221. Springer, Berlin, 1991.
- [Lib03] D. Liberzon. *Switching in Systems and Control*. Birkhäuser, 2003.
- [MA01] E. Mosca and T. Agnoloni. Inference of candidate loop performance and data filtering for switching supervisory control. *Automatica*, 37:527–534, 2001.
- [MCC01] E. Mosca, F. Capecchi, and A. Casavola. Designing predictors for mimo switching supervisory control. *Int. J. Adaptive Control Signal Proc.*, 15:265–286, 2001.



- [MCMS07] C. Manuelli, S. G. Cheong, E. Mosca, and M. G. Safonov. Stability of unfalsified adaptive control with non-scli controllers and related performance under different prior knowledge. *Proc. of the European Control Conference, Kos, Greece, 2007*.
- [MMG92] A. S. Morse, D. Q. Mayne, and G. C. Goodwin. Applications of hysteresis switching in parameter adaptive control. *IEEE Trans. on Automatic Control*, 37:1343–1354, 1992.
- [MN95] E. Mosca and C. Nava. Identification and dynamic weights for lqg control with integral action. *IEE Proceeding - Control Theory and Applications*, 142:647–653, 1995.
- [Mor95] A. S. Morse. Control using logic-based switching. In A. Isidori, editor, *Trends in Control: An European perspective*, pages 69–113. London: Springer, 1995.
- [Mor97] A. S. Morse. Supervisory control of families of linear set-point controllers, part 2: robustness. *IEEE Trans. on Automatic Control*, 42(11):1500–1515, 1997.
- [Mos95] E. Mosca. *Optimal, Predictive, and Adaptive Control*. Prentice Hall, 1995.
- [NB97] K.S. Narendra and J. Balakrishnan. Adaptive control using multiple models. *IEEE Trans. on Automatic Control*, 42:171–187, 1997.
- [NRR93] R.A. Nichols, R.T. Reichert, and W.J. Rugh. Gain scheduling for h-infinity controllers: A flight control example. *IEEE Trans. on Control System Technology*, 1:69–79, 1993.
- [NX00] K.S. Narendra and C. Xiang. Adaptive control of discrete-time systems using multiple models. *IEEE Trans. on Automatic Control*, 45:1669–1686, 2000.
- [OS62] A. Ostrowski and H. Schneider. Some theorems on the inertia of general matrices. *J. of Math. Analysis and Applications*, 4:72–84, 1962.
- [PHGne] F. R. Pour Safaei, J. P. Hespanha, and Stewart G. On controller initialization in multivariable switching systems. *Automatica*, 2012, In press, Available online.
- [PK01] F. M. Pait and F. Kassab. On a class of switched, robustly stable, adaptive systems. *Int. J. Adaptive Control and Signal Processing*, 15:213–238, 2001.

- [PVH96] Y. Peng, D. Vrancic, and R. Hanus. Anti-windup, bumpless, and conditioned transfer techniques for pid controllers. *IEEE Control Systems Magazine*, 14(4):48–57, 1996.
- [PVHW88] Y. Peng, D. Vrancic, R. Hanus, and S. S. Wellers. Anti-windup designs for multivariable controllers. *Automatica*, 34(12):1559–1565, 1988.
- [RS00] W.J. Rugh and J.S. Shamma. Research on gain scheduling. *Automatica*, 36:1401–1425, 2000.
- [SA90] J.S. Shamma and M. Athans. Analysis of nonlinear gain scheduled control systems. *IEEE Trans. on Automatic Control*, 35:898–907, 1990.
- [SAB06] S. W. Su, B. D. O. Anderson, and T.S. Brinsmead. Minimal multirealization of mimo linear systems. *IEEE Trans. on Automatic Control*, 51:690–695, 2006.
- [SB89] S. Sastry and M. Bodson. *Adaptive Control: Stability, Convergence and Robustness*. Prentice Hall, Englewood Cliffs, NJ, 1989.
- [SL92] B.L. Stevens and F.L. Lewis. *Aircraft Control and Simulation*. Jhon Wiley and Sons, Inc., 1992.
- [Sny05] J.A. Snyman. *Practical Mathematical Optimization*. Springer Science and Business Media, Inc. New York, 2005.
- [SP97] M. W. Spong and L. Praly. Energy based control of underactuated mechanical systems using switching and saturation. In A. S. Morse, editor, *Control using logic-based switching, Lecture Notes in Control and Information Sciences*, pages 162–172. London: Springer, 1997.
- [SS08] M. Stefanovic and M. G. Safonov. Safe adaptive switching control: Stability and convergence. *IEEE Trans. on Automatic Control*, 53:2012–2021, 2008.
- [SS11] M.G. Safonov and M. Stefanovic. Safe adaptive control: Data-driven stability analysis and robust synthesis. *Series: Lecture Notes in Control and Information Sciences*, 405:1–156, 2011.
- [ST97] M. G. Safonov and T. C. Tsao. The unfalsified control concept and learning. *IEEE Trans. on Automatic Control*, 42:843–847, 1997.

- [SWPS07] M. Stefanovic, R. Wang, A. Paul, and M. G. Safonov. Cost detectability and stability of adaptive control systems. *Int. J. Robust Nonlinear Control*, 17:549–561, 2007.
- [Tao03] G. Tao. *Adaptive control: Design and Analysis*. John Wiley & Sons, 2003.
- [TW00] M. C. Turner and D. J. Walker. Linear quadratic bumpless transfer. *Automatica*, 36:1089–1101, 2000.
- [TWY07] A.S. Morse T.-W. Yoon, J.-S. Kim. Supervisory control using a new control-relevant switching. *Automatica*, 43:1791–1798, 2007.
- [VS95] P.M.J. Van den Hof and R.J.P. Schrama. Identification and control: Closed-loop issues. *Automatica*, 31:1751–1770, 1995.
- [WF79] W.A. Wolovich and P. Ferreira. Output regulation and tracking in linear multivariable systems. *IEEE Trans. on Aut. Contr.*, 24(3):460–465, 1979.
- [WG94] S. R. Weller and G. C. Goodwin. Hysteresis switching adaptive control of linear multivariable systems. *IEEE Trans. on Automatic Control*, 39:1360–1374, 1994.
- [YQK07] J. J. Yamè, H. Qiao, and M. Kinnaert. On bumps and reduction of switching transients in multicontroller systems. *Mathematical problems in Engineering*, 2007, 2007.
- [YQK10] J. J. Yamè, H. Qiao, and M. Kinnaert. A self-conditioned implementation of switching controllers for smooth transition in multimode systems. *Conference on Control and Fault Tolerant Systems, Nice, France*, 2010.
- [YSTH96] T. Yamaguchi, K. Shishida, S. Tohyama, and Hirai H. Mode switching control design with initial value compensation and its application to head positioning control on magnetic disk drives. *IEEE Trans. on Industrial Electronics*, 43(1):65–73, 1996.
- [ZDG95] K. Zhou, J. C. Doyle, and K. Glover. *Robust and Optimal Control*. Prentice Hall, 1995.

## Bibliography

---

- [ZMF00] P. V. Zhivoglyadov, R. H. Middleton, and M. Fu. Localization based switching adaptive control for time-varying discrete-time systems. *IEEE Trans. on Automatic Control*, 45:752–755, 2000.
- [ZT02] L. Zaccarian and A. R. Teel. A common framework for anti-windup, bumpless transfer and reliable designs. *Automatica*, 38:1735–1744, 2002.
- [ZT05] L. Zaccarian and A. R. Teel. The  $\mathcal{L}_2$  ( $l_2$ ) bumpless transfer problem for linear plants: Its definition and solution. *Automatica*, 41:1273–1280, 2005.